

LEARNING TO REGULATE HOMEOSTATIC BRAIN NETWORKS

Dissertation

zur Erlangung des Grades eines
Doktors der Naturwissenschaften

der Mathematisch-Naturwissenschaftlichen Fakultät
und
der Medizinischen Fakultät
der Eberhard-Karls-Universität Tübingen

vorgelegt

von

Rahim Malekshahi

aus Eilam, Iran

March - 2016

Tag der mündlichen Prüfung: 17.05.2016

Dekan der Math.-Nat. Fakultät: Prof. Dr. W. Rosenstiel

Dekan der Medizinischen Fakultät: Prof. Dr. I. B. Autenrieth

1. Berichterstatter: Prof. Dr. Dr. hc. mult. Niels Birbaumer

2. Berichterstatter: Prof. Dr. Christoph Braun

Prüfungskommission:

Prof. Dr. Dr. hc. mult. Niels Birbaumer

Prof. Dr. Christoph Braun

Prof. Dr. Hubert Preissl

Prof. Dr. Wolfgang Larbig

I hereby declare that I have produced the work entitled "*Learning to regulate homeostatic brain networks*", submitted for the award of a doctorate, on my own (without external help), have used only the sources and aids indicated and have marked passages included from other works, whether verbatim or in content, as such. I swear upon oath that these statements are true and that I have not concealed anything. I am aware that making a false declaration under oath is punishable by a term of imprisonment of up to three years or by a fine.

Tübingen, den
Datum / Date

.....
Unterschrift /Signature

To my:

“Beloved Wife”, “Dear Son”, and “Beautiful and Precious Family”

It was impossible to succeed without you

Acknowledgements

I would like to express my deepest appreciation to my supervisors, Prof. Dr. Dr. hc. mult. Niles Birbaumer, and Prof. Andrea Caria for their support. Dear Niels working with you was a real pleasure. I learned a lot from you. You were there for me, despite your busy agenda, whenever I needed your advice on both research and personal matters. Dear Andrea, your supervision was invaluable to me. Without your guidance and persistent help, this dissertation would not have been possible.

I would also like to express my sincere gratitude to my PhD advisor Prof. Christoph Braun for following my projects enthusiastically, and supported me on this journey. Very special thanks go to Dr. Ralf Veit, Prof. Masataka Watanabe, and Dr. Michael Erb for sharing their brilliant experimental MRI knowledge throughout this PhD.

I would like to extend my thanks to my dear colleagues, Dr. Gisela Hagberg, Prof. Hubert Preissl, Dr. Maartje Spetter, Dr. Manfred Hallschmid, Angela Straub, Dr. Amalia Papanikolaou, Dr. Karim Ansari Asl, Dr. Cesare Magri, and Prof. Nikos Logothetis for their guidance and support over the years.

I would like to gratefully acknowledge Dr. Tina Lampe for coordinating doctoral program in the excellent way. Dear Tina thanks for your great advices during my PhD. I would like to also thank Prof. Dr. Horst Herbert, head of the Graduate Training Centre, and Dr. Katja Thieltges, administration - finance Coordinator. Many thanks for providing the opportunity to grow through diverse and rich training courses.

Immeasurable appreciation to my dear friends for their moral support, thank you.

Contents

Abstract	13
Abstract (English)	15
Abstract (German)	17
Synopsis	19
Neurofeedback and neuroplasticity	20
Real time fMRI neurofeedback principles	21
Real time fMRI clinical applications and technical considerations	22
Single region of interest versus brain networks	24
Brain connectivity	25
fMRI a tool for studying brain connectivity	27
Connectivity-based rtfMRI neurofeedback	30
Homeostatic brain networks – obesity, OCD and interoception	31
Literature	40
Presentation of own contributions to papers and manuscripts	53
Volitional regulation of brain responses to food stimuli in overweight and obese subjects: A real-time fMRI feedback study	55
Simultaneous learned regulation of anterior insula and somatosensory cortex improves interoceptive but not exteroceptive awareness	65
Self-regulation of anterior insula with real-time fMRI and its behavioral effects in obsessive-compulsive disorder: a feasibility study	89

Abstract

Abstract (English)

Dynamic equilibrium of internal conditions such as body temperature, blood pressure, blood pH, hormones, blood glucose, insulin concentrations, and the like is vital for health and survival, and indeed many diseases involve a disturbance of homeostasis. Mainly the nervous system and the endocrine system control regulation mechanisms, and in general after sensing imbalance, appropriate biochemical or physiological feedback loops regulate the condition to the normal balance set-point. This dissertation aimed to investigate novel real-time functional magnetic resonance imaging neurofeedback (rt-fMRI-NF) methodologies enable healthy individuals, and patients to learn to regulate homeostatic brain networks. The first study targeted the effect of rt-fMRI-NF training-induced up-regulation of functional connectivity (FC) between reward value- and impulse-control-related brain areas on eating behaviour in a proof-of-principle correlative pre-post pilot experiment. The second study explored the possibility of manipulating functional connectivity between anterior insular cortex (AIC) and somatosensory cortex (SC) by rewarding simultaneous activity in these two brain regions. We postulated that the functional interconnection between AIC and SC, regions which receive visceral and skin afferents respectively, organizes the processing of bodily signals from the viscera and somatic tissues which represents the core aspect of emotional regulation in the James-Lang concept of emotion. Finally in the third study, we investigated whether patients with contamination obsessions and washing compulsions can learn to volitionally decrease (down-regulate) BOLD activity in the insula in the presence of disgust/anxiety provoking stimuli. The result of the first study showed that conscious voluntary up-regulation of correlation results in an increased functional connectivity between the dorsolateral prefrontal cortex (dlPFC) and ventromedial prefrontal cortex (vmPFC), a connectivity that is involved in self-control and healthy food choices. The behavioural results indicated a tendency towards healthier food choices comparing post transfer session with respect to the pre-test session. The second study confirmed our hypothesis that volitional up-regulation of simultaneous combined BOLD activity of AIC and SC leads to enhanced functional connectivity between them, a connectivity that permits enriched feelings from the body and subjective feeling of emotions. We observed that the modulation of functional connectivity between the AI and SC predicted performance in the heartbeat perception task. In the third study, we found that OCD patients could gain self-control of the BOLD activity of insula after few training sessions. Together behavioral findings from our three studies provide new insights that the homeostatic self-regulating ability of the brain can be strengthened by rt-fMRI-NF training. They clarify that changing and modulating neuronal pathways in brain networks underling self-control, decision making, and emotional experiences will result in promising behavioral consequences.

Abstrakt (German)

Eine dynamische Balance der physiologischen Gegebenheiten wie Körpertemperatur, Blutdruck, Blut-PH-Wert, Hormonspiegel, Blutzucker und Insulinkonzentration ist für die Gesundheit und das Überleben unverzichtbar. Viele Krankheiten haben eine Störung der Homöostase zur Folge. Vor allem das Nerven- und das Hormonsystem steuern Regulationsmechanismen und sobald diese ein Ungleichgewicht feststellen, gibt es passende biochemische oder physiologische Feedback-Kreisläufe, die den Gesamtzustand in die Balance zurückführen. Diese Dissertation untersucht neuartige Methoden des Echtzeit-Neurofeedbacks, das auf funktioneller Magnetresonanztomographie basiert (Real-time functional magnetic resonance imaging – rt-fMRI-NF), um es gesunden Probanden und Patienten zu ermöglichen, homöostatische Netzwerke des Gehirns zu regulieren. Die erste Studie hatte zum Ziel, die Auswirkungen der Hochregulierung der funktionellen Konnektivität durch rt-fMRI-NF-Training (engl. Functional connectivity – FC) zwischen Belohnungs- und impulsivitätsregulierenden Gehirnarealen auf das Essverhalten zu untersuchen. Diese Studie war ein Pilotexperiment im Pre-Post-Schema. Die zweite Studie untersuchte die Möglichkeit, die funktionelle Konnektivität zwischen der anterioren Insula (AIC) und dem somatosensorischen Kortex (SC) durch Belohnung von gleichzeitiger Aktivität dieser Regionen zu beeinflussen. AIC und SC sind Gehirnregionen, die physiologische Zustandsinformationen von Körpergewebe und großflächigen Hautsegmenten erhalten. Wir nahmen an, dass die funktionelle Verbindung zwischen diesen Regionen die Verarbeitung dieser Signale der inneren Organe und Körpergewebe übernimmt. Dies stellt einen Kernbereich des Gefühlskonzeptes von James-Lang dar. In der dritten Studie untersuchten wir, ob Patienten mit kontaminationsbezogenen Zwangsgedanken und Waschzwang lernen können, ihre BOLD-Aktivität in der Insula herunterzuregulieren, wenn sie mit ekelerregenden oder Angst hervorrufenden Stimuli konfrontiert werden. Die Ergebnisse der ersten Studie zeigten, dass die willentliche Hochregulierung der Korrelation zu einer erhöhten funktionellen Konnektivität zwischen dem dorsolateralen präfrontalen Kortex (dlPFC) und dem ventromedialen präfrontalen Kortex (vmPFC) führt. Diese Konnektivität betrifft Selbstkontrolle und die Entscheidung für gesunde Nahrungsmittel. Die Verhaltenstests deuten darauf hin, dass die Probanden sich in der Transfersitzung (nach der Intervention) für weniger ungesunde Nahrungsmittel entscheiden als in der Sitzung vor der Intervention. Die zweite Studie bestätigte unsere Hypothese, dass die willentliche Hochregulierung von gleichzeitiger BOLD-Aktivität von AIC und SC deren funktionale Konnektivität erhöht. Diese Verbindung ermöglicht eine verstärkte Körperwahrnehmung und ein verändertes subjektives Gefühlserleben. Wir beobachteten, dass die Veränderung der funktionellen Konnektivität zwischen AIC und SC die Leistung der Probanden in der Aufgabe (Wahrnehmung des Herzschlags) verbesserte. In der dritten Studie fanden wir heraus, dass Patienten mit Zwangsstörungen (OCD) nach einigen Trainingseinheiten die Selbstkontrolle der BOLD-Aktivität der Insula

erreichen konnten. Fasst man die Ergebnisse der drei Studien zusammen, konnten wir zeigen, dass die Fähigkeit des Gehirns zur homöostatischen Selbstregulierung durch die Verwendung von rt-fMRI-Training verbessert werden kann. Zudem ist nun klarer, dass die Veränderung und die Modulation von neuronalen Pfaden in Gehirnnetzwerken, die der Selbstkontrolle, der Entscheidungsfindung und der Gefühlswahrnehmung zugrunde liegen, zu vielversprechenden Verhaltensveränderungen führt.

Synopsis

Neurofeedback and neuroplasticity

Neuroplasticity, brain plasticity, is the brain's ability to restructure itself by forming new neural connections and/or prune irrelevant connections and pathways after training or practice throughout life. Neurofeedback is defined as a learning process utilizing operant learning mechanisms to control brain activity. Neurofeedback takes advantage of the brain's plasticity and by providing continuous information about the brain activity, or physiological process to humans or animals, permits a voluntary self-regulation of that activity through feedback and reward (Birbaumer et al. 2013, Birbaumer et al. 2009). Different imaging modalities have been used for neurofeedback. Electro-encephalography (EEG), and electro-physiology use neuroelectric activity (Neuper et al. 2003, Fetz 1969, Fetz et al. 1971, Spilker et al. 1969, Wolpaw et al. 2002, Turnip et al. 2011, Turnip et al. 2012, Kim et al. 2014, Soekadar et al. 2014, Pineda et al. 2008), magneto-encephalography (MEG) uses magnetic fields produced by electrical currents in the brain (Florin et al. 2014), and functional near-infrared spectroscopy (fNIRS) (Sitaram et al. 2009, Sitaram et al. 2007, Naito et al. 2007, Fazli et al. 2012, Hong et al. 2015) and real time functional magnetic resonance imaging (rtfMRI) (Weiskopf et al. 2004, LaConte 2011, Caria et al. 2007, Sulzer et al. 2013) benefit from metabolic activity of the brain.

The first study on neurofeedback reported the use of the alpha waves of human participants (Spilker et al. 1969). This promising study triggered other work, where they showed that animals are also able to alter their brain activity by providing feedback (Fetz 1969, Fetz et al. 1971). However, it took many years until neurofeedback found its way into clinical applications. Recently researchers showed that during and after training self-regulation of slow cortical potentials (SCPs), patient with drug-resistant epilepsy experienced less frequent ictal events (Kotchoubey et al. 2001, Rockstroh et al. 1993). Strehl et al. showed that children with attention deficit–hyperactivity disorder (ADHD) could learn to regulate negative SCPs. This well-controlled study resulted in significant improvement in behavior, attention, and IQ (Strehl et al. 2006).

Real time fMRI neurofeedback principles

RtfMRI allows noninvasive and real time measurement of metabolic brain activity, and was first introduced in 1995 (Cox et al. 1995). Advances in hardware and software, made the rtfMRI a powerful technique with potential applications from diagnosis to monitoring and treatment of disorders (Birbaumer et al. 2009, Birbaumer et al. 2006, deCharms et al. 2004, deCharms et al. 2005, deCharms 2007, deCharms 2008, Weiskopf et al. 2007, Weiskopf et al. 2004, Weiskopf 2012). In contrast to the conventional fMRI, in rtfMRI the dependent variable is behavior while brain activity is noninvasively manipulated as the independent variable (Caria et al. 2012, Weiskopf 2012). The principal advantages of rtfMRI lie in its noninvasive nature, ever-increasing availability, relatively high spatiotemporal resolution, and its capacity to demonstrate the entire network of brain areas engaged when subjects undertake particular tasks.

Normal functioning of brain depends on neurovascular coupling which is the basis of functional MRI and rtfMRI. Hemodynamic response (HR) allows homeostatically adjustment of blood flow to deliver nutrients such as oxygen and glucose to active neurons. One disadvantage of these techniques is that, like all hemodynamic-based modalities, it measures a surrogate signal whose spatial specificity and temporal response are subject to both physical and biological constraints (Logothetis 2008). The Blood-oxygen-level dependent (BOLD) signal reflects neural activity indirectly, and the exact relationship between the measured fMRI signal and the underlying neuronal activity is only partly understood and remains under vigorous investigation (Logothetis et al. 2001, Logothetis et al. 2004, Magri et al. 2011). However, compared to other modalities such as TMS, EEG, and even fNIRS, rtfMRI owns higher spatial resolution and subcortical regions can be precisely studied. With modern multi-channel EEG systems, the source localization is an intrinsically ill-posed problem (Baillet et al. 2001). Due to this problem in EEG, brain areas underlying learning of self-regulation and the relationship with behavior is not clear (Weiskopf 2012).

RtfMRI-BCI works as a closed loop system, and normally has three main components (brain signal acquisition, online analysis, and feedback) which are usually executed by separate computers connected via TCP/IP protocol. MRI scanner using the fast echo planar imaging (EPI)

sequences measures spatially circumscribed brain activity. Data are retrieved and exported to a feedback computer every repetition time (TR). There, real time data pre-processing and statistical analysis are performed using dedicated software. Motion and image distortion correction, temporal filtering, spatial smoothing, and normalization are among important pre-processing steps. Modern technologies allow applying online real time statistical analysis as powerful as their offline counterparts (Weiskopf 2012). Univariate general linear model (GLM) (Bagarinao et al. 2003, Goebel et al. 2001, Caria et al. 2007, Caria et al. 2012, Weiskopf et al. 2004, Sulzer et al. 2013), and multivariate support vector machines (SVMs) (Sitaram et al. 2011, LaConte et al. 2007, Hollmann et al. 2011) are among important model-based methods widely used in rtfMRI. Independent component analysis (ICA) on the other hand is a potential data-driven approach, which has been applied successfully to the fMRI data in real time (Esposito et al. 2003, Wang et al. 2013). After performing statistical analysis, contingent feedback is provided to the participant in the scanner via a projector (commonly visually, in the form of a thermometer icon, with the temperature measure indicating the current level of brain activity. However, not only visual but also auditory or haptic feedback is possible) using stimulus computer. Information from the feedback, almost real time, helps subjects to learn to voluntarily control their brain activity in the targeted brain regions or network.

Real time fMRI clinical applications and technical considerations

Over years, patient studies support the feasibility of rtfMRI-based neurofeedback training, where they have reported neurophysiological and/or behavioral effects. Some of these investigations include chronic Pain (deCharms et al. 2005), chronic tinnitus (Haller et al. 2010), schizophrenia (Ruiz et al. 2013, Cordes et al. 2015), major depression (Linden et al. 2012, Young et al. 2014), alcohol abuse/addiction (Karch et al. 2015, Kirsch et al. 2015), nicotine addiction (Li et al. 2013, Hartwell et al. 2013, Hartwell et al. 2016, Hanlon et al. 2013), chronic stroke (Sitaram et al. 2012), Parkinson disease (Subramanian et al. 2011), obesity (Frank et al. 2012), obsessive-compulsive-disorder (Scheinost et al. 2013, Buyukturkoglu et al. 2015), spider phobia (Zilverstand et al. 2015),

and psychopathy (Sitaram et al. 2014). Although clinical application of rtfMRI seems promising, but so far most of the aforementioned studies suffer from small size test/control groups and partially successful transfer when participants need to perform the task inside or outside the MR scanner without feedback. Moreover, intermediate or long lasting behavioral effects were not investigated or have not been found (Brühl 2015). Hence, still there should be many methodological considerations for the use of rtfMRI-based neurofeedback for treating (psychiatric/neurological) disorders. The number and the optimal duration of a training session, inter-session interval, necessity of adaptation based on targeted disorder, implicit or explicit instruction, the best interface for feedback display, interventions to be used in the control group, intermittent or continuous feedback are among critical issues that need to be addressed in future works (Sulzer et al. 2013, Fovet et al. 2015, Stoeckel et al. 2014).

Although ambiguous instruction to participants in a neurofeedback study might lead to a substantial rate of non-learners, Birbaumer, a pioneer in the field of neurofeedback and rtfMRI, does not support explicit instruction for regulating brain activity in neurofeedback studies. As long as a single region in the brain such as amygdala might have a multiple functions, instructing subjects to use specific mental imagery (i.e. imagining fearful situation) to regulate activity in that region would not be the best solution. Instead, he believes in using pure reward and contingency of feedback (Birbaumer et al. 2013). Patients often have cognitive deficits, or are not able to follow instructions.

Another critical point in neurofeedback is the learning curve (Birbaumer et al. 2013). With rtfMRI within a very short time, almost less than half an hour, people are able to control their brain activity in any circumscribed brain region inside the MR scanner, while in EEG-based neurofeedback it might be longer than several hours. The brain is usually continuously informed about the blood flow and it has to regulate the blood flow extremely tightly in order to equilibrium function. In neuro-vascular coupling, the feedback comes from the vessels to the brain, and that is probably one reason why people are able to control metabolic changes in the brain better than neuroelectric activity. There are no specific sensors in the brain to update the brain about its

underlying electrical activity; therefore, in rtfMRI the feedback to the brain is faster, more reliable and specific. Birbaumer et al. propose that learning regulation of brain activity is similar to skill learning (Birbaumer et al. 2013). The striatum and basal ganglia are critical brain areas for skill learning. Feedback from brain's vascular system to these areas constrains the abstract nature of the skill to be acquired (Birbaumer et al. 2013, Koralek et al. 2012). Emmert et al. by performing a meta-analysis of several rtfMRI studies also observed the activation of both the basal ganglia and the anterior insula (AI) during the regulation of brain activation across the studies (Emmert et al. 2016).

Single region of interest versus brain networks

The majority of early rtfMRI studies, targeted diverse but single brain areas such as amygdala (Posse et al. 2003, Zotev et al. 2011), anterior insula (Caria et al. 2007, Caria et al. 2010, Veit et al. 2012, Ruiz et al. 2013), several subdivisions of the ACC (Weiskopf et al. 2003, Hamilton et al. 2011, deCharms et al. 2005), several sensorimotor areas (Lee et al. 2009, Yoo et al. 2008, Johnson et al. 2012, Chiew et al. 2012, Berman et al. 2012), and auditory cortex (Yoo et al. 2006). They have shown that self-regulation of BOLD activity inside these region of interests (ROIs) could be learned specifically. However, the brain consists of many different networks (Van Den Heuvel et al. 2010). Spatially distributed but functionally linked regions in the brain are continuously exchanging information during resting state and functioning of the brain. Concert action of several brain regions and even networks is essential for performing complex cognitive processes. In fact, in the brain processes of emotion, language, perception, etc., which have been examined in rtfMRI studies, the activation of multiple brain regions have been observed (Ruiz et al. 2014). However, understanding dynamic flow of information across neuronal networks has been always a challenge for neuroscience.

Brain connectivity

Altered brain connectivity has been observed in a number of diseases such as obesity, ADHD, stroke, autism spectrum disorder (ASD), and Alzheimer disease (AD). How brain connectivity and integration of information might be disturbed during neurological or psychiatric diseases and its relationship with behavior has attracted considerable attention (Bullmore et al. 2009, Greicius 2008). Brain connectivity which has gained a considerable popularity among neuroscientists refers to a network of anatomical coupling (anatomical connectivity), statistical dependencies mainly temporal correlation (functional connectivity), and causal interaction (effective connectivity) between spatially distinct units in the nervous system (Ribeiro et al. 2015, Guye et al. 2008). It can be defined at several levels of scale, microscale, mesoscale and macroscale. At the microscale (micrometer resolution), several techniques such as histological staining and post-mortem dissections of neural tissues have been employed (Van Buren et al. 1958, Eickhoff et al. 2006, Schmahmann et al. 2007). These techniques unravel the interactions at the level of individual neurons, and their synaptic connections. Mesoscale corresponds to networks connecting neuronal populations such as cortical columns. It deals with a spatial resolution of hundreds of micrometers. However to link brain structure to function, studying connectivity at macroscale (interacting regions) is needed.

In recent years, there is a tendency towards functional integration than segregation, and the main approach to characterize integration is brain connectivity. Structural connectivity defines as synaptic connection between adjacent neurons or fiber tracks between spatially remote brain regions. It mostly relies on diffusion tensor imaging (DTI) which measures the directionality of water diffusion within brain structures. DTI is a suitable technique for evaluating the integrity of white matter tracts. White matter consists of myelinated axonal fibres that connect cortical regions. Although structural connectivity itself would not fully describe brain connectivity, but effective connectivity partially depends on structural connectivity. In a visual interhemispheric integration task, superior dynamic causal models (DCMs) were those models that profited from tractography information (Stephan et al. 2009). However, the degree to which the effective connectivity

relies on structural constraints has not been fully understood yet. In fact, the intact anatomy is needed but the effective connectivity of a structural connectivity cannot be inferred from its quantitative information and it does not need to rely on monosynaptic connections (Friston 2011). Therefore, in general, functional links may not be observed necessarily upon anatomical connection (Biswal et al. 2010). While functional connectivity is a descriptive observable phenomenon, effective connectivity is an abstract notion, a model-based approach trying to explain the existing correlation, coherence or other measures of dependencies of measurement of neural activities (Friston et al. 1993, Friston 1994, Friston 2011). In functional connectivity, there is no inference about the coupling between regions, and it only tests some deviations of correlation against the null hypothesis. Difference in correlation between two regions among different conditions would reflect that the neural activity differed between conditions but the underlying coupling can still be the same. Change in coupling elsewhere in the network via a third region, change in amplitude of fluctuation of neural activity, and even change in noise level could explain the change in functional connectivity with intact effective connectivity (Friston 2011).

Various imaging modalities (electrophysiological recording, EEG, MEG, PET and fMRI) that vary in temporal, and spatial resolution and also differ in many other features such as data representation (neuron or neuronal ensembles), nature of activity (electrical or hemodynamic) have been employed to study different levels of description of connectivity (Fingelkurts et al. 2005) which makes it a complicated concept. In addition, applying different computational algorithms even to the same dataset based on different definitions, introduce more complexity (Horwitz 2003). Another major issue which studying brain connectivity suffers from, would be the fact that none of the imaging modalities, due to either inherent or technological limitation is truly able to capture the delicate spatio-temporal characteristics of brain's electrical activity (Duyn 2012). However, there is no direct way to measure connectivity in the brain, and each imaging modality has its own merits and limitations in characterizing brain connectivity, and therefore, the interpretation have always been challenging and a vast simplification of brain networks have been considered.

fMRI a tool for studying brain connectivity

Functional MRI has been extensively used for studying both segregation as well as integration of information being processed. Several researchers have been using fMRI for studying functional connectivity in many different experimental contexts such as resting state (Biswal et al. 1995, Damoiseaux et al. 2006, Greicius 2008, Salvador et al. 2005) as well as in tasks or stimulus-based experiments. Although functional MRI provides precise spatial localization, it relies on hemodynamic activity, and indeed any connectivity measure using fMRI reflects the co-fluctuation in BOLD signal in segregated brain regions. Therefore, its limitations such as inherent delay due to the nature of the hemodynamic response, and the variation of HRF in different regions across entire brain and even different subjects should be considered.

Two main classes of algorithms have been used for calculating functional connectivity, knowledge-based (supervised) and data-driven (unsupervised) algorithms. Knowledge-based approaches need prior knowledge about a model behind data generation process (Lang et al. 2012). They are biased by the seed selection, which mostly anatomically or by performing a cognitive task is defined. They employ several regions of interest (ROI) as seed and looks for co-variation elsewhere in the brain with the average BOLD activity of the seeds (seed to voxel analysis) or between seeds (ROI to ROI analysis). The pairwise co-variation is specified based on cross correlation analysis (CCA) with mostly zero lag (Pearson correlation), mutual information and coherence. Head motion, physiological artifacts from breathing and cardiac rhythms, and low frequency scanner noise could lead to increased Pearson correlation. To distinguish direct from indirect connections, and connectivity arising from the correlation of interfering signals other than the neural sources, the partial correlation analysis has been employed (Zhen et al. 2007). Many studies have been applying knowledge-based techniques to the resting state functional connectivity (Andrews-Hanna et al. 2007, Andrews-Hanna et al. 2010, Biswal et al. 1995, Cordes et al. 2000, Fransson 2005, Larson-Prior et al. 2009, Song et al. 2015), as well as task/stimulus based functional connec-

tivity (Gordon et al. 2012, Li et al. 2012, Newton et al. 2011, Hampson et al. 2006, Buckner et al. 2009, Demb et al. 1995, DeSalvo et al. 2014).

On the other hand, unsupervised data-driven approaches including clustering and decomposition algorithms need no prior knowledge or model. These methods rely on the assumption that the brain is organized in a finite set of functional networks. Singular value decomposition (SVD), principal component analysis (PCA), independent component analysis (ICA) are among decomposition techniques, while Hierarchical, partitional, and spectral clustering are some important unsupervised clustering techniques which have been employed in studying functional connectivity by several researchers (clustering techniques: (Cordes et al. 2002, Salvador et al. 2005, Thirion et al. 2006, Van Den Heuvel et al. 2008), and decomposition techniques: (Friston et al. 1993, Beckmann et al. 2005, Calhoun et al. 2001, van de Ven et al. 2004, Esposito et al. 2006).

In resting state fMRI (RS-fMRI) volunteers/patients are instructed to relax, and not to perform any explicit cognitive, motor or language tasks. RS-fMRI connectivity provides important insight on intrinsic functional networks in the brain in the absence of any explicit task. Even it allows studying how the connectivity of different brain areas can be adopted for engaging in different networks at different times (Smith 2012). Many functional connectivity studies assume temporal stationary of brain signals, but functional connectivity is not static (Chang et al. 2010), and in addition to average functional connectivity, its dynamic nature should also be considered (Lang et al. 2012). Multiple brain resting-state networks associated with visual (Beckmann et al. 2005, Power et al. 2011, Smith et al. 2009), attention (Fox et al. 2006, Power et al. 2011), sensorimotor (Biswal et al. 1995), as well as default mode network (Greicius et al. 2003) have been identified. Deviation in networks associated with mental and neurodegenerative diseases have also been studied (Bassett et al. 2009). For example, several studies confirm the decreased functional or structural connectivity of distributed brain regions in ASD patients (Müller et al. 2011, Hughes 2007).

In resting state data, the correlation analysis could be applied across whole time series. In task data, if two brain areas both respond to the task stimulus, then they will be correlated, even

if there is no connectivity between them. Psychophysiological interactions (PPI) analysis solves this problem. In fact, PPI detects task-specific (context-specific) enhancement in the coupling between seed of interest and the rest of brain (O'Reilly et al. 2012). In other words, to regress out the confounding effect, the psychological and physiological time courses are also included in the analysis.

Dynamic causal modeling (DCM) (Friston et al. 2003), and Granger causality (G-causality) analysis (Goebel et al. 2003) are the two most popular methodologies for describing effective, directional, connectivity. DCM is a generic Bayesian model comparison approach, which compares the carefully selected models (neurobiologically motivated models) of how data were generated. A DCM is fitted to the data (parameter estimation at neuronal level) such that modelled and measured signals are maximally similar. In fact, it infers hidden neural states from measurement of neural activity (Stephan et al. 2010, Stephan et al. 2008). Dynamical causal interaction between neural populations and experimental (context or time) perturbation of this interaction is estimated by DCM (Friston et al. 2003). Lohmann et al. stated that due to serious inconsistency between model evidence and priors, even winning model in DCM cannot be trusted (Lohmann et al. 2012, Lohmann et al. 2013). On the other hand, G-causality which is a statistical concept can be directly applied to any given time series. It tests whether the information of one time series (X) could be used for forecasting the future of another(Y), even better than the information from the past of Y itself (Granger 1969, Friston et al. 2013, Seth et al. 2015). Then it is said that X Granger causes Y. However, G-causality of fMRI signals has been always controversial (David et al. 2008, Roebroeck et al. 2011). Hemodynamic delay, and low sampling rate (very slow repetition time) of fMRI sequences are two main concerns and limitations of applying G-causality to fMRI data. Although G-causality is insensitive to HRF regional variability, it should be used under careful consideration. Comparison between different conditions would be one possible approach to assume unchanged HRF. Correlating causal influences between ROIs and behavioral performance was also employed by different researchers (Wen et al. 2012, Bressler et al. 2008). Bressler et al. showed that top-down G-causality from parietal to occipital regions predicted behavioral performance (Bressler et

al. 2008). Wen et al. also showed that Granger causal influences from ventral attention network to dorsal attention network predicts degraded performance while reciprocal direction was associated with enhanced performance(Wen et al. 2012).

Connectivity-based rtfMRI neurofeedback

As it has been discussed in the previous sections, in traditional fMRI studies the analyses are performed offline. However, real time fMRI neurofeedback studies benefit from acquiring, retrieving, and analysing functional data in a real time scale. This allows subjects to be informed and updated about their brain activity in circumscribed regions every repetition time (TR), almost less than 2 seconds. As described earlier, several rtfMRI neurofeedback studies have been trying to train subjects to regulate brain activity in a single region. They have shown that volitionally regulation of a specific region leads to behavioral consequences that are specific to the functional role of that region in the brain. However, large-scale neural systems are coupled functionally, and indeed any high level cognitive function is achieved by involving multiple brain regions or neural systems. Therefore, recently a lot of attention have been attracted towards establishing new methodologies or adopting available offline approaches to make it possible to use the information from brain networks or multiple brain regions for building neurofeedback systems. Several researchers implemented and developed real-time multivariate classifiers especially based on SVMs for application in rtfMRI neurofeedback experiments (LaConte et al. 2007, Rana et al. 2013, Sato et al. 2013, Shibata et al. 2011). Connectivity-based neurofeedback is another alternative network-based approach, which is highly promising in noninvasively and nonpharmacologically modulating brain connections. In the rest of this synopsis, the concentration would be on real-time functional and effective connectivity methodologies in rtfMRI neurofeedback and their applications in regulating homeostatic brain networks.

Scharnowski et al. by using offline DCM showed that successful up-regulation of activity in visual cortex was associated with enhanced connectivity between visual cortex and superior parietal lobe (Scharnowski et al. 2014). By employing offline multivariate G-causality, Lee et al. showed that extended training of self-regulation of insular cortex was associated with reducing

the extend of superfluous connection and strengthening relevant connections (Lee et al. 2011). Several other studies also have shown that successful regulation of a single brain region leads to change in the brain network connectivity (Veit et al. 2012, Zotev et al. 2011, Hamilton et al. 2011). Although all these studies suggest modulating brain connectivity through self-regulation of brain activity in a circumscribed brain region, but they had no prior assumption about brain regions on the other side of augmented connections. Based on these findings for the first time, Ruiz et al. showed that healthy participants are able to enhance functional connectivity between inferior frontal gyrus (IFG) and superior temporal gyrus (STG) after a few training sessions by providing contingent feedback from correlation coefficient between these regions (Ruiz et al. 2011). In the formula they used for calculating feedback, emphasis was more on the correlation resulted from high amplitude BOLD signals than low amplitude random fluctuation. Koush et al. proposed a DCM-based approach for manipulating causal interaction between brain regions for rtfMRI neurofeedback studies (Koush et al. 2013). Two years later, Koush and his colleagues applied their proposed real-time DCM methodology to the emotion regulation network. They showed that healthy participants were able to learn to enhance top down connectivity from the dorsomedial prefrontal cortex (dmPFC) onto the amygdala (Koush et al. 2015). These encouraging evidences suggest that regarding clinical application towards treatment of diseases (obesity, schizophrenia, addiction, and ASD among many), targeting brain network connectivity may be more suitable than a single brain region.

Homeostatic brain networks – obesity, OCD and interoception

Homeostasis in general, refers to the characteristic of a system that helps maintaining equilibrium. Human homeostasis is defined as self-regulating processes by which the internal conditions and systems of body remain stable despite external environmental changes due to eating, pregnancy, and the like. Dynamic equilibrium of conditions such as body temperature, blood pressure, blood pH, hormones, blood glucose and insulin concentrations, etc. is vital for health and survival, and indeed many diseases involve a disturbance of homeostasis. Constant monitoring and ad-

justment of physiological conditions is called homeostatic regulation. Mainly the nervous system and the endocrine system control regulation mechanisms, and in general after sensing imbalance, appropriate biochemical or physiological feedback loops regulate the condition to the normal balance set-point (Matthews et al. 1985). For instance, regulating body temperature is supervised by the nervous system, in which brain and specifically temperature-sensitive neurons of preoptic area of the hypothalamus control the adjustment of body temperature by tuning the metabolic rate, the breathing rate, the circulation of blood near the skin and some other subtle parameters. Specific to this dissertation, homeostatic brain networks underling obesity and interoception will be reviewed. Furthermore, three novel rtfMRI neurofeedback experiments will be discussed, and will be elucidated that these novel methodologies enable healthy and overweight individuals to learn to regulate homeostatic brain networks.

Obesity is at least partially due to an imbalance of homeostasis, emerged through genetic, environmental and biopsychosocial mechanisms (Wells 2006, Marks 2015). Psychological feature of homeostatic theory of obesity (Circle of Discontent) implies that disequilibrium is resulted from feedback loops of weight gain, body disappointment, negative affect and emotional energy-dense overconsumption. Based on this theory, once weight rises due to whatever reason (i.e. body disappointment), then reciprocal causal interaction between these items leads to instability of the system which makes it very difficult to control overweight (Marks 2015). Energy dis-homeostasis is another important feature of obesity (Woods et al. 1998). Energy homeostasis is achieved when anabolic and catabolic processes are in balance over long intervals. There exist two negative feedback loops which keep the level of adipose mass in a stable set-point over time. Energy imbalance follows by changes in hormonal (Leptin, Insulin, and Glucocorticoid) concentration. In case of negative energy balance, less insulin and leptin are secreted and reach the brain while glucocorticoid concentration increases. This stimulates appetite and results in more food intake and energy storage. Opposite mechanisms and effects, follow positive energy balance (Woods et al. 1998). However, defects to these regulatory mechanisms lead to different eating disorders.

The brain is the most important organ of energy homeostasis. The hypothalamus, by integrating information from different systems and organs, is a key region in several homeostatic regulation mechanisms such as weight supervision and regulating body temperature. In fact, the hypothalamus is a link between the autonomous nervous system and the endocrine system. By integrating information from inside and outside the brain, the hypothalamus drives appropriate actions to the organs and tissues outside the brain through the autonomous nervous system and the endocrine system. The hypothalamus sends its messages inside and outside the brain using neurotransmitters. The neurotransmitter dopamine plays an important role in controlling feeding behavior, and its amount positively correlates with the level of pleasure while eating. Obese patients have lower concentration of the D2 dopamine receptors, therefore obesity could be interpreted as imbalance between energy homeostasis and reward network. Neuroimaging studies have confirmed that reward network in obese patients show altered activation compared to lean individuals (Stoeckel et al. 2008, Martin et al. 2010).

Another determining factor in food intake is cognitive control including decision-making. Several studies have shown that obesity is associated with alteration in brain structures, functional connectivity, and purposeful behavior (Raschpichler et al. 2012, Weygandt et al. 2013, Carnell et al. 2013). Weygandt et al. showed that being able to lose more weight over time could be predicted from the degree of functional connectivity between dorsolateral prefrontal cortex (dlPFC) (area for controlling eating behaviour) and ventromedial prefrontal cortex (vmPFC) (region that process food value) (Weygandt et al. 2013). Hare et al. showed that activity in vmPFC correlated with combination of competing factors (healthiness and tastiness) while dlPFC activity was increased by exercising self-control (Hare et al. 2009). In addition to the dlPFC and the inferior frontal gyrus (IFG), the activity of the anterior insula and the temporo-parietal junction (TPJ) was also observed during active regulation of desire for food. This finding implies the importance of interoceptive awareness as a key process underlying conscious regulation of appetite (Hollmann et al. 2012). Herbert et al. showed that obese and overweight individuals have lower interoceptive awareness than healthy people (Herbert et al. 2014).

Interoception is defined as the sense of the internal physiological condition of the body (Craig 2003). The intensity of subjective feeling of emotion reflect the interoceptive sensitivity (IS) (sensitivity to the variation of internal bodily signals) (Critchley et al. 2004). According to the interoceptive inference (also known as interoceptive predictive coding) theory, top-down predictive inference of the causes of interoceptive sensory signals determines the subjective feeling of emotion (Seth 2013, Seth et al. 2011). Based on this model, the top-down expectation is updated by interoceptive predictive error signals arise from any undesired variation in the internal conditions (i.e. blood sugar level). Then subjective feeling of emotion is experienced (i.e. experiencing hunger or thirst for sugary foods). Next, the resulting high-level prediction error can be resolved by employing autonomic control (change in metabolic rate) or allostatic behaviour (eating available food) (or both) (Seth 2014, Gu et al. 2014). In addition, somatic marker hypothesis links the interoception with decision-making. Based on this theory, somatic markers (interoceptive responses) guide decision-making (Damasio 1991). According to this hypothesis, when individuals face conflicting choices, they may be unable to decide merely based on cognitive processes.

Bud Craig in a series of articles presented a lot of evidences from psychiatry, psychology and neuroscience that insular cortex is where interoception generates feeling (Craig 2002, Craig 2003, Craig 2005, Craig 2009, Craig 2011, Craig 2013, Craig 2015). Feeling from the body are the most fundamental sensations, which underlie most of our affective responses. Bodily feelings could be a direct (i.e. am I warm enough?) or indirect (i.e. do I need a fresh air?) reflection of body's physiological conditions. Lamina I (a thin layer of cells at the top of gray matter in the spinal cord) receives input from small-diameter sensory fibers of the body. From there, the information continues its travel to the brain by Lamina I's fibers (or, axons) through the lateral spinothalamic pathway. Indeed, the destination are thalamic nuclei in the center of the forebrain. During the route, in the medulla (the lower part of the brain stem), nucleus tractus solitarii's (NTS) axons incorporate Lamina I's axons. NTS neurons receive input from different set of small-diameter sensory fibers that innervate the heart, the tongue and all of the viscera. Thalamic nuclei, in turn convey the sensory activity to the cerebral cortex, including dorsal posterior insula. In

fact, not only sensory input from viscera, but also the small-diameter sensory fibers (conveying information about the condition of the tissue itself) from all tissues of the body, including skin, muscle, and bone provide the continuous information required for homeostatic control of ongoing changes in blood flow and respiration. This pathway supports sensations from the body such as pain, itch, vascular flush, and so on. In contrast, sensory fibers which have large-diameter axons and cell bodies provide the exteroceptive sensory information elicited by external world. These evidences reasonably explain the presence of two separate anatomical ascending sensory pathways: spinothalamic and dorsal column-medial lemniscal pathways conveying interoceptive and exteroceptive signals respectively. Based on these findings, interoception include the sensory information from not only viscera (heart, liver, and stomach), muscles, and teeth, but also skin (the largest organ in the body). All and all, interoception directly support homeostatic energy efficiency. In other words, the sensors which report the physiological conditions of all tissues in the body, enable the neural, endocrine and behavioral functions for supporting the process of homeostasis to perform optimally and efficiently together (Kanosue et al. 2010, Amann et al. 2011). For example, the same small-diameter sensory receptors of muscles which involve in energy self-regulation, also contribute to the subjective feeling of fatigue. They signal workload, metabolite concentration, vascular distension, mechanical distortion and temperatures. In the Craig homeostatic model, primary interoceptive representation, the high-resolution representation of ongoing metabolic and vascular conditions, which are conveyed by small-diameter sensory fibers, is embedded in the posterior insula. For example, objective feeling of painful heat intensity is correlated with the activity in the dorsal posterior insula. According to this model, based on comprehensive evidences, there is a multimodal integration in the mid-insula. In the mid-insula, interoceptive image of the body is sequentially integrated with exteroceptive sensory activity such as those from skin and muscles, with homeostatic motor activity (i.e. breathing), with environmental sensory information (auditory, and visual), and with hedonic activity from accumbens and orbitofrontal. The PET study of cool feelings showed that subjective rating of cool temperature correlated first with activation in mid-insula and then strongly with the anterior insula. Therefore, feelings from

the body emerge first in the mid-insula. In the last step, AIC (where conscious experience of emotion emerges) incorporates emotionally salient activity from limbic cortical regions (ACC, OFC), as well as social and cognitive activities from vmPFC, and dlPFC. Sequential re-representations of bodily sensations across IC, provides a foundation for the integration of homeostatic conditions of the body, with the sensory environment, the internal autonomic states and motivational and social conditions.

Alternative hypothesis on interoceptive awareness's pathways suggests that the insula would not be necessary for interoceptive awareness, and pathways projecting to the somatosensory cortex (SC) would be involved. Khalsa et al. had a unique opportunity to study the existence of different pathways. Their subject suffered from complete damage to the bilateral IC, ACC, OFC and amygdala, but the bilateral SC was intact. Any dose-dependent increase in heart rate after bolus administrations of isoproterenol (a sympathetic agonist) was precisely reported verbally and by turning a dial by the patient. However, as soon as the lower left chest skin was anesthetized (using a topical lidocaine), he was not anymore aware of any change in the heart rate. Their result showed that both pathways independently mediate interoceptive awareness (Khalsa et al. 2009). It clarified that the skin sensory afferents to the primary and secondary somatosensory cortices (SC: S1 and S2), which usually believed to support exteroception, independently from sensory afferents to IC and ACC enable awareness of the cardiovascular status of the body. Couto et al. in a case study showed that their patient who was using an external heart (an extracorporeal left-univentricular cardiac assist device, LVAD) relies on somatosensory beats from LVAD in the modified heartbeat detection task, rather than direct vagal enervation of the endogenous heart (Couto et al. 2014). He showed lack of empathy when observed painful pictures of accidents, and compared to the control group he performed significantly worse in theory of mind tasks.

Another interesting converging evidence on multiple interoceptive pathways is that, all other studies which reported activation of insular cortex (IC) during cardiac interoception, showed the activation of somatosensory cortex (SC) as well (Cameron et al. 2002, Pollatos et al. 2007,

Critchley et al. 2004). One more clue of skin relevance in the cardiac interoceptive awareness is the negative correlation between BMI and heartbeat detection performance (Rouse et al. 1998).

To summarize, people have non-identical bodily awareness, and therefore different subjective emotional experience (Wiens 2005). Those with higher awareness have more intense reactions to emotive pictures and are better at describing their emotions. Even they are better at recognizing other people emotions from their faces. Furthermore, interoceptive awareness influences decision-making (Dunn et al. 2010, Kirk et al. 2011), and theory of mind (Lutz et al. 2009).

In this doctoral dissertation, the effort has been on designing and performing experiments for modulating homeostatic networks by using rtfMRI neurofeedback in order to improve interoceptive awareness, decision-making related eating behavior in obese patients, and self-control in obsessive-compulsive disorder (OCD) patients. Three studies have been conducted. In the first study, we wanted to investigate if overweight participants are able to learn to enhance their functional connectivity between vmPFC and dlPFC using neurofeedback training, and whether successful training of functional connectivity improves the inhibitory control of eating behaviour. Towards this purpose, participants were trained to volitionally up-regulate the functional connectivity (partial correlation) between vmPFC and dlPFC over several sessions. In the second study, we aimed at enhancing interoceptive awareness by modulating functional connectivity between SC and AIC indirectly in healthy participants. In contrast to the first study, we tried to boost functional connectivity between SC, and AIC by neurofeedback training of voluntarily up-regulation of simultaneous combined activity from both regions. Therefore, the two studies shared the fact that both targeted modulating functional connectivity for improving homeostatic regulation, but their approaches for enhancing the strength of coupling were different.

As we discussed earlier, the neural mechanisms underlying learning regulation of BOLD activity have been investigated and is understood (Birbaumer et al. 2013). On the other hand, although there exist many encouraging evidences for neurofeedback training of functional connectivity, but still underlying mechanism of regulating connectivity needs to be investigated. As a result, neuroscientifically, modulating coupling between distributed regions in the brain by target-

ing the BOLD activity is preferred over connectivity's measures such as correlation. In fact, Hebbian theory that explains the fundamental mechanism for synaptic plasticity was the basis for our second study. According to the Hebbian theory, any two cells or systems of cells that are repeatedly active at the same time will tend to become associated (Hebb 1949). In other words, cells that fire together wire together (Lowel et al. 1992). Although applying both methodologies successfully resulted in enhancing functional connectivity in our studies, but there has been a limitation to employ the same Hebbian-based approach for modulating connectivity in eating-related brain areas in the first study. The limitation arises from the fact that employing successful strategies for up-regulating BOLD activity in dlPFC might lead to deactivation or co-activation of vmPFC. Therefore, learning processes would be difficult, if not impossible.

Finally in the last study, we investigated whether patients with contamination obsessions and washing compulsions can learn to volitionally decrease (down-regulate) BOLD activity in the insula in the presence of disgust/anxiety provoking stimuli. In concordance with the role of insula in disgust processing, new neural models based on neuroimaging studies suggest that abnormal high activations of insula could be implicated in OCD psychopathology, at least in the subgroup of patients with contamination fears and washing compulsions. We employed rtfMRI-NF technique for training OCD patients to volitionally down-regulate the insula activation. Post treatment, the effect of down-regulation on clinical, behavioural and physiological changes pertaining to OCD symptoms was evaluated.

The result of the first study showed that conscious voluntary up-regulation of correlation results in an increased functional connectivity between the dlPFC and vmPFC, a connectivity that is involved in self-control and healthy food choices. The behavioural results indicated a tendency towards healthier food choices comparing post transfer session with the pre-test session. Offline partial correlation analysis in the second study confirmed our hypothesis that volitional up-regulation of simultaneous combined BOLD activity of AIC and SC leads to enhanced functional connectivity between them, a connectivity that permits enriched feelings from the body and subjective feeling of emotions. Very interestingly, the results elucidated that coupling strength be-

tween right AIC and SC predicts the interoceptive sensitivity measured by heartbeat perception task. Results of the third study showed that OCD patients could gain self-control of the BOLD activity of insula, albeit to different degrees. Positive changes in behaviour in the Ecological disgust test (EDT) were observed following the rtfMRI trainings. Behavioural changes were also confirmed by reductions in the negative valence and in the subjective perception of disgust towards symptom provoking images.

This dissertation clarifies that rtfMRI neurofeedback is a powerful efficient technique for neuroplasticity and enhancing altered or interrupted homeostatic equilibrium. Specifically, functional connectivity between areas that process food value (vmPFC) and those that control eating behaviour(dIPFC) in overweight subjects, and also functional connectivity in brain regions which mediate interoceptive awareness (AIC, and SC) in healthy participants can be enhanced by rtfMRI neurofeedback training. Promisingly, we showed that not only up-regulation, but also down-regulation of BOLD activity in AIC is achievable.

Behavioral findings from our three studies provide new insights that the homeostatic self-regulating ability of the brain can be strengthened by neurofeedback. They clarify that changing and modulating neuronal pathways in brain networks underling self-control, decision making, and emotional experiences will result in promising behavioral consequences. Despite the costs and accessibility of MR technology, the possibility to manipulate homeostatic brain networks through few sessions of training is highly important and represents a novel approach for clinical application.

Literature

- Amann, M., et al. (2011). "Implications of group III and IV muscle afferents for high-intensity endurance exercise performance in humans." The Journal of physiology **589**(21): 5299-5309.
- Andrews-Hanna, J. R., et al. (2010). "Functional-anatomic fractionation of the brain's default network." Neuron **65**(4): 550-562.
- Andrews-Hanna, J. R., et al. (2007). "Disruption of large-scale brain systems in advanced aging." Neuron **56**(5): 924-935.
- Bagarinao, E., et al. (2003). "Estimation of general linear model coefficients for real-time application." Neuroimage **19**(2): 422-429.
- Baillet, S., et al. (2001). "Electromagnetic brain mapping." Signal Processing Magazine, IEEE **18**(6): 14-30.
- Bassett, D. S. and E. T. Bullmore (2009). "Human brain networks in health and disease." Curr Opin Neurol **22**(4): 340-347.
- Beckmann, C. F., et al. (2005). "Investigations into resting-state connectivity using independent component analysis." Philosophical Transactions of the Royal Society of London B: Biological Sciences **360**(1457): 1001-1013.
- Berman, B. D., et al. (2012). "Self-modulation of primary motor cortex activity with motor and motor imagery tasks using real-time fMRI-based neurofeedback." Neuroimage **59**(2): 917-925.
- Birbaumer, N., et al. (2009). "NEUROFEEDBACK AND BRAIN-COMPUTER INTERFACE: CLINICAL APPLICATIONS." International Review of Neurobiology **86**: 107-117.
- Birbaumer, N., et al. (2013). "Learned regulation of brain metabolism." Trends Cogn Sci **17**(6): 295-302.
- Birbaumer, N., et al. (2006). "Physiological regulation of thinking: brain-computer interface (BCI) research." Progress in brain research **159**: 369-391.
- Biswal, B., et al. (1995). "Functional connectivity in the motor cortex of resting human brain using echo-planar mri." Magn Reson Med **34**(4): 537-541.
- Biswal, B. B., et al. (2010). "Toward discovery science of human brain function." Proceedings of the National Academy of Sciences **107**(10): 4734-4739.
- Bressler, S. L., et al. (2008). "Top-down control of human visual cortex by frontal and parietal cortex in anticipatory visual spatial attention." J Neurosci **28**(40): 10056-10061.
- Brühl, A. B. (2015). "Making sense of real-time functional magnetic resonance imaging (rtfMRI) and rtfMRI neurofeedback." International Journal of Neuropsychopharmacology **18**(6): pyv020.
- Buckner, R. L., et al. (2009). "Cortical hubs revealed by intrinsic functional connectivity: mapping, assessment of stability, and relation to Alzheimer's disease." The Journal of Neuroscience **29**(6): 1860-1873.
- Bullmore, E. and O. Sporns (2009). "Complex brain networks: graph theoretical analysis of structural and functional systems." Nature Reviews Neuroscience **10**(3): 186-198.

- Buyukturkoglu, K., et al. (2015). "Correction: Self-Regulation of Anterior Insula with Real-Time fMRI and Its Behavioral Effects in Obsessive-Compulsive Disorder: A Feasibility Study." PLoS One **10**(12).
- Calhoun, V., et al. (2001). "A method for making group inferences from functional MRI data using independent component analysis." Hum Brain Mapp **14**(3): 140-151.
- Cameron, O. G. and M. Satoshi (2002). "Regional Brain Activation Due to Pharmacologically Induced Adrenergic Interoceptive Stimulation in Humans." Psychosomatic Medicine **64**: 851–861
- Caria, A., et al. (2012). "Real-time fMRI: a tool for local brain regulation." Neuroscientist **18**(5): 487-501.
- Caria, A., et al. (2010). "Volitional control of anterior insula activity modulates the response to aversive stimuli. A real-time functional magnetic resonance imaging study." Biol Psychiatry **68**(5): 425-432.
- Caria, A., et al. (2007). "Regulation of anterior insular cortex activity using real-time fMRI." Neuroimage **35**(3): 1238-1246.
- Carnell, S., et al. (2013). "Appetitive traits from infancy to adolescence: Using behavioral and neural measures to investigate obesity risk." Physiology & behavior **121**: 79-88.
- Chang, C. and G. H. Glover (2010). "Time–frequency dynamics of resting-state brain connectivity measured with fMRI." Neuroimage **50**(1): 81-98.
- Chiew, M., et al. (2012). "Investigation of fMRI neurofeedback of differential primary motor cortex activity using kinesthetic motor imagery." Neuroimage **61**(1): 21-31.
- Cordes, D., et al. (2002). "Hierarchical clustering to measure connectivity in fMRI resting-state data." Magn Reson Imaging **20**(4): 305-317.
- Cordes, D., et al. (2000). "Mapping functionally related regions of brain with functional connectivity MR imaging." American Journal of Neuroradiology **21**(9): 1636-1644.
- Cordes, J. S., et al. (2015). "Cognitive and neural strategies during control of the anterior cingulate cortex by fMRI neurofeedback in patients with schizophrenia." Front Behav Neurosci **9**.
- Couto, B., et al. (2014). "The man who feels two hearts: the different pathways of interoception." Soc Cogn Affect Neurosci **9**(9): 1253-1260.
- Cox, R. W., et al. (1995). "Real-Time Functional Magnetic Resonance Imaging." Magn Reson Med **33**(2): 230-236.
- Craig, A. (2003). "Interoception: the sense of the physiological condition of the body." Current Opinion in Neurobiology **13**(4): 500-505.
- Craig, A. (2005). "Forebrain emotional asymmetry: a neuroanatomical basis?" Trends Cogn Sci **9**(12): 566-571.
- Craig, A. (2011). "Significance of the insula for the evolution of human awareness of feelings from the body." Annals of the New York Academy of Sciences **1225**: 72-82.

- Craig, A. (2013). "An interoceptive neuroanatomical perspective on feelings, energy, and effort." Behavioral and Brain Sciences **36**(06): 685-686.
- Craig, A. (2015). How do you feel?: an interoceptive moment with your neurobiological self.
- Craig, A. D. (2002). "How do you feel? Interoception: the sense of the physiological condition of the body." Nature Reviews Neuroscience **3**(8): 655-666.
- Craig, A. D. (2003). "Interoception: the sense of the physiological condition of the body." Current Opinion in Neurobiology **13**(4): 500-505.
- Craig, A. D. (2009). "How do you feel—now? the anterior insula and human awareness." Nature Reviews Neuroscience **10**(1).
- Critchley, H. D., et al. (2004). "Neural systems supporting interoceptive awareness." Nat Neurosci **7**(2): 189-195.
- Damasio, A. R. (1991). "Behavior: Theory and Preliminary Testing." Frontal lobe function and dysfunction: 217.
- Damoiseaux, J., et al. (2006). "Consistent resting-state networks across healthy subjects." Proceedings of the National Academy of Sciences **103**(37): 13848-13853.
- David, O., et al. (2008). "Identifying neural drivers with functional MRI: an electrophysiological validation." PLoS Biol **6**(12): e315.
- deCharms, R. C. (2007). "Reading and controlling human brain activation using real-time functional magnetic resonance imaging." Trends Cogn Sci **11**(11): 473-481.
- deCharms, R. C. (2008). "Applications of real-time fMRI." Nature Reviews Neuroscience **9**(9): 720-729.
- deCharms, R. C., et al. (2004). "Learned regulation of spatially localized brain activation using real-time fMRI." Neuroimage **21**(1): 436-443.
- deCharms, R. C., et al. (2005). "Control over brain activation and pain learned by using real-time functional MRI." Proc Natl Acad Sci U S A **102**(51): 18626-18631.
- Demb, J. B., et al. (1995). "Semantic encoding and retrieval in the left inferior prefrontal cortex: a functional MRI study of task difficulty and process specificity." The Journal of Neuroscience **15**(9): 5870-5878.
- DeSalvo, M. N., et al. (2014). "Task-dependent reorganization of functional connectivity networks during visual semantic decision making." Brain and behavior **4**(6): 877-885.
- Dunn, B. D., et al. (2010). "Listening to your heart how interoception shapes emotion experience and intuitive decision making." Psychol Sci.
- Duyn, J. H. (2012). "EEG-fMRI Methods for the Study of Brain Networks during Sleep." Front Neurol **3**: 100.
- Eickhoff, S. B., et al. (2006). "Testing anatomically specified hypotheses in functional imaging using cytoarchitectonic maps." Neuroimage **32**(2): 570-582.

- Emmert, K., et al. (2016). "Meta-analysis of real-time fMRI neurofeedback studies using individual participant data: How is brain regulation mediated?" Neuroimage **124**: 806-812.
- Esposito, F., et al. (2006). "Independent component model of the default-mode brain function: Assessing the impact of active thinking." Brain research bulletin **70**(4): 263-269.
- Esposito, F., et al. (2003). "Real-time independent component analysis of fMRI time-series." Neuroimage **20**(4): 2209-2224.
- Fazli, S., et al. (2012). "Enhanced performance by a hybrid NIRS–EEG brain computer interface." Neuroimage **59**(1): 519-529.
- Fetz, E. E. (1969). "Operant conditioning of cortical unit activity." Science **163**(3870): 955-958.
- Fetz, E. E. and D. V. Finocchio (1971). "Operant conditioning of specific patterns of neural and muscular activity." Science **174**(4007): 431-435.
- Fingelkurts, A. A., et al. (2005). "Functional connectivity in the brain—is it an elusive concept?" Neuroscience & Biobehavioral Reviews **28**(8): 827-836.
- Florin, E., et al. (2014). "Targeted reinforcement of neural oscillatory activity with real-time neuroimaging feedback." Neuroimage **88**: 54-60.
- Fovet, T., et al. (2015). "Current issues in the use of fMRI-based neurofeedback to relieve psychiatric symptoms." Current pharmaceutical design **21**(23): 3384-3394.
- Fox, M. D., et al. (2006). "Spontaneous neuronal activity distinguishes human dorsal and ventral attention systems." Proceedings of the National Academy of Sciences **103**(26): 10046-10051.
- Frank, S., et al. (2012). "The obese brain athlete: self-regulation of the anterior insula in adiposity." PLoS One **7**(8): e42570.
- Fransson, P. (2005). "Spontaneous low-frequency BOLD signal fluctuations: An fMRI investigation of the resting-state default mode of brain function hypothesis." Hum Brain Mapp **26**(1): 15-29.
- Friston, K. (2011). "Dynamic causal modeling and Granger causality Comments on: The identification of interacting networks in the brain using fMRI: Model selection, causality and deconvolution." Neuroimage **58**(2): 303-305.
- Friston, K., et al. (1993). "Time-dependent changes in effective connectivity measured with PET." Hum Brain Mapp **1**(1): 69-79.
- Friston, K., et al. (2013). "Analysing connectivity with Granger causality and dynamic causal modelling." Current Opinion in Neurobiology **23**(2): 172-178.
- Friston, K. J. (1994). "Functional and effective connectivity in neuroimaging: a synthesis." Hum Brain Mapp **2**(1-2): 56-78.
- Friston, K. J., et al. (2003). "Dynamic causal modelling." Neuroimage **19**(4): 1273-1302.
- Goebel, R., et al. (2001). "Sustained extrastriate cortical activation without visual awareness revealed by fMRI studies of hemianopic patients." Vision Res **41**(10): 1459-1474.

- Goebel, R., et al. (2003). "Investigating directed cortical interactions in time-resolved fMRI data using vector autoregressive modeling and Granger causality mapping." Magn Reson Imaging **21**(10): 1251-1261.
- Gordon, E. M., et al. (2012). "Effect of dopamine transporter genotype on intrinsic functional connectivity depends on cognitive state." Cereb Cortex **22**(9): 2182-2196.
- Granger, C. W. (1969). "Investigating causal relations by econometric models and cross-spectral methods." Econometrica: Journal of the Econometric Society: 424-438.
- Greicius, M. (2008). "Resting-state functional connectivity in neuropsychiatric disorders." Current opinion in neurology **21**(4): 424-430.
- Greicius, M. D., et al. (2003). "Functional connectivity in the resting brain: a network analysis of the default mode hypothesis." Proceedings of the National Academy of Sciences **100**(1): 253-258.
- Gu, X. and T. H. FitzGerald (2014). "Interoceptive inference: homeostasis and decision-making." Trends Cogn Sci **18**(6): 269-270.
- Guye, M., et al. (2008). "Imaging structural and functional connectivity: towards a unified definition of human brain organization?" Current opinion in neurology **21**(4): 393-403.
- Haller, S., et al. (2010). "Real-time fMRI feedback training may improve chronic tinnitus." European radiology **20**(3): 696-703.
- Hamilton, J. P., et al. (2011). "Modulation of subgenual anterior cingulate cortex activity with real-time neurofeedback." Hum Brain Mapp **32**(1): 22-31.
- Hampson, M., et al. (2006). "Brain connectivity related to working memory performance." The Journal of Neuroscience **26**(51): 13338-13343.
- Hanlon, C. A., et al. (2013). "Reduction of cue-induced craving through realtime neurofeedback in nicotine users: the role of region of interest selection and multiple visits." Psychiatry Research: Neuroimaging **213**(1): 79-81.
- Hare, T. A., et al. (2009). "Self-control in decision-making involves modulation of the vmPFC valuation system." Science **324**(5927): 646-648.
- Hartwell, K. J., et al. (2016). "Individualized real-time fMRI neurofeedback to attenuate craving in nicotine-dependent smokers." Journal of psychiatry & neuroscience: JPN **41**(1): 48.
- Hartwell, K. J., et al. (2013). "Real-time fMRI in the treatment of nicotine dependence: A conceptual review and pilot studies." Psychology of Addictive Behaviors **27**(2): 501.
- Hebb, D. O. (1949). "The Organization of Behavior. New York: Wiley & Sons."
- Herbert, B. M. and O. Pollatos (2014). "Attenuated interoceptive sensitivity in overweight and obese individuals." Eating behaviors **15**(3): 445-448.
- Hollmann, M., et al. (2012). "Neural correlates of the volitional regulation of the desire for food." International Journal of Obesity **36**(5): 648-655.
- Hollmann, M., et al. (2011). "Predicting decisions in human social interactions using real-time fMRI and pattern classification." PLoS One **6**(10): e25304.

- Hong, K.-S., et al. (2015). "Classification of prefrontal and motor cortex signals for three-class fNIRS-BCI." Neuroscience Letters **587**: 87-92.
- Horwitz, B. (2003). "The elusive concept of brain connectivity." Neuroimage **19**(2): 466-470.
- Hughes, J. R. (2007). "Autism: the first firm finding= underconnectivity?" Epilepsy & Behavior **11**(1): 20-24.
- Johnson, K. A., et al. (2012). "Intermittent "Real-time" fMRI feedback is superior to continuous presentation for a motor imagery task: a pilot study." Journal of Neuroimaging **22**(1): 58-66.
- Kanosue, K., et al. (2010). "Concepts to utilize in describing thermoregulation and neurophysiological evidence for how the system works." European journal of applied physiology **109**(1): 5-11.
- Karch, S., et al. (2015). "Modulation of Craving Related Brain Responses Using Real-Time fMRI in Patients with Alcohol Use Disorder." PLoS One **10**(7): e0133034.
- Khalsa, S. S., et al. (2009). "The pathways of interoceptive awareness." Nat Neurosci **12**(12): 1494-1496.
- Kim, S. and N. Birbaumer (2014). "Real-time functional MRI neurofeedback: a tool for psychiatry." Current opinion in psychiatry **27**(5): 332-336.
- Kirk, U., et al. (2011). "Interoception drives increased rational decision-making in meditators playing the ultimatum game." Front. Neurosci **5**(49).
- Kirsch, M., et al. (2015). "Real-time functional magnetic resonance imaging neurofeedback can reduce striatal cue-reactivity to alcohol stimuli." Addiction biology.
- Koralek, A. C., et al. (2012). "Corticostriatal plasticity is necessary for learning intentional neuroprosthetic skills." Nature **483**(7389): 331-335.
- Kotchoubey, B., et al. (2001). "Modification of slow cortical potentials in patients with refractory epilepsy: a controlled outcome study." Epilepsia **42**(3): 406-416.
- Koush, Y., et al. (2015). "Learning Control Over Emotion Networks Through Connectivity-Based Neurofeedback." Cereb Cortex.
- Koush, Y., et al. (2013). "Connectivity-based neurofeedback: dynamic causal modeling for real-time fMRI." Neuroimage **81**: 422-430.
- LaConte, S. M. (2011). "Decoding fMRI brain states in real-time." Neuroimage **56**(2): 440-454.
- LaConte, S. M., et al. (2007). "Real-time fMRI using brain-state classification." Hum Brain Mapp **28**(10): 1033-1044.
- Lang, E. W., et al. (2012). "Brain connectivity analysis: a short survey." Comput Intell Neurosci **2012**: 412512.
- Larson-Prior, L. J., et al. (2009). "Cortical network functional connectivity in the descent to sleep." Proceedings of the National Academy of Sciences **106**(11): 4489-4494.

- Lee, J.-H., et al. (2009). "Brain-machine interface via real-time fMRI: preliminary study on thought-controlled robotic arm." Neuroscience Letters **450**(1): 1-6.
- Lee, S., et al. (2011). "Detection of cerebral reorganization induced by real-time fMRI feedback training of insula activation: a multivariate investigation." Neurorehabil Neural Repair **25**(3): 259-267.
- Li, R., et al. (2012). "Attention-related networks in Alzheimer's disease: A resting functional MRI study." Hum Brain Mapp **33**(5): 1076-1088.
- Li, X., et al. (2013). "Volitional reduction of anterior cingulate cortex activity produces decreased cue craving in smoking cessation: a preliminary real-time fMRI study." Addiction biology **18**(4): 739-748.
- Linden, D. E., et al. (2012). "Real-time self-regulation of emotion networks in patients with depression." PLoS One **7**(6): e38115.
- Logothetis, N. K. (2008). "What we can do and what we cannot do with fMRI." Nature **453**(7197): 869-878.
- Logothetis, N. K., et al. (2001). "Neurophysiological investigation of the basis of the fMRI signal." Nature **412**(6843): 150-157.
- Logothetis, N. K. and B. A. Wandell (2004). "Interpreting the BOLD signal." Annu. Rev. Physiol. **66**: 735-769.
- Lohmann, G., et al. (2012). "Critical comments on dynamic causal modelling." Neuroimage **59**(3): 2322-2329.
- Lohmann, G., et al. (2013). "Response to commentaries on our paper: critical comments on dynamic causal modelling." Neuroimage **75**: 279-281.
- Lowel, S. and W. Singer (1992). "Selection of intrinsic horizontal connections in the visual cortex by correlated neuronal activity." Science **255**(5041): 209-212.
- Lutz, A., et al. (2009). "BOLD signal in insula is differentially related to cardiac function during compassion meditation in experts vs. novices." Neuroimage **47**(3): 1038-1046.
- Magri, C., et al. (2011). "Different LFP frequency bands convey complementary information about the BOLD signal." BMC Neuroscience **12**(Suppl 1): P204.
- Marks, D. F. (2015). "Homeostatic theory of obesity." Health Psychology Open **2**(1).
- Martin, L. E., et al. (2010). "Neural mechanisms associated with food motivation in obese and healthy weight adults." Obesity **18**(2): 254-260.
- Matthews, D., et al. (1985). "Homeostasis model assessment: insulin resistance and β -cell function from fasting plasma glucose and insulin concentrations in man." Diabetologia **28**(7): 412-419.
- Müller, R.-A., et al. (2011). "Underconnected, but how? A survey of functional connectivity MRI studies in autism spectrum disorders." Cereb Cortex **21**(10): 2233-2243.

Naito, M., et al. (2007). "A communication means for totally locked-in ALS patients based on changes in cerebral blood volume measured with near-infrared light." IEICE transactions on information and systems **90**(7): 1028-1037.

Neuper, C., et al. (2003). "Clinical application of an EEG-based brain-computer interface: a case study in a patient with severe motor impairment." Clinical neurophysiology **114**(3): 399-409.

Newton, A. T., et al. (2011). "Modulation of steady state functional connectivity in the default mode and working memory networks by cognitive load." Hum Brain Mapp **32**(10): 1649-1659.

O'Reilly, J. X., et al. (2012). "Tools of the trade: psychophysiological interactions and functional connectivity." Soc Cogn Affect Neurosci **7**(5): 604-609.

Pineda, J., et al. (2008). "Positive behavioral and electrophysiological changes following neurofeedback training in children with autism." Research in Autism Spectrum Disorders **2**(3): 557-581.

Pollatos, O., et al. (2007). "Brain structures mediating cardiovascular arousal and interoceptive awareness." Brain Res **1141**: 178-187.

Posse, S., et al. (2003). "Real-time fMRI of temporolimbic regions detects amygdala activation during single-trial self-induced sadness." Neuroimage **18**(3): 760-768.

Power, J. D., et al. (2011). "Functional network organization of the human brain." Neuron **72**(4): 665-678.

Rana, M., et al. (2013). "A toolbox for real-time subject-independent and subject-dependent classification of brain states from fMRI signals." Front Neurosci **7**: 170.

Raschpichler, M., et al. (2012). "Evaluating childhood obesity: magnetic resonance-based quantification of abdominal adipose tissue and liver fat in children." RoFo: Fortschritte auf dem Gebiete der Rontgenstrahlen und der Nuklearmedizin **184**(4): 324-332.

Ribeiro, A. S., et al. (2015). "Multimodal Imaging Brain Connectivity Analysis (MIBCA) toolbox." PeerJ **3**: e1078.

Rockstroh, B., et al. (1993). "Cortical self-regulation in patients with epilepsies." Epilepsy research **14**(1): 63-72.

Roebroeck, A., et al. (2011). "The identification of interacting networks in the brain using fMRI: model selection, causality and deconvolution." Neuroimage **58**(2): 296-302.

Rouse, C. H., et al. (1998). "The effect of body composition and gender on cardiac awareness." Psychophysiology **25**(4): 400-407.

Ruiz, S., et al. (2014). "Real-time fMRI brain computer interfaces: self-regulation of single brain regions to networks." Biological psychology **95**: 4-20.

Ruiz, S., et al. (2013). "Acquired self-control of insula cortex modulates emotion recognition and brain network connectivity in schizophrenia." Hum Brain Mapp **34**(1): 200-212.

Ruiz, S., et al. (2011). Brain network connectivity and behaviour enhancement: a fMRI-BCI study. 17th Annual Meeting of the Organization for Human Brain Mapping.

- Salvador, R., et al. (2005). "Neurophysiological architecture of functional magnetic resonance images of human brain." Cereb Cortex **15**(9): 1332-1342.
- Sato, J. R., et al. (2013). "Real-time fMRI pattern decoding and neurofeedback using FRIEND: an FSL-integrated BCI toolbox." PLoS One **8**(12): e81658.
- Scharnowski, F., et al. (2014). "Connectivity changes underlying neurofeedback training of visual cortex activity." PLoS One **9**(3): e91090.
- Scheinost, D., et al. (2013). "Orbitofrontal cortex neurofeedback produces lasting changes in contamination anxiety and resting-state connectivity." Translational psychiatry **3**(4): e250.
- Schmahmann, J. D., et al. (2007). "Association fibre pathways of the brain: parallel observations from diffusion spectrum imaging and autoradiography." Brain **130**(3): 630-653.
- Seth, A. K. (2013). "Interoceptive inference, emotion, and the embodied self." Trends Cogn Sci **17**(11): 565-573.
- Seth, A. K. (2014). The Cybernetic Bayesian Brain. Open MIND, Open MIND. Frankfurt am Main: MIND Group.
- Seth, A. K., et al. (2015). "Granger causality analysis in neuroscience and neuroimaging." The Journal of Neuroscience **35**(8): 3293-3297.
- Seth, A. K., et al. (2011). "An interoceptive predictive coding model of conscious presence." Front Psychol **2**: 395.
- Shibata, K., et al. (2011). "Perceptual learning incepted by decoded fMRI neurofeedback without stimulus presentation." Science **334**(6061): 1413-1415.
- Sitaram, R., et al. (2009). "Hemodynamic brain-computer interfaces for communication and rehabilitation." Neural networks **22**(9): 1320-1328.
- Sitaram, R., et al. (2014). "Volitional control of the anterior insula in criminal psychopaths using real-time fMRI neurofeedback: a pilot study." Front Behav Neurosci **8**: 344.
- Sitaram, R., et al. (2011). "Real-time support vector classification and feedback of multiple emotional brain states." Neuroimage **56**(2): 753-765.
- Sitaram, R., et al. (2012). "Acquired control of ventral premotor cortex activity by feedback training: an exploratory real-time FMRI and TMS study." Neurorehabil Neural Repair **26**(3): 256-265.
- Sitaram, R., et al. (2007). "Temporal classification of multichannel near-infrared spectroscopy signals of motor imagery for developing a brain-computer interface." Neuroimage **34**(4): 1416-1427.
- Smith, S. M. (2012). "The future of FMRI connectivity." Neuroimage **62**(2): 1257-1266.
- Smith, S. M., et al. (2009). "Correspondence of the brain's functional architecture during activation and rest." Proceedings of the National Academy of Sciences **106**(31): 13040-13045.

- Soekadar, S. R., et al. (2014). "Learned EEG-based brain self-regulation of motor-related oscillations during application of transcranial electric brain stimulation: feasibility and limitations." Front. Behav. Neurosci **8**(93): 10.3389.
- Song, H., et al. (2015). "Love-related changes in the brain: a resting-state functional magnetic resonance imaging study." Front Hum Neurosci **9**.
- Spilker, B., et al. (1969). "Visual evoked responses in subjects trained to control alpha rhythms." Psychophysiology **5**(6): 683-695.
- Stephan, K. E., et al. (2008). "Nonlinear dynamic causal models for fMRI." Neuroimage **42**(2): 649-662.
- Stephan, K. E., et al. (2010). "Ten simple rules for dynamic causal modeling." Neuroimage **49**(4): 3099-3109.
- Stephan, K. E., et al. (2009). "Tractography-based priors for dynamic causal models." Neuroimage **47**(4): 1628-1638.
- Stoeckel, L., et al. (2014). "Optimizing real time fMRI neurofeedback for therapeutic discovery and development." NeuroImage: Clinical **5**: 245-255.
- Stoeckel, L. E., et al. (2008). "Widespread reward-system activation in obese women in response to pictures of high-calorie foods." Neuroimage **41**(2): 636-647.
- Strehl, U., et al. (2006). "Self-regulation of slow cortical potentials: a new treatment for children with attention-deficit/hyperactivity disorder." Pediatrics **118**(5): e1530-e1540.
- Subramanian, L., et al. (2011). "Real-time functional magnetic resonance imaging neurofeedback for treatment of Parkinson's disease." The Journal of Neuroscience **31**(45): 16309-16317.
- Sulzer, J., et al. (2013). "Real-time fMRI neurofeedback: progress and challenges." Neuroimage **76**: 386-399.
- Sulzer, J., et al. (2013). "Real-time fMRI neurofeedback: Progress and challenges." Neuroimage **76**: 386-399.
- Thirion, B., et al. (2006). "Detection of signal synchronizations in resting-state fMRI datasets." Neuroimage **29**(1): 321-327.
- Turnip, A. and K.-S. Hong (2012). "Classifying mental activities from EEG-P300 signals using adaptive neural network." Int. J. Innov. Comp. Inf. Control **8**(9): 6429-6443.
- Turnip, A., et al. (2011). "Real-time feature extraction of P300 component using adaptive nonlinear principal component analysis." Biomed. Eng. Online **10**(1): 83.
- Van Buren, J. M. and M. Baldwin (1958). "The architecture of the optic radiation in the temporal lobe of man." Brain **81**(1): 15-40.
- van de Ven, V. G., et al. (2004). "Functional connectivity as revealed by spatial independent component analysis of fMRI measurements during rest." Hum Brain Mapp **22**(3): 165-178.
- Van Den Heuvel, M., et al. (2008). "Normalized cut group clustering of resting-state FMRI data." PLoS One **3**(4): e2001.

- Van Den Heuvel, M. P. and H. E. H. Pol (2010). "Exploring the brain network: a review on resting-state fMRI functional connectivity." European Neuropsychopharmacology **20**(8): 519-534.
- Veit, R., et al. (2012). "Using real-time fMRI to learn voluntary regulation of the anterior insula in the presence of threat-related stimuli." Soc Cogn Affect Neurosci **7**(6): 623-634.
- Wang, N., et al. (2013). "SACICA: A sparse approximation coefficient-based ICA model for functional magnetic resonance imaging data analysis." Journal of neuroscience methods **216**(1): 49-61.
- Weiskopf, N. (2012). "Real-time fMRI and its application to neurofeedback." Neuroimage **62**(2): 682-692.
- Weiskopf, N., et al. (2004). "Principles of a brain-computer interface (BCI) based on real-time functional magnetic resonance imaging (fMRI)." Biomedical Engineering, IEEE Transactions on **51**(6): 966-970.
- Weiskopf, N., et al. (2007). "Real-time functional magnetic resonance imaging: methods and applications." Magn Reson Imaging **25**(6): 989-1003.
- Weiskopf, N., et al. (2003). "Physiological self-regulation of regional brain activity using real-time functional magnetic resonance imaging (fMRI): methodology and exemplary data." Neuroimage **19**(3): 577-586.
- Wells, J. C. (2006). "The evolution of human fatness and susceptibility to obesity: an ethological approach." Biological Reviews **81**(2): 183-205.
- Wen, X., et al. (2012). "Causal interactions in attention networks predict behavioral performance." The Journal of Neuroscience **32**(4): 1284-1292.
- Weygandt, M., et al. (2013). "The role of neural impulse control mechanisms for dietary success in obesity." Neuroimage **83**: 669-678.
- Wiens, S. (2005). "Interoception in emotional experience." Current opinion in neurology **18**(4): 442-447.
- Wolpaw, J. R., et al. (2002). "Brain-computer interfaces for communication and control." Clinical neurophysiology **113**(6): 767-791.
- Woods, S. C., et al. (1998). "Signals that regulate food intake and energy homeostasis." Science **280**(5368): 1378-1383.
- Yoo, S.-S., et al. (2006). "Increasing cortical activity in auditory areas through neurofeedback functional magnetic resonance imaging." Neuroreport **17**(12): 1273-1278.
- Yoo, S. S., et al. (2008). "Neurofeedback fMRI-mediated learning and consolidation of regional brain activation during motor imagery." International journal of imaging systems and technology **18**(1): 69-78.
- Young, K. D., et al. (2014). "Real-time FMRI neurofeedback training of amygdala activity in patients with major depressive disorder." PLoS One **9**(2): e88785.
- Zhen, Z., et al. (2007). Partial correlation mapping of brain functional connectivity with resting state fMRI. Medical Imaging, International Society for Optics and Photonics.

Zilverstand, A., et al. (2015). "fMRI neurofeedback facilitates anxiety regulation in females with spider phobia." Front Behav Neurosci **9**.

Zotev, V., et al. (2011). "Self-regulation of amygdala activation using real-time fMRI neurofeedback." PLoS One **6**(9): e24522.

Presentation of own contributions to papers and manuscripts

(Darstellung des Eigenanteils bei Gemeinschaftsarbeiten nach §9 para. 2)

Study 1: Volitional regulation of brain responses to food stimuli in overweight and obese subjects: A real-time fMRI feedback study. *M.S. Spetter**, *R. Malekshahi**, *N. Birbaumer*, *M Lührs*, *A. van der Veer*, *K. Scheffler*, *S. Spuckti*, *H.Preissl*, *R. Veit*, and *M. Hallschmid*. *Appetite* 112 (2017) 188-195.

***M.S. Spetter and R. Malekshahi equally contributed to this work as first author.**

Conceived, and designed the experiment: M.S. Spetter, R. Malekshahi, N. Birbaumer, H. Preissl, M. Hallschmid, and R. Veit. I mainly contributed to designing neurofeedback sessions, and pre/post transfer sessions with M.S. Spetter, and R. Veit.

Real-time fMRI technical setup and programming: designing optimal feedback, programming stimulus presentations codes, designing, implementing, and programming neurofeedback setup: R. Malekshahi. Designing optimal plugins together with M. Lührs.

Performed the experiment: M.S. Spetter, and R. Veit.

Analyzed the data: R. Malekshahi, M.S. Spetter, and R. Veit.

Wrote the paper: M.S. Spetter, R. Malekshahi, R. Veit, N. Birbaumer, H. Preissl, and M. Hallschmid. My contribution here was writing methods corresponding to neurofeedback sessions, and their offline/online data processing, and online neurofeedback setup. Writing all results corresponding to neurofeedback training' effect size, offline/online connectivity, and pre/post transfer sessions. Writing part of discussion. Correction/improvement all parts of the manuscript.

Study 2: Simultaneous learned regulation of anterior insula and somatosensory cortex improves interoceptive but not exteroceptive awareness. *R. Malekshahi*, *M.S. Spetter*, *N. Birbaumer*, and *A. Caria*. (Will be submitted to NeuroImage). It was presented as poster in OHBM 2016.

Conceived, and designed the experiment: R. Malekshahi, and A. Caria.

Real-time fMRI setup design: R. Malekshahi, and A. Caria.

Programming stimulus presentations codes, implementing, and programming neurofeedback setup: R. Malekshahi.

Performed the experiment: R. Malekshahi (all sessions), M.S. Spetter (half of sessions), and A. Caria (half of sessions).

Analyzed the data: R. Malekshahi, with support from A. Caria.

Wrote the paper: R. Malekshahi, A. Caria, M.S. Spetter, and N. Birbaumer. I wrote abstract, introduction, material and methods, results, and discussion. N. Birbaumer corrected all parts of the manuscript. M.S. Spetter, and A. Caria corrected the introduction.

Study 3: Self-Regulation of Anterior Insula with Real- Time fMRI and Its Behavioral Effects in Obsessive-Compulsive Disorder: A Feasibility Study. *K. Buyukturkoglu, H. Roettgers, J. Sommer, M. Rana, L. Dietzsch, E.B. Arikan, R. Veit, R. Malekshahi, T. Kircher, N. Birbaumer, R. Sitaram, S. Ruiz.* Published in PLOS ONE, August 24, 2015.

Conceived and designed the experiments: KB RS SR JS MR HR NB. Performed the experiments: KB JS LD EA. Analyzed the data: KB JS LD EA RV R. Malekshahi. Contributed reagents/materials/analysis tools: KB JS RS SR TK MR. Wrote the paper: KB RS SR JS TK NB.

I contributed to analysing the neurofeedback and skin conductance data. I also contributed in programming stimulus presentation codes.

Volitional regulation of brain responses to food stimuli

in overweight and obese subjects: a real-time fMRI feedback study

Maartje S. Spetter^{a*}, Rahim Malekshahi^{a,b*}, Niels Birbaumer^{a,c,d}, Michael Lührs^{e,f}, Albert H. van der Veer^a, Klaus Scheffler^{g,h}, Sophia Spuckti^a, Hubert Preissl^{i-m}, Ralf Veit^{a,h,i,j*}, Manfred Hallschmid^{a,i,j*}

^aInstitute of Medical Psychology and Behavioral Neurobiology, University of Tübingen, Germany;

^bGraduate School of Neural & Behavioral Sciences, International Max Planck Research School, Tübingen, Germany;

^cOspedale San Camillo, IRCCS, Venice, Italy;

^dWyssCenter for Bio and Neuroengineering, Geneva, Switzerland;

^eDepartment of Cognitive Neuroscience, Maastricht University, Netherlands;

^fBrain Innovation B.V., Maastricht, Netherlands;

^gHigh-Field Magnetic Resonance Center, Max Planck Institute for Biological Cybernetics, Tübingen, Germany;

^hDepartment of Biomedical Magnetic Resonance, University of Tübingen, Germany;

ⁱInstitute for Diabetes Research and Metabolic Diseases (IDM) of the Helmholtz Center Munich at the University of Tübingen, Germany;

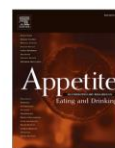
^jGerman Center for Diabetes Research (DZD e.V.), Tübingen, Germany;

^kDepartment of Internal Medicine, Division of Endocrinology, Diabetology, Angiology, Nephrology and Clinical Chemistry, Eberhard Karls University Tübingen, Tübingen, Germany;

^lInstitute of Pharmaceutical Sciences, Department of Pharmacy and Biochemistry, Eberhard Karls Universität Tübingen, Tübingen, Germany (Auf der Morgenstelle 8, 72076 Tübingen);

^mInterfaculty Center for Pharmacogenomics and Pharma Research at the Eberhard Karls University Tübingen, Tübingen, Germany

**These authors contributed equally to this work.*



Volitional regulation of brain responses to food stimuli in overweight and obese subjects: A real-time fMRI feedback study



Maartje S. Spetter^{a,*,1}, Rahim Malekshahi^{a,b,1}, Niels Birbaumer^{a,c,d}, Michael Lührs^{e,f},
Albert H. van der Veer^a, Klaus Scheffler^{g,h}, Sophia Spuckti^a, Hubert Preissl^{i,j,k,l,m},
Ralf Veit^{a,h,i,j,1}, Manfred Hallschmid^{a,i,j,**,1}

^a Department of Medical Psychology and Behavioral Neurobiology, University of Tübingen, Germany

^b Graduate School of Neural & Behavioral Sciences, International Max Planck Research School, Tübingen, Germany

^c Ospedale San Camillo, IRCCS, Venice, Italy

^d WyssCenter for Bio and Neuroengineering, Geneva, Switzerland

^e Department of Cognitive Neuroscience, Maastricht University, The Netherlands

^f Brain Innovation B.V., Maastricht, The Netherlands

^g High-Field Magnetic Resonance Center, Max Planck Institute for Biological Cybernetics, Tübingen, Germany

^h Department of Biomedical Magnetic Resonance, University of Tübingen, Germany

ⁱ Institute for Diabetes Research and Metabolic Diseases (IDM) of the Helmholtz Center Munich at the University of Tübingen, Germany

^j German Center for Diabetes Research (DZD e.V.), Tübingen, Germany

^k Department of Internal Medicine, Division of Endocrinology, Diabetology, Angiology, Nephrology and Clinical Chemistry, University of Tübingen, Germany

^l Institute of Pharmaceutical Sciences, Department of Pharmacy and Biochemistry, Interfaculty Center for Pharmacogenomics and Pharma Research, University of Tübingen, Germany

^m Institute for Diabetes and Obesity, Helmholtz Diabetes Center, Helmholtz Center Munich, German Research Center for Environmental Health, Neuherberg, Germany

ARTICLE INFO

Article history:

Received 5 October 2016

Received in revised form

23 December 2016

Accepted 21 January 2017

Available online 25 January 2017

Keywords:

Overweight

Obesity

Neurofeedback

Real-time functional magnetic resonance imaging

Dorsolateral prefrontal cortex

Ventromedial prefrontal cortex

ABSTRACT

Obese subjects who achieve weight loss show increased functional connectivity between dorsolateral prefrontal cortex (dlPFC) and ventromedial prefrontal cortex (vmPFC), key areas of executive control and reward processing. We investigated the potential of real-time functional magnetic resonance imaging (rt-fMRI) neurofeedback training to achieve healthier food choices by enhancing self-control of the interplay between these brain areas. We trained eight male individuals with overweight or obesity (age: 31.8 ± 4.4 years, BMI: 29.4 ± 1.4 kg/m²) to up-regulate functional connectivity between the dlPFC and the vmPFC by means of a four-day rt-fMRI neurofeedback protocol including, on each day, three training runs comprised of six up-regulation and six passive viewing trials. During the up-regulation runs of the four training days, participants successfully learned to increase functional connectivity between dlPFC and vmPFC. In addition, a trend towards less high-calorie food choices emerged from before to after training, which however was associated with a trend towards increased covertly assessed snack intake. Findings of this proof-of-concept study indicate that overweight and obese participants can increase functional connectivity between brain areas that orchestrate the top-down control of appetite for high-calorie foods. Neurofeedback training might therefore be a useful tool in achieving and maintaining weight loss.

© 2017 Elsevier Ltd. All rights reserved.

1. Introduction

The prevalence of overweight and obesity has increased rapidly in less than half a century and the spread of many comorbidities including type 2 diabetes and cardiovascular diseases has followed suit (Finkelstein, Trogon, Cohen, & Dietz, 2009). Obesity is strongly associated with increased intake of high-calorie and energy-dense palatable food (Berthoud & Zheng, 2012).

* Corresponding author.

** Corresponding author. Department of Medical Psychology and Behavioral Neurobiology, University of Tübingen, Otfried-Müller-Straße 25, 72076 Tübingen, Germany.

E-mail addresses: maartje.spetter@uni-tuebingen.de (M.S. Spetter), manfred.hallschmid@uni-tuebingen.de (M. Hallschmid).

¹ These authors contributed equally to this work.

Accordingly, obese in comparison to lean individuals display altered activity of brain areas involved in reward processing, eating motivation, and cognitive control, which may contribute to the persistence of elevated body weight (Carnell, Gibson, Benson, Ochner, & Geliebter, 2012; Ng, Stice, Yokum, & Bohon, 2011; Val-Laillet et al., 2015). These insights rely on neuroimaging as an effective means of investigating the neural networks underlying the regulation of appetite and food preference in normal-weight and overweight subjects (Carnell, Benson, Pryor, & Driggin, 2013). Neuroimaging has moreover turned out to be a potential non-invasive neurotherapeutic tool in the treatment of disorders such as depression (Linden et al., 2012) and eating disorders (Bartholdy, Musiat, Campbell, & Schmidt, 2013). Thus, recent experiments have shown that individuals can learn to voluntarily control their brain activity with the help of real-time functional magnetic resonance imaging (rt-fMRI) providing online feedback of neural activity (Weiskopf, 2012).

Since rt-fMRI paradigms have been found to trigger intended behavioral effects (Caria, Sitaram, Veit, Begliomini, & Birbaumer, 2010) and factors critical for food intake control like self-regulation and impulse control are suitable targets of neurofeedback (Birbaumer, Ruiz, & Sitaram, 2013; Schlogl, Horstmann, Villringer, & Stumvoll, 2016; Val-Laillet et al., 2015), respective interventions might be a promising avenue to the modulation of eating behavior (Frank et al., 2012; Ihssen, Sokunbi, Lawrence, Lawrence, & Linden, 2016). In this context, areas that process reward or mediate inhibitory control can be assumed to be of major relevance (Val-Laillet et al., 2015). Overeating in obese subjects may be conceptualized to stem from hyper-responsivity of reward-processing structures or, rather, from diminished sensitivity triggering surplus calorie intake (Kenny, 2011). Therefore, targeting reward-processing areas by neurofeedback might bear the risk of unintended effects, whereas impairments in impulse control and decision making have been conclusively observed in obese subjects (Rangel, 2013). Neuroimaging studies have indeed indicated that the interplay between the dorsolateral and the ventromedial prefrontal cortices (dlPFC and vmPFC) may be of particular significance in this regard. While the vmPFC is assumed to encode the valence of a stimulus (Hare, O'Doherty, Camerer, Schultz, & Rangel, 2008), the dlPFC rather mediates self-control over consummatory behaviors (Hollmann et al., 2012). Functional connectivity between dlPFC and vmPFC is increased during exposure to food pictures when healthy individuals are satiated as compared to being fasted (Thomas et al., 2015). Accordingly, healthy food choice is positively related to functional connectivity between dlPFC and vmPFC, and dlPFC activity is increased when participants exercise self-control (Hare, Camerer, & Rangel, 2009). In line with these results, individuals who show greater diet-induced weight loss than others exhibit stronger dlPFC-vmPFC functional connectivity (Weygandt et al., 2013). Improving the connectivity between these brain areas may therefore normalize eating behavior and support weight loss in obese subjects. In the present proof-of-principle study we investigated whether rt-fMRI neurofeedback training enables overweight and obese subjects to increase dlPFC-vmPFC functional connectivity during visual stimulation with unhealthy, high-calorie food stimuli and, if so, how such changes relate to food choices and eating behavior.

2. Methods

2.1. Participants

Eight healthy male participants with overweight or obesity participated in the study (age: 31.8 ± 4.4 years, BMI: 29.4 ± 1.4 kg/m²). Exclusion criteria included weight loss exceeding 5 kg within 3

months before participation, eating disorders, neurological or psychiatric diseases, use of medication, and contraindications for MRI. Prior to participation subjects were informed about the procedure and gave written informed consent. The study protocol was approved by the local Ethics Committee and in accordance with the Declaration of Helsinki.

2.2. Experimental protocol

Within four weeks, subjects participated in six sessions separated by at least two days, a pre-training session in the first week, four neurofeedback training sessions in the second and third week, and one post-training session in the fourth week. Sessions took place in the late morning after at least two hours of post-breakfast fasting.

2.2.1. Pre-training

In the pre-training session, individual regions of interest (ROI) for neurofeedback training (dlPFC and vmPFC) were determined (Hare et al., 2009) (Supplementary Fig. S1). Participants first rated 90 food images (Hare et al., 2009) on tastiness (1 = not tasty at all, 2 = not tasty, 3 = neutral, 4 = tasty, 5 = very tasty) and healthiness (1 = very unhealthy, 2 = unhealthy, 3 = neutral, 4 = healthy, 5 = very healthy) in separate sessions on 5-point scales while they were scanned. One item that was rated as neutral both regarding tastiness and healthiness was selected as the reference image for the subsequent choice task. (If necessary, a tastiness rating of 4 was taken to represent relative neutrality). In that task, participants first saw their personalized reference image and were told that in each of the following trials they would have to indicate if they preferred to eat the food item presented in the trial or their reference food (Hare et al., 2009). This procedure yielded healthy, neutral and unhealthy choices. Food images were displayed for 3 s on a computer screen (Presentation, Neurobehavioral Systems Inc, www.neurobs.com) and ratings during the scan were given via a fMRI-compatible button box (www.curdes.com).

2.2.2. Training sessions

In the training sessions, participants learned to self-control dlPFC-vmPFC functional connectivity. On the first neurofeedback day, the idea of neurofeedback (self-regulation) was explained and suggestions to control the specific brain areas were given (reappraisal techniques (Greer, Trujillo, Glover, & Knutson, 2014); see Supplementary File 1). Subsequently the participant was placed in the scanner and underwent three training runs of 9 min each (see Fig. 1 for neurofeedback set-up). Each run consisted of 6 trials of 30 s up-regulation of functional connectivity between dlPFC and vmPFC and 30 s of passive viewing, including 12 s of rest in-between and between trials. During up-regulation and viewing, an appetitive high-calorie food picture (rated high in tastiness and low in healthiness in the rating task of the pre-training session), two black thermometers on the right and respectively left side of the food image (providing feedback on functional connectivity) and two additional symbols indicating the type of the trial (upward arrow during up-regulation, plus sign during passive viewing) were displayed. The thermometer bars included ten levels which turned from black to grey in an upward, incremental fashion whenever functional connectivity between the ROIs increased by 0.1. Only increases in functional connectivity were fed back to the participants, otherwise the thermometer bars were displayed as empty. Participants received feedback only during up-regulation trials. During passive viewing, participants were instructed to relax, and the same visual cues as during up-regulation were shown without updating the feedback thermometers. During rest, a cross appeared. Stimuli were displayed on a screen through a computer

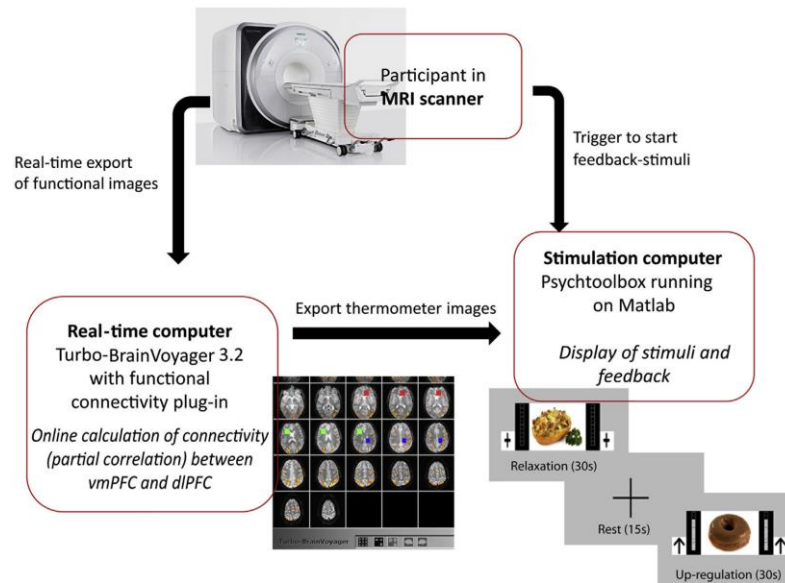


Fig. 1. Setup of rt-fMRI neurofeedback training. BOLD signals were acquired via fMRI scans, processed in real-time and presented as visual feedback on the stimulation computer. Visual feedback was provided in the form of thermometer bars indicating increases in functional connectivity between the dorsolateral prefrontal cortex (dlPFC) and the ventromedial prefrontal cortex (vmPFC; partial correlation). Visual feedback was updated only during up-regulation phases (cued by arrows appearing next to the thermometer bars). During the up-regulation phases participants were instructed to increase the thermometer bars, whereas during passive viewing and rest phases, participants were instructed to relax and no feedback was provided.

interface and run with the program Psych-toolbox on Matlab (version 17). Procedures were identical during all four neurofeedback days. After the training sessions, subjects were advised to use in real-life conditions of food choice the strategies they assumed to have worked during feedback training.

2.2.3. Post-training

During post-training, all procedures of the pre-training were repeated. Psychometric ratings were obtained in all sessions. At pre- and post-training, food preferences were determined and snack intake was covertly assessed (see 2.4, Behavioral Assessments).

2.3. Neuroimaging assessments

2.3.1. fMRI data acquisition

All scans were performed with a 3-Tesla PRISMA Siemens scanner equipped with a 20-channel head coil at the Max Planck Institute of Biological Cybernetics, High-Field MR Center, Tübingen, Germany. T1-weighted anatomical scans were acquired with the following parameters: TR/TE = 2300/4.18 ms, flip angle = 9°, FOV = 256 × 175 mm, 176 axial slices, and voxel size = 1 × 1 × 1 mm³ (MPRAGE GRAPPA). Functional images at pre- and post-training were acquired with a single-shot echo-planar imaging (EPI) sequence with the following parameters: repetition time TR = 2500 ms, flip angle = 70°, echo time TE = 30 ms, matrix size = 64 × 64, and 40 slices (thickness = 3 mm), resulting in a voxel size of 3 × 3 × 3. Functional images in the neurofeedback training sessions (comprising 356 scans) were acquired with a

single-shot EPI sequence with a short repetition time TR = 1500 ms, flip angle of 79°, echo time TE = 30 ms, matrix size = 64 × 64, and 20 slices (thickness = 4 mm), resulting in a voxel size of 3 × 3 × 4. In order to assure scanning the same slices (and hence ROIs) in the brain during the different training days of each participant, we used the landmark-based automated positioning system (AutoAlign Head using AC-PC line). Positioning parameters were saved at the beginning of the pre-training and the neurofeedback training sessions.

2.3.2. fMRI data preprocessing and analyses

All functional imaging data were pre-processed and analysed using SPM 12 (Wellcome Department of Cognitive Neurology, London, UK) run with MATLAB 2013 (The Mathworks Inc, Natick, MA) and the WFU Pickatlas-tool. Images were first motion-corrected and realigned. The high-resolution T1 image was then co-registered to the mean image of the EPI series for each participant. Segmentation was performed to compute spatial transformation parameters that were used to normalize the structural (1 × 1 × 1) and the functional (3 × 3 × 3.5) scans to a standard Montreal Neurological Institute (MNI) template. Normalized images were spatially smoothed with a 9 mm full-width half-maximum Gaussian kernel. Low frequency drifts were removed using a high-pass filter with 128 s cut off. After functional data preprocessing, a general linear model was adopted to perform first-level statistical analysis.

2.3.3. ROI analyses

For ROI determination the functional images obtained during

tastiness and healthiness ratings and the choice task (see above) were pre-processed and analysed. For both tasks separate GLM analyses with two regressors representing mean activation and covariation with the individual ratings (parametric modulation) were performed. Significant clusters within the vmPFC mask (based on Hare et al., 2009) that showed a positive covariation with the individual tastiness ratings were selected to define ROI 1. In the choice task two regressors were defined, i.e., healthy choice (selection of a low-calorie food) and unhealthy choice (high-calorie item), resulting in the contrast image healthy vs. unhealthy choice. ROI 2 was determined by comparing brain activity within a dlPFC mask (covering Brodmann areas 9 and 46) during healthy and unhealthy choices (Hare, Schultz, Camerer, O'Doherty, & Rangel, 2011). A rectangular box (comprising 6×6 voxels) centered on the individual peak voxels covering three slices was selected to represent each of the two ROI. In all models, the six movement parameters from the corresponding sessions were added as covariates of no interest to correct for motion-related variance. Brain activation determining the ROI was considered significant when exceeding a threshold of $P < 0.005$ uncorrected on an individual level (see Supplementary Fig. S1). In the post-training session participants underwent the same tasks as outlined above, this time without determining the ROI for neurofeedback training.

2.3.4. Analyses of neurofeedback training results

For the whole-brain analysis of neurofeedback training data, a design matrix was constructed for all days and sessions using up-regulation and passive viewing as separate regressors. Conditions were modelled with a canonical hemodynamic response. For each participant contrast images were created for up-regulation versus viewing for each session on each day. Contrast images were then entered into a second-level full factorial design with the factors day \times run to allow population-level inferences. A threshold of $P < 0.05$ Family-wise-error (FWE) was considered as significant brain activation.

2.3.5. Online analysis of functional connectivity

During the neurofeedback sessions, all functional images were analysed with Turbo Brain Voyager (TBV; Version 3.2; Brain innovation, Maastricht, Netherlands). The MR images were exported in real-time from the MRI console computer to a computer running TBV. To avoid T1 saturation effects the first 10 images were excluded. Real-time motion correction was achieved by aligning all functional images to the first recorded volume in the first session; images in all other sessions were aligned accordingly. Motion corrected functional images were then spatially smoothed by a kernel of 9 mm. Incoming images were used for calculating functional connectivity using partial correlations (plugin TBV, Version 3.2; Brain innovation, Maastricht, Netherlands) between the mean time courses within individually selected ROI in the vmPFC, dlPFC, and white matter (parietal lobes) as a reference area to adjust for global signal changes. Partial correlations were used to regress out any global fluctuations or unwanted movement artefacts that may not have been corrected by pre-processing algorithms. Time windows of 12 s including 8 data points were used to calculate partial correlations. Feedback was updated at every repetition time. In subsequent analyses the online connectivity values were compared between runs and sessions by means of aligned rank transformation and a nonparametric analysis of variance on repeated measures (R-version of ARTool). Post-hoc Tukey-Kramer tests were applied for single-step multiple comparisons.

2.3.6. Offline analysis of functional connectivity

Offline connectivity analysis was performed using CONN toolbox (version v15 <http://www.nitrc.org/projects/conn>)

implemented in SPM12. Functional connectivity was determined by evaluating the temporal correlation between seed regions as well as between each seed and all remaining voxels in the brain. Seeds were left and right dlPFC and vmPFC (Weygandt et al., 2013). Subsequently, an additional control analysis was performed that included the amygdala as a seed to investigate connectivity changes in emotion-processing networks. Spheres of 6 mm radius centered at the most significant voxel were imported for connectivity analyses. Before computing connectivity, confounds from blood oxygen level-dependent (BOLD) signals from white matter, cerebrospinal fluid, estimated subject motion parameters, and all main task effects were removed by linear regression analysis. A threshold of $P < 0.05$ (FWE-corrected) was considered significant.

2.4. Behavioral assessments

2.4.1. Rating tasks

In each session, participants gave hunger- and mood-related ratings on 0–100 mm visual analogue scales (VAS). At pre- and post-training, tastiness and healthiness of food items were rated on 5 point-scales. In a choice task, participants had to indicate preferred food items, resulting in healthy, unhealthy high-calorie, and neutral choices.

2.4.2. Assessment of calorie intake

For the covert investigation of snack intake, three plates were placed on a table containing snacks which were different in taste but roughly comparable in calorie content and macronutrient composition (Higgs, Williamson, & Atwood, 2008; Ott et al., 2013). They were labelled snack A, B, and C, respectively. The three types were, "TUC Cracker Classic" (salty taste; Griesson-de Beukelaer, Polch, Germany, 488 kcal/100 g), "Rice Waffles" (bland taste; Continental Bakeries B.V., Dordrecht, The Netherlands, 389 kcal/100 g), and "Double Chocolate Cookies" (sweet taste; EDEKA, Hamburg, Germany, 503 kcal/100 g), all broken down into bite-sized pieces. Of each variety a considerable amount could be eaten without the plates appearing empty, to ensure that participants would not restrict snack intake based on whether the experimenter could see how much had been consumed. In addition, a glass of water was provided. The participant was instructed to taste and rate each type of cookie on a visual analogue scale assessing palatability, sweetness and saltiness, anchored at 0 (not at all) and 10 cm (very palatable/sweet/salty). The importance of giving accurate ratings was emphasized and participants were informed that during and after completion of the rating task they could eat as many snacks as they liked because any remaining snacks would be discarded, and were left alone for 10 min. Snack intake was covertly measured by weighing before and after the test without awareness of the participant.

2.4.3. Statistical analyses

Statistical analyses of behavioral data were based on repeated-measures ANOVA (SPSS 22.0) and post-hoc, paired t-tests ($P < 0.05$, Bonferroni-corrected). Ratings and snack intake were analysed by repeated-measure ANOVAs with the within-subject factor "time point". Healthiness and tastiness ratings of food pictures were analysed by 2×2 repeated-measure ANOVA with the factors "time point" (pre-vs. post-training) and "calorie" (high vs. low). In addition, the percentages of healthy and unhealthy food items chosen during the choice task before and after the training sessions were analysed by repeated-measures ANOVA. Post-hoc, paired t-tests were used to specify comparisons ($P < 0.05$, Bonferroni-corrected for multiple comparisons). Data are presented as means \pm SEM.

3. Results

3.1. Functional connectivity

Collapsed across all four training days, participants successfully increased dlPFC-vmPFC functional connectivity across the three consecutive runs ($F(2,14) = 5.69$, $P = 0.01$), yielding increased functional connectivity during up-regulation in run 3 compared to run 1 ($P < 0.05$; Fig. 2A). In contrast, there was no respective change during passive viewing runs ($F(2,14) = 1.76$, $P = 0.22$). Across the four individual training days, there was no incremental increase in functional connectivity ($F(3,21) = 1.06$, $P = 0.31$; see [Supplementary Fig. S2](#)). In dlPFC seed-based offline analyses, an increase in functional connectivity to the vmPFC was found across all days and runs during up-regulation compared to viewing (FWE-corrected $P < 0.05$; Fig. 2B). Respective analyses with amygdala as a seed did not yield differences between up-regulation and passive viewing.

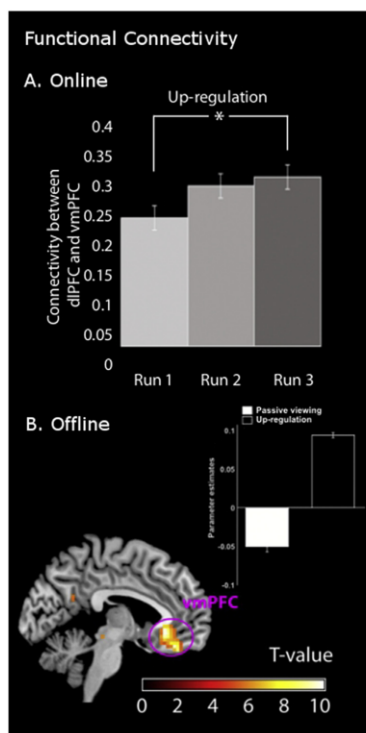


Fig. 2. Effects of rt-fMRI up-regulation training on functional connectivity. (A) Offline analysis of functional connectivity. The dorsolateral prefrontal cortex (dlPFC) was selected as a seed in the whole brain seed-to-voxel analysis. The ventromedial prefrontal cortex (vmPFC) was the only region to show significant connectivity with the dlPFC across all days and runs when up-regulation vs. passive viewing were compared. T-value was thresholded at $P < 0.05$ (FWE-corrected). (B) Online connectivity analysis. Changes in dlPFC-vmPFC functional connectivity assessed online during up-regulation. During up-regulation runs 1–3, a significant increase in connectivity emerged.

3.2. Regional activation

During up-regulation of functional connectivity, activity of bilateral insula/inferior frontal gyrus (IFG), left and right dlPFC and bilateral striatum was increased compared to viewing (FWE-corrected $P < 0.05$; Fig. 3A and Table 1). In contrast, viewing did not lead to any significant activation compared to up-regulation. Comparing the first to the fourth training day, increased activity of the right dlPFC (up-regulation vs. viewing) was observed (FWE-corrected $P < 0.05$), while dlPFC activity during viewing was not changed. We did not observe significant differences in vmPFC activity between up-regulation and passive viewing (see Fig. 3B for dlPFC and vmPFC effect size during up-regulation).

3.3. Behavioral results

In the food choice task, a trend towards less high-calorie food choices emerged from pre- (51%) to post-training (40%; $P = 0.095$; $F(1,7) = 3.67$, $P = 0.097$ for Time). Hunger, fullness, satiety and appetite ratings remained unchanged (all $P > 0.1$) while fear ($F(1,7) = 7.89$, $P = 0.026$) and agitation ($F(1,7) = 7.47$, $P = 0.029$) ratings declined across training sessions. Ratings of tastiness and healthiness of foods presented in the scanner did not change (all $P > 0.71$). From before to after training, a trend towards increased snack intake emerged ($F(1,7) = 4.19$, $P = 0.08$). See [Supplementary Table S1](#) for detailed behavioral results and [Table S2](#) for an overview of applied up-regulation strategies.

4. Discussion

We demonstrate that overweight and obese male subjects can up-regulate functional connectivity between dlPFC and vmPFC during rt-fMRI neurofeedback training. Moreover, we found increased activation in the dlPFC and IFG/bilateral insula during active up-regulation compared to viewing of food pictures. These effects were associated with a trend towards less high-calorie food choices but also with a tendency to increased actual food intake. The results of our proof-of-concept study are the first to indicate that neurofeedback training may enable subjects with increased body weight who are exposed to appetitive food stimuli to effectively modulate the activity of brain areas that process dietary self-control (Hare et al., 2009).

Functional connectivity between dlPFC and vmPFC has been linked to reward-related decisions (Chen, Jimura, White, Maddox, & Poldrack, 2015) both regarding food (Hare et al., 2009; Hare, Malmaud, & Rangel, 2011) and monetary reward (Hare, Hakimi, & Rangel, 2014). Accordingly, it has been proposed that dlPFC activation mediates volitional control over reward value signals processed by the vmPFC (Hare et al., 2014; Hare et al., 2009; Hare et al., 2011; Weygandt et al., 2013). Responsivity of the vmPFC changes in dependence of dlPFC input when participants focus on health aspects of a food (Hare et al., 2011), and the interplay between both areas may reflect food-related impulse control (Weygandt et al., 2013). Our participants with overweight or obesity were able to up-regulate dlPFC-vmPFC functional connectivity, but there was no additional effect of the four consecutive training days. This pattern might indicate that the training effect does not persist between sessions or that only a higher number of training sessions might induce incremental effects. Corresponding rt-fMRI neurofeedback interventions in depressive patients aiming at brain areas that process positive emotions yielded successful up-regulation of prefrontal and insular areas which, notably, also emerged across the three respective runs but not the four training days (Linden et al., 2012). These findings underline that the mechanisms behind the successful acquisition of volitional control of brain

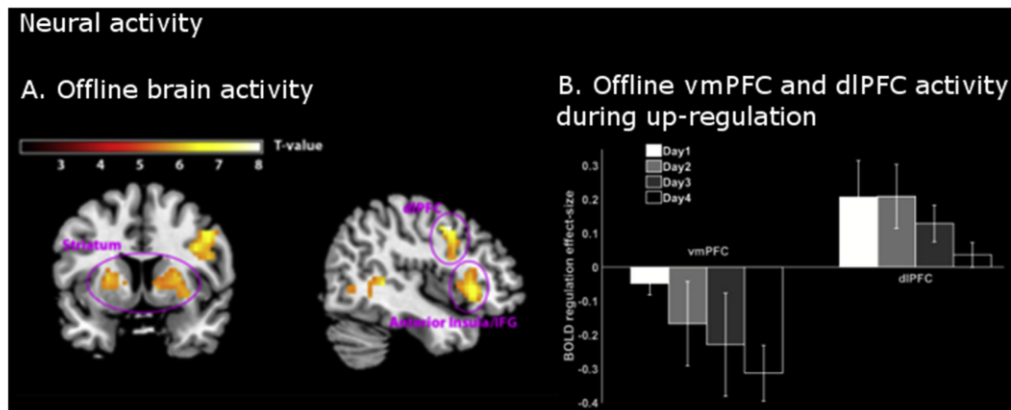


Fig. 3. Effects of rt-fMRI up-regulation training on neural activity. (A) Offline analysis of brain activity. Brain regions with increased responses during up-regulation as compared to passive viewing are indicated by activation maps of up-regulation vs. passive viewing collapsed across all days and all runs. Left panel, activation in bilateral striatum; right panel, activation in bilateral anterior insula/inferior frontal gyrus (IFG) and dlPFC. T-value was thresholded at $P < 0.05$ (FWE-corrected). (B) Offline analysis of BOLD effect size of vmPFC and dlPFC activity during up-regulation depicted per day.

Table 1
Up-regulation of functional connectivity compared to passive viewing.

Brain region	Peak voxel coordinates			z-score
	x	y	z	
R dlPFC	45	5	43	5.7
	39	8	28	5.0
	48	8	22	4.8
L dlPFC	-42	2	43	4.7
R striatum	24	20	7	5.45
L striatum	-24	17	7	5.1
	-9	2	10	4.7
R IFG/Insular cortex	36	26	4	5.3
	48	20	1	5.3
L IFG/Insular cortex	-36	20	-2	4.8
R Mid/Superior temporal gyrus	54	-43	7	5.5
	66	-37	25	5.2
	60	-31	40	4.8
	48	-67	1	4.6
R Occipital superior cortex	30	-73	19	5.4

Contrasts between up-regulation and viewing were calculated using second-level GLM analyses. Reported clusters were thresholded at $P < 0.05$, FWE-corrected with a cluster extent threshold $k > 10$ voxels. Voxel coordinates are given in MNI space. dlPFC, dorsolateral prefrontal cortex; IFG, inferior frontal gyrus.

activation patterns should be scrutinized in studies focusing on methodological aspects of neurofeedback training. They might also unravel the nature of respective learning effects and how they can be optimized on an individual level (Sulzer et al., 2013).

Against the background of previous studies suggesting that local BOLD regulation modulates functional connectivity (Lee, Kim, & Yoo, 2012; Ruiz, Buyukturkoglu, Rana, Birbaumer, & Sitaram, 2013), we were particularly interested in whether increases in functional connectivity are associated with changes in local neural activation. During up-regulation vs. passive viewing, we observed enhanced activation of dlPFC, IFG/insula and striatum, i.e., key areas of food intake regulation (Carnell et al., 2012; Val-Laillet et al., 2015), in particular on the first training day. Fittingly, enhanced self-control is associated with increased dlPFC activity that modulates vmPFC activation (Hare et al., 2009). Insular activity is a regular concomitant of brain self-regulation (Emmert et al., 2016), and

EEG feedback training to reduce food craving is associated with increased activation of the insula (Imperatori et al., 2016). This area has been implied in food intake- and appetite-related processes (Wang et al., 2004; Wood et al., 2016) and previous studies of our group indicate that obese individuals are able to regulate its activity (Frank et al., 2012). Since the insula has also turned out to be a feasible target of neurofeedback training aiming at emotional regulation (Kadosh et al., 2016), respective eating-related interventions may also invoke emotional effects.

The striatum is involved in reward- and instrumental skill-learning (Birbaumer et al., 2013) and might also reflect the rewarding impact of successful self-regulation (Emmert et al., 2016). Striatal responses to palatable foods appear to differ between lean and obese subjects (Kenny, 2011), but it is unclear if this pattern is related to food hyposensitivity (Stice, Spoor, Bohon, Veldhuizen, & Small, 2008) or hypersensitivity (Stice, Yokum,

Bohon, Marti, & Smolen, 2010) in overweight individuals (Val-Laillet et al., 2015). Increased activity of dlPFC and IFG contributes to inhibitory top-down control of behavior, be it related to monetary or dietary rewards (Harris, Hare, & Rangel, 2013; Ochsner & Gross, 2005), and is involved in selective attention and working memory (Ochsner, Silvers, & Buhle, 2012). Hollman and coworkers (2012) observed similar activation patterns when they asked participants to use cognitive reappraisal strategies to down-regulate their desire for appealing food. Likewise, Yokum and Stice (2013) found that the suppression of craving for palatable food was associated with increased activation of inhibitory areas such as the superior frontal gyrus and ventrolateral prefrontal cortex. In these studies, no neurofeedback was provided and participants were merely asked to suppress and resist their appetite for the presented food items. There is increasing evidence that obesity is associated with decreased prefrontal cortical activation (Le et al., 2007). Thus, external stimulation of the dlPFC by transcranial direct current stimulation (tDCS) in comparison to sham stimulation results in significant weight loss (Gluck et al., 2015), while theta burst stimulation of the area increases snack intake and craving (Lowe, Hall, & Staines, 2014).

Our results suggest that neurofeedback training improves top-down control of the desire for palatable foods, a conclusion supported by the tendency to choosing less high-calorie food items after neurofeedback training. The surprising opposite trend towards increased snack intake after training may have been due to effects of anticipation and habituation to the experimental set-up emerging between the initial pre-training and the final post-training session (Wansink, 2004). Effects of habituation are likely considering that ratings of agitation and fear displayed a decrease across sessions. Studies relying on crossover comparisons with sham trainings may allow more definite conclusions about the (long-term) behavioral implications of food-focused rt-fMRI neurofeedback training. Such experiments should also investigate whether providing real-time feedback on local neural activation of areas like the dlPFC rather than on functional connectivity might be a more efficient and feasible approach (Zilverstand, Sorger, Zimmermann, Kaas, & Goebel, 2014). Technically, such an approach would be easier to apply and might also be expected to be easier to process for the participants. It is also to note that a number of brain areas show differences in activation between normal-weight and obese humans, including emotion-regulating and reward-processing regions such as the amygdala or striatum (see Schlogl et al., 2016 for review), and might be suitable targets of neurofeedback-based interventions.

In sum, our proof-of-principle exploration of the potential of rt-fMRI neurofeedback training to influence eating motivation demonstrates that participants with elevated body weight are able to up-regulate functional connectivity between dlPFC and vmPFC, regions of high relevance for food intake control. This effect is achieved mainly by enhanced dlPFC activation and is associated with behavioral implications that should be further specified in future studies, which may also investigate whether successful neurofeedback interventions may induce persistent changes in brain architecture or rather rely on the application of newly learned regulatory skills outside the scanner.

Funding

Supported by funding within the framework of the F7 EUproject BRAINTRAIN (602186) as well as by grants from the Deutsche Forschungsgemeinschaft (DFG BI 195/69-1 Koselleck), the Italian Ministry of Health progetto corrente RC 2614726, the Eva and Horst Köhler Stiftung, the Baden-Württemberg-Stiftung (GRUENS, ROB-1), the German Federal Ministry of Education and Research (BMBF

EMOIO grant 16SV7196), the Volkswagen Stiftung (87819), the Helmholtz Alliance Imaging and Curing Environmental Metabolic Diseases (ICEMED), through the Initiative and Networking Fund of the Helmholtz Association, and from the BMBF to the German Center for Diabetes Research (DZD e.V.; v01GI0925). The funding sources had no input in the design and conduct of this study; in the collection, analysis, and interpretation of the data, or in the preparation, review, or approval of the manuscript.

Declaration

The authors declare no conflict of interest.
ClinicalTrials.gov identifier: NCT02148770.

Appendix A. Supplementary data

Supplementary data related to this article can be found at <http://dx.doi.org/10.1016/j.appet.2017.01.032>.

References

- Bartholdy, S., Musiat, P., Campbell, I. C., & Schmidt, U. (2013). The potential of neurofeedback in the treatment of eating disorders: A review of the literature. *European Eating Disorders Review*, 21(6), 456–463. Journal Article <https://doi.org/10.1002/erv.2250>.
- Berthoud, H. R., & Zheng, H. (2012). Modulation of taste responsiveness and food preference by obesity and weight loss. *Physiology & Behavior*, 107(4), 527–532. Journal Article <https://doi.org/10.1016/j.physbeh.2012.04.004>.
- Birbaumer, N., Ruiz, S., & Sitaram, R. (2013). Learned regulation of brain metabolism. *Trends in Cognitive Sciences*, 17(6), 295–302. Journal Article <https://doi.org/10.1016/j.tics.2013.04.009>.
- Caria, A., Sitaram, R., Veit, R., Begliomini, C., & Birbaumer, N. (2010). Volitional control of anterior insula activity modulates the response to aversive stimuli. A real-time functional magnetic resonance imaging study. *Biological Psychiatry*, 68(5), 425–432 (Journal Article).
- Carnell, S., Benson, L., Pryor, K., & Driggin, E. (2013). Appetitive traits from infancy to adolescence: Using behavioral and neural measures to investigate obesity risk. *Physiology & Behavior*. Journal Article <https://doi.org/10.1016/j.physbeh.2013.02.015>.
- Carnell, S., Gibson, C., Benson, L., Ochner, C. N., & Geliebter, A. (2012). Neuroimaging and obesity: Current knowledge and future directions. *Obesity Reviews*, 13(1), 43–56. Journal Article <https://doi.org/10.1111/j.1467-789X.2011.00927.x>.
- Chen, M. Y., Jimura, K., White, C. N., Maddox, W. T., & Poldrack, R. A. (2015). Multiple brain networks contribute to the acquisition of bias in perceptual decision-making. *Frontiers in Neuroscience*, 9, 63. Journal Article <https://doi.org/10.3389/fnins.2015.00063>.
- Emmert, K., Kopel, R., Sulzer, J., Bruhl, A. B., Berman, B. D., Linden, D. E., ... Haller, S. (2016). Meta-analysis of real-time fMRI neurofeedback studies using individual participant data: How is brain regulation mediated? *NeuroImage*, 124(Pt A), 806–812. Journal Article <https://doi.org/10.1016/j.neuroimage.2015.09.042>.
- Finkelstein, E. A., Trogdon, J. G., Cohen, J. W., & Dietz, W. (2009). Annual medical spending attributable to obesity: Payer- and service-specific estimates. *Health Affairs*, 28(5), w822–w831. Journal Article <https://doi.org/10.1377/hlthaff.28.5.w822>.
- Frank, S., Lee, S., Preissl, H., Schultes, B., Birbaumer, N., & Veit, R. (2012). The obese brain athlete: Self-regulation of the anterior insula in adiposity. *PLoS One*, 7(8), e42570. Journal Article <https://doi.org/10.1371/journal.pone.0042570>.
- Gluck, M. E., Alonso-Alonso, M., Piaggi, P., Weise, C. M., Jumpertz-von Schwartzberg, R., Reinhardt, M., ... Krakoff, J. (2015). Neurostimulation targeted to the prefrontal cortex induces changes in energy intake and weight loss in obesity. *Obesity (Silver Spring, Md.)*, 23(11), 2149–2156. <https://doi.org/10.1002/oby.21313>.
- Greer, S. M., Trujillo, A. J., Glover, G. H., & Knutson, B. (2014). Control of nucleus accumbens activity with neurofeedback. *NeuroImage*, 96, 237–244. Journal Article <https://doi.org/10.1016/j.neuroimage.2014.03.073>.
- Hare, T. A., Camerer, C. F., & Rangel, A. (2009). Self-control in decision-making involves modulation of the vmPFC valuation system. *Science*, 324(5927), 646–648. Journal Article.
- Hare, T. A., Hukimi, S., & Rangel, A. (2014). Activity in dlPFC and its effective connectivity to vmPFC are associated with temporal discounting. *Frontiers in Neuroscience*, 8, 50. Journal Article <https://doi.org/10.3389/fnins.2014.00050>.
- Hare, T. A., Malmaud, J., & Rangel, A. (2011). Focusing attention on the health aspects of foods changes value signals in vmPFC and improves dietary choice. *Journal of Neuroscience*, 31(30), 11077–11087. Journal Article <https://doi.org/10.1523/JNEUROSCI.6383-10.2011>.
- Hare, T. A., O'Doherty, J., Camerer, C. F., Schultz, W., & Rangel, A. (2008). Dissociating the role of the orbitofrontal cortex and the striatum in the computation of goal values and prediction errors. *Journal of Neuroscience*, 28(22), 5623–5630.

- Journal Article <https://doi.org/10.1523/JNEUROSCI.1309-08.2008>.
- Hare, T. A., Schultz, W., Camerer, C. F., O'Doherty, J. P., & Rangel, A. (2011). Transformation of stimulus value signals into motor commands during simple choice. *Proceedings of the National Academy of Sciences of the United States of America*, 108(44), 18120–18125. Journal Article <https://doi.org/10.1073/pnas.1109322108>.
- Harris, A., Hare, T., & Rangel, A. (2013). Temporally dissociable mechanisms of self-control: Early attentional filtering versus late value modulation. *Journal of Neuroscience*, 33(48), 18917–18931. Journal Article <https://doi.org/10.1523/JNEUROSCI.5816-12.2013>.
- Higgs, S., Williamson, A. C., & Attwood, A. S. (2008). Recall of recent lunch and its effect on subsequent snack intake. *Physiology & Behavior*, 94(3), 454–462. Journal Article <https://doi.org/10.1016/j.physbeh.2008.02.011>.
- Hollmann, M., Hellrung, L., Pleger, B., Schlogl, H., Kabisch, S., Stumvoll, M., ... Horstmann, A. (2012). Neural correlates of the volitional regulation of the desire for food. *International Journal of Obesity (London)*, 36(5), 648–655. Journal Article <https://doi.org/10.1038/ijo.2011.125>.
- Ihsen, N., Sokunbi, M. O., Lawrence, A. D., Lawrence, N. S., & Linden, D. E. (2016). Neurofeedback of visual food cue reactivity: A potential avenue to alter incentive sensitization and craving. *Brain Imaging and Behavior*. Journal Article <https://doi.org/10.1007/s11682-016-9558-x>.
- Imperatori, C., Valenti, E. M., Della Marca, G., Amoroso, N., Massullo, C., Carbone, G. A., ... Farina, B. (2016). Coping food craving with neurofeedback: Evaluation of the usefulness of alpha/theta training in a non-clinical sample. *International Journal of Psychophysiology*. <https://doi.org/10.1016/j.ijpsycho.2016.11.010>.
- Kadosh, K. C., Luo, Q., de Burca, C., Sokunbi, M. O., Feng, J., Linden, D. E. J., et al. (2016). Using real-time fMRI to influence effective connectivity in the developing emotion regulation network. *NeuroImage*, 125, 616–626. <https://doi.org/10.1016/j.neuroimage.2015.09.070>.
- Kenny, P. J. (2011). Reward mechanisms in obesity: New insights and future directions. *Neuron*, 69(4), 664–679. Journal Article <https://doi.org/10.1016/j.neuron.2011.02.016>.
- Lee, J. H., Kim, J., & Yoo, S. S. (2012). Real-time fMRI-based neurofeedback reinforces causality of attention networks. *Neuroscience Research*, 72(4), 347–354. Journal Article <https://doi.org/10.1016/j.neures.2012.01.002>.
- Le, D. S. N., Pannacciulli, N., Chen, K., Salbe, A. D., Del Parigi, A., Hill, J. O., ... Krakoff, J. (2007). Less activation in the left dorsolateral prefrontal cortex in the reanalysis of the response to a meal in obese than in lean women and its association with successful weight loss. *The American Journal of Clinical Nutrition*, 86(3), 573–579. Retrieved from <http://www.ncbi.nlm.nih.gov/pubmed/17823419>.
- Linden, D. E., Habes, I., Johnston, S. J., Linden, S., Tatineni, R., Subramanian, L., ... Goebel, R. (2012). Real-time self-regulation of emotion networks in patients with depression. *PLoS One*, 7(6), e38115. Journal Article <https://doi.org/10.1371/journal.pone.0038115>.
- Lowe, C. J., Hall, P. A., & Staines, W. R. (2014). The effects of continuous theta burst stimulation to the left dorsolateral prefrontal cortex on executive function, food cravings, and snack food consumption. *Psychosomatic Medicine*, 76(7), 503–511. <https://doi.org/10.1097/PSY.0000000000000090>.
- Ng, J., Stice, E., Yokum, S., & Bohon, C. (2011). An fMRI study of obesity, food reward, and perceived caloric density. Does a low-fat label make food less appealing? *Appetite*, 57(1), 65–72. Journal Article.
- Ochsner, K. N., & Gross, J. J. (2005). The cognitive control of emotion. *Trends in Cognitive Sciences*, 9(5), 242–249. <https://doi.org/10.1016/j.tics.2005.03.010>.
- Ochsner, K. N., Silvers, J. A., & Buhle, J. T. (2012). Functional imaging studies of emotion regulation: A synthetic review and evolving model of the cognitive control of emotion. *Annals of the New York Academy of Sciences*, 1251, E1–E24. Journal Article <https://doi.org/10.1111/j.1749-6632.2012.06751.x>.
- Ott, V., Finlayson, G., Lehner, H., Heitmann, B., Heinrichs, M., Born, J., et al. (2013). Oxytocin reduces reward-driven food intake in humans. *Diabetes*, 62(10), 3418–3425. Journal Article <https://doi.org/10.2337/db13-0663>.
- Rangel, A. (2013). Regulation of dietary choice by the decision-making circuitry. *Nature Neuroscience*, 16(12), 1717–1724. Journal Article <https://doi.org/10.1038/nn.3561>.
- Ruiz, S., Buyukturkoglu, K., Rana, M., Birbaumer, N., & Sitaram, R. (2013). Real-time fMRI brain computer interfaces: Self-regulation of single brain regions to networks. *Biological Psychology*. Journal Article <https://doi.org/10.1016/j.biopsycho.2013.04.010>.
- Schlögl, H., Horstmann, A., Villringer, A., & Stumvoll, M. (2016). Functional neuroimaging in obesity and the potential for development of novel treatments. *The Lancet Diabetes & Endocrinology*. Journal Article [https://doi.org/10.1016/S2213-8587\(15\)00475-1](https://doi.org/10.1016/S2213-8587(15)00475-1).
- Stice, E., Spoor, S., Bohon, C., Veldhuizen, M. G., & Small, D. M. (2008). Relation of reward from food intake and anticipated food intake to obesity: A functional magnetic resonance imaging study. *Journal of Abnormal Psychology*, 117(4), 924–935. Journal Article <https://doi.org/10.1037/a0013600>.
- Stice, E., Yokum, S., Bohon, C., Marti, N., & Smolen, A. (2010). Reward circuitry responsiveness to food predicts future increases in body mass: Moderating effects of DRD2 and DRD4. *NeuroImage*, 50(4), 1618–1625. <https://doi.org/10.1016/j.neuroimage.2010.01.081>.
- Sulzer, J., Haller, S., Scharnowski, F., Weiskopf, N., Birbaumer, N., Belfari, M. L., ... Sitaram, R. (2013). Real-time fMRI neurofeedback: Progress and challenges. *NeuroImage*, 76, 386–399. Journal Article <https://doi.org/10.1016/j.neuroimage.2013.03.033>.
- Thomas, J. M., Higgs, S., Dourish, C. T., Hansen, P. C., Harmer, C. J., & McCabe, C. (2015). Satiation attenuates BOLD activity in brain regions involved in reward and increases activity in dorsolateral prefrontal cortex: An fMRI study in healthy volunteers. *The American Journal of Clinical Nutrition*, 101(4), 697–704. <https://doi.org/10.3945/ajcn.114.097543>.
- Val-Laillet, D., Aarts, E., Weber, B., Ferrari, M., Quaresima, V., Stoeckel, L. E., ... Stice, E. (2015). Neuroimaging and neuromodulation approaches to study eating behavior and prevent and treat eating disorders and obesity. *NeuroImage: Clinical*, 8, 1–31. Journal Article <https://doi.org/10.1016/j.nicl.2015.03.016>.
- Wang, G.-J., Volkow, N. D., Telang, F., Jayne, M., Ma, J., Rao, M., ... Fowler, J. S. (2004). Exposure to appetitive food stimuli markedly activates the human brain. *NeuroImage*, 21(4), 1790–1797. <https://doi.org/10.1016/j.neuroimage.2003.11.026>.
- Wansink, B. (2004). Environmental factors that increase the food intake and consumption volume of unknowing consumers. *Annual Review of Nutrition*, 24, 455–479. Journal Article.
- Weiskopf, N. (2012). Real-time fMRI and its application to neurofeedback. *NeuroImage*, 62(2), 682–692. Journal Article <https://doi.org/10.1016/j.neuroimage.2011.10.009>.
- Weygandt, M., Mai, K., Dommes, E., Leupelt, V., Hackmack, K., Kahnt, T., ... Haynes, J. D. (2013). The role of neural impulse control mechanisms for dietary success in obesity. *NeuroImage*, 83C, 669–678. Journal Article <https://doi.org/10.1016/j.neuroimage.2013.07.028>.
- Wood, S. M. W., Schembre, S. M., He, Q., Engelmann, J. M., Ames, S. L., & Bechara, A. (2016). Emotional eating and routine restraint scores are associated with activity in brain regions involved in urge and self-control. *Physiology & Behavior*, 165, 405–412. <https://doi.org/10.1016/j.physbeh.2016.08.024>.
- Yokum, S., & Stice, E. (2013). Cognitive regulation of food craving: Effects of three cognitive reappraisal strategies on neural response to palatable foods. *International Journal of Obesity (London)*, 37(12), 1565–1570. Journal Article <https://doi.org/10.1038/ijo.2013.39>.
- Zilverstand, A., Sorger, B., Zimmermann, J., Kaas, A., & Goebel, R. (2014). Windowed correlation: A suitable tool for providing dynamic fMRI-based functional connectivity neurofeedback on task difficulty. *PLoS One*, 9(1), e85929. Journal Article <https://doi.org/10.1371/journal.pone.0085929>.

Simultaneous learned regulation of anterior insula and somatosensory cortex improves interoceptive but not exteroceptive awareness

R. Malekshahi^{1,2}, M.S. Spetter¹, N. Birbaumer³, A. Caria⁴

¹ *Institute for Medical Psychology and Behavioral Neurobiology, University of Tübingen, Tübingen, Germany*

² *Graduate School of Neural & Behavioural Sciences, International Max Planck Research School, Tübingen, Germany*

³ *Ospedale San Camillo, IRCCS, Venice, Italy*

⁴ *Department of Psychology and Cognitive Science, University of Trento, Rovereto, Italy*

Abstract

Background: Individual differences in interoceptive awareness explain some of the variations in emotional information processing. Several studies have shown that activity of the right anterior insular cortex (AIC) is associated with accuracy in heartbeat perception and detection tasks. On the other hand, there exist alternative hypotheses about the functional neuroanatomy of interoception suggesting that the AIC is not critical for processing interoception. It has been shown that different pathways play a role in interoceptive awareness including visceral afferents projecting to the AIC and anterior cingulate cortex (ACC), and skin afferents projecting to the somatosensory cortex (SC). We assumed that AIC and SC interoceptive pathways have a different and complementary role for heartbeat interoception. The anterior insula (AI) pathway conveys pressure related heartbeat signals, whereas the SC pathway transmits the exogenous somatosensory component associated with cardiac activity; together they would then permit to analyse emotional activations and probably emotional valence.

Objective: we postulated that the functional interconnection between AIC and SC, regions which receive visceral and skin afferents respectively, organizes the processing of bodily signals from the viscera and somatic tissues which represents the core aspect of emotional regulation in the James-Lang concept of emotion. We trained healthy participants to volitionally regulate BOLD activity in the AIC and SC simultaneously using real-time functional magnetic resonance imaging neurofeedback (rtfMRI-NF). We specifically aimed to manipulate functional connectivity between AIC and SC by rewarding simultaneous activity in these two brain regions.

Design: 12 healthy individuals were trained to regulate simultaneous BOLD activity in the AIC and SC over one training day consisting of four neurofeedback sessions and one localiser session. Average BOLD activity of ROIs in AIC and SC, selected based on localiser session, was used for calculating feedback (Turbo-BrainVoyager 3.2, Brain Innovation B.V.).

Results: 9 out of 12 participants were able to regulate BOLD magnitude successfully in the right AIC and SC. Training resulted in a significantly increased BOLD activity, increased effect-size, in both the right AIC, and SC. Offline partial correlation connectivity analysis showed significant increase of correlation between right AI and SC over sessions during regulation. Regression analysis revealed that learned coupling between right AIC and SC predicted interoceptive sensitivity.

Conclusion: We employed a novel neurofeedback approach to increase functional connectivity. Accordingly, by rewarding BOLD response in both AIC and SC simultaneously through rtfMRI-NF training we tightened their functional interconnection. At behavioral level, we observed that the modulation of functional connectivity between the AI and SC predicted performance in the heartbeat perception task. The possibility to manipulate interoceptive sensitivity through self-

regulation of specific neuronal network activity might represent a novel approach for clinical application aiming at treating disorders of interoceptive awareness i.e. obesity and anorexia-bulimia.

Keywords: Interoceptive awareness, rtfMRI-neurofeedback, functional connectivity, learning

1. Introduction

Interoception denotes the sense for visceral and somatic afferent bodily information originating from inside the body (Craig 2002, Craig 2003, Seth 2013). Detection of internal bodily sensation has been defined as interoceptive awareness (Garfinkel 2013). Interoceptive feedback keeps the internal physiological state in a stable equilibrium (Critchley et al. 2013, Ondobaka et al. 2015, Craig 2009, Seth et al. 2011). It has been proposed that heightened interoceptive awareness could be associated with more intense emotional experiences (Wiens 2000). This is in line with the James–Lange theory of emotion, and its more recent version of somatic marker according to which subjective emotional experience depends upon the perception of physiological changes of the body (Damasio 1991, Craig 2009, Seth et al. 2011, Seth 2013).

Functional imaging studies have provided evidence that the right anterior insular cortex (AIC) is a critical region for interoceptive and subjective emotional awareness (Gu et al. 2013, Craig 2009, Pollatos et al. 2007). Several studies have shown that activity of the right AIC is associated with accuracy in heartbeat and other visceral perception and detection tasks (Critchley et al. 2004, Pollatos et al. 2005). Awareness of emotionally salient stimuli also correlates with AIC activity (Critchley et al. 2004).

The AIC forms the substrate for a neural representation of interoceptive bodily states and generates regulatory signals necessary to maintain bodily homeostasis (Craig 2002, Craig 2003, Craig 2009, Critchley et al. 2004, Craig 2005). Craig in his model of human awareness suggested a mechanism of a global instantiation of bodily status within the right anterior insula, “the material me”. In this model, the posterior insula and the primary interoceptive cortex are associated with somatotopic representation of bodily states, and sequential integration of salient visceral/bodily activity with cognitive and motivational information progresses from the posterior to the anterior insula. According to this model, damage to the AIC would result in the lack of interoceptive awareness (Craig 2002, Craig 2003, Craig 2005, Craig 2009). Recently, Seth et al. also proposed an interoceptive predictive coding model of conscious presence pointing to the anterior insula as key region for assessing top-down predictions of interoceptive signals evoked (directly) by autonomic

control signals and (indirectly) by bodily responses to afferent sensory signals. Within this framework, interoceptive prediction error would then result from comparing top-down interoceptive predictions with bottom-up bodily signals. As claimed by this model, the anterior insula plays a critical role as a neural comparator of top-down interoceptive predictions and bottom-up bodily signals (Seth 2013).

On the other hand, there exist alternative hypotheses about the functional neuroanatomy of interoception suggesting that the AIC might not be the sole region for mediating interoception. It has been shown that additional pathways play a role in interoceptive awareness including visceral/bodily afferents projecting to the insular cortex and ACC (Anterior cingulate cortex), and skin afferents projecting to somatosensory cortex (SC) (Cameron et al. 2002, Khalsa et al. 2009, Pollatos et al. 2007, Couto et al. 2014). Khalsa et al. by combining lesion and pharmacological methods studied a patient with bilateral damage to insula and ACC, and intact bilateral SC. This patient showed good performance on heartbeat detection task, but after chest skin anaesthesia interoceptive sensitivity was impaired (Khalsa et al. 2009). This important study challenged current neuroimaging findings of the insula as the exclusive cortical substrate for interoceptive awareness. Instead, these results supported the existence of two, possibly independent, pathways mediating interoceptive awareness: one constituted of visceral afferents projecting to the insular cortex (IC) and ACC, and one including skin afferents projecting to secondary somatosensory cortex.

This finding is also supported by studies showing that lower body mass index predicts better heart beat detection accuracy, thus suggesting that skin receptors are important for interoceptive awareness (Rouse et al. 1998, Couto et al. 2014). In addition, most of previous neuroimaging studies reporting AIC activation associated with interoceptive sensitivity also reported activation of SC (Critchley et al. 2004, Pollatos et al. 2005, Pollatos et al. 2007). Furthermore, several different interoceptive awareness/attention tasks were associated with SC activity (Dickenson et al. 2013, Kashkouli Nejada et al. 2015, Kilpatrick et al. 2011).

The present study aimed at clarifying the neural correlates underlying interoceptive awareness using a novel approach based on instrumental learning of BOLD response through real-time fMRI. In the last decade, a number of investigations have demonstrated that learned regulation of the blood-oxygen-level dependent (BOLD) signal is possible in brain areas related to different type of processing: sensorimotor, cognitive and emotion (Birbaumer et al. 2013, Caria et al. 2012, Weiskopf 2012, Sulzer et al. 2013). More importantly, real-time functional magnetic resonance imaging (rtfMRI) studies have shown that neurofeedback training, besides allowing specific control of localized BOLD signal, leads to changes in human behavior (Sulzer et al. 2013, Caria et al. 2012, Weiskopf 2012, Weiskopf et al. 2007). In particular, changes in emotional responses were reported concurrently with successful regulation of AI activity (Caria et al. 2012, Caria et al. 2015).

In this study we postulated a critical role of the functional interconnection between AI and SC, regions which receive visceral and skin afferents respectively, mediates the processing of bodily signals from the viscera and somatic tissues which represents a core aspect of motivational regulation (Bechara et al. 2004, Craig 2002). We assumed that AI and SC interoceptive pathways have different and complementary roles for heartbeat interoception. AI pathway conveys endogenous, more visceral heartbeat signals, whereas the SC pathway transmits the exogenous somatic somatosensory component associated with cardiac activity; together they would then permit a complete perceptive model of heart rate changes.

Hence, we hypothesized that interoceptive awareness would be modulated by the functional coupling between anterior insula and somatosensory cortex more than by the isolated activity of each single region. To this aim, we trained healthy participants to volitionally regulate simultaneous combined BOLD activity in the AI and SC using rtfMRI neurofeedback. We specifically aimed to manipulate functional connectivity between AI and SC by reinforcing activity in these two brain regions simultaneously. This novel approach is based on Hebbian learning mechanisms (Hebb 1949) indicating that neuronal assemblies are formed through their successful coactivations. Accordingly, by rewarding BOLD response in both AI and SC through neurofeedback training

we aimed to reinforce their functional interconnection. At behavioral level, we then expected that the modulation of functional connectivity between AI and SC would predict performance on heartbeat perception task. As a first step, we intended to demonstrate that learning of brain functional connectivity is possible as a proof-of-principle approach. It is obvious however that differential training of both areas probably needs to be realized as a control condition. However, in order to secure the specificity of training changes to interoception, a comparable exteroception task was introduced.

Ultimately, the possibility to manipulate interoceptive sensitivity through self-regulation of specific neuronal network activity might represent an approach for clinical application aiming at treating psychological and psychiatric disorders where altered interoceptive and emotional awareness is often observed.

2. Methods

2.1. Participants

Twelve healthy volunteers participated to the study (mean age 27 ± 3.62 years, 9 females, 11 right handed). They had no history of neurological or psychiatric disorders including substance abuse/dependence or psychotropic medications, or any other medical condition that requires regular medical treatment. All participants were previously involved in at least one MR experiment. They signed a written informed consent and were monetary compensated for their effort and participation at the end of the experiment (12 €/hr). This study was approved by the local ethics committee of the Faculty of Medicine of the University of Tübingen. Participants were instructed not to move and to breath regularly in order to avoid artefacts.

2.2. Experimental procedure

All participants underwent a single fMRI day. The experiment was preceded by a preparation phase, and included MR data acquisition for a high resolution brain anatomy, a functional localizer, and four neurofeedback training sessions.

2.2.1. Preparation

Few days before the scanning sessions, participants were provided with written instructions about the experimental task. Participants were administered the Vividness of Visual Imagery Questionnaire—(VVIQ-2, Marks, 1995) and the Body Perception Questionnaire (BPQ) in order to test for the individuals' imagery ability and awareness of bodily changes respectively. The items of the VVIQ-2 test will possibly bring certain images to the mind. During the VVIQ-2 participants are asked to rate the vividness of each image on a 5-point scale. For example, if the image is dim or vague, participants are supposed to give a rating of 2. High scores on the VVIQ-2 indicate vivid visual imagery. The BPQ includes 5 subtests: bodily awareness, stress response, autonomic nervous system reactivity, stress style, and health history inventory. Subjects required scoring their answers on a 5-point scale (ranging from never to always).

At the experimental day, participants were debriefed about the experiment, and at the very beginning, they were trained to use a keypad composed of 10 keys (zero, 1, 2... 9) by asking them to report numbers between 1 and 19 (while they were lying on the scanner table, the experimenter instructed random numbers to them auditorily). Participants were trained until their response was sufficiently fast and reliable (100% correct in 60 responses).

2.2.2. Localizer

The functional localizer permitted to delineate AI and SC. It consisted of 3 interoception and 3 exteroception trials alternated with rest. During the interoceptive task (16 seconds), subjects were asked to attend to their own heart, and silently count their heartbeat for as long as the task-type indicator (a dark coloured heart on a light background) was displayed (Figure 1B). The exteroceptive task (16 seconds) was indicated by a dark coloured musical note symbol on a light background, and participants had to silently count the number of tones during the period the indicator was on the screen (Figure 1A). After each condition, subjects were asked to report the number of heartbeats or tones using the keypad (3 seconds). During rest (16 seconds) a dark cross was presented on a light gray background (Figure 1E), and subjects were instructed to relax.

2.2.3. Feedback training

Participants underwent four neurofeedback training sessions in one day where they learned to voluntarily regulate their own brain activity. Each neurofeedback session composed of 8 regulation, and 8 baseline trials which were followed by interoception/exteroception trials pseudo-randomly and alternated with rest. During regulation, a thermometer and an up-arrow sign next to it were shown to the subjects (Figure 1C). The thermometer informed them in real-time about the current level of combined brain activation. The number of grey lines in the thermometer reflected the level of activation. Their task was to increase the number of grey lines. We instructed participants to figure out cognitive strategies that work for them to accomplish better regulation, and once they find one, they should keep using it. We proposed some additional suggestions.

These suggestions included a) using emotional imagery, recalling some of the most emotional episodes of his/her life, and try to feel the same emotion as they felt in the past b) to concentrate on internal bodily signals, such as breathing, heartbeats, gastrointestinal movement or c) body perception (focus on perception of your arms, legs etc.). They were told that feedback is a bit delayed and they will see the effect of a strategy after about six or seven seconds. During the baseline, only the thermometer frame with a small plus sign (symbol of the trial) next to it was presented, but no feedback was provided (without updating gray thermometer's lines) (Figure 1D). During the baseline, participants were instructed to relax and reduce any cognitive load and not to think about the experiment. During the interoceptive and exteroceptive tasks, participants were supposed to do the same as they did during the localizer session. The duration of each trial was as follow: regulation: 30 seconds, baseline: 30 seconds, extro- and interoception trial: 14, 15, 16, 17 seconds (these times include 3 seconds for reporting numbers) pseudo-randomised, rest: 30 seconds – (duration of interoception or exteroception trial). All stimulus presentation programs were implemented in Matlab using Psychtoolbox version 3.0.12.

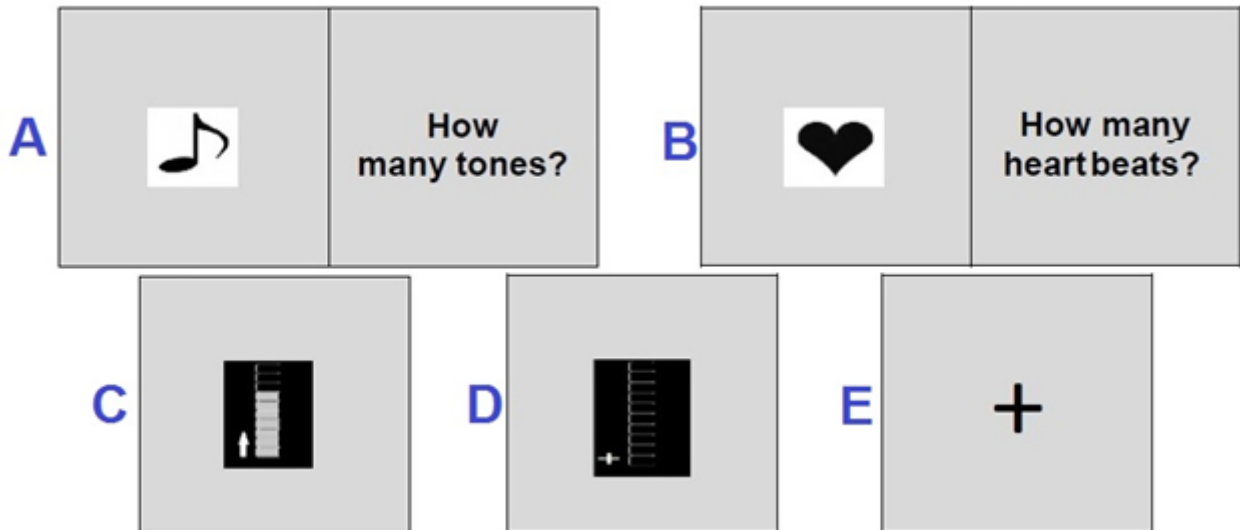


Figure 1: Experimental protocol – the experiment consisted of a localizer and 4 neurofeedback sessions. Localizer permitted to estimate the localization of the AI and SC cortices. It included 3 interoception and 3 exteroception trials alternated to rest. Each neurofeedback session composed of 8 regulation, and 8 baseline trials which were followed by interoception/exteroception trials pseudo-randomly and alternated with rest. Below are the description of different trials:

- A. Exteroception trial:** participants were asked to attend to the auditory tones, and silently count them as long as the task-type indicator (a dark coloured musical note symbol on a light background) was displayed. The duration of each exteroception trial was 20 seconds in the localizer session, but pseudo-randomly varied during neurofeedback sessions (14, 15, 16, 17 seconds). Subjects were asked to report the number of tones using the keypad. All of the aforementioned times include 3 seconds for reporting number of tones.
- B. Interoception trial:** participants were asked to attend to their own heart, and silently count the heartbeat for as long as the task-type indicator (a dark coloured heart on a light background) was displayed. The duration of interoception trial was 20 seconds in the localizer session, but pseudo-randomly varied during neurofeedback sessions (14, 15, 16, 17 seconds). Subjects were asked to report the number of heartbeats using the keypad. All aforementioned times include 3 seconds for reporting number of heartbeats.
- C. Regulation trial:** The regulation was cued with an up-arrow next to the thermometer. The combined BOLD-activity of AI and SC was reflected by the grey lines inside the thermometer, and were updated every $TR=1.5$ seconds. Subjects were required to increase the number of lines. The duration of regulation was 30 seconds.
- D. Baseline trial:** The baseline was cued with a plus sign next to the thermometer. During this trial, only the empty thermometer frame and plus sign were shown to the subjects. Subjects were required to relax and reduce any cognitive work during this period. The duration of baseline was 30 seconds.
- E. Rest:** It was cued by a plus sign in the center of the screen. Subjects were required to relax during this period. The duration of the rest trial was 16 seconds in the localizer, and 30 seconds – (duration of interoception or exteroception trial) in neurofeedback training sessions.

MR compatible headphones were used for presenting tones during exteroceptive task (Figure 1A). In order to make the difficulty of both the intero- and exteroceptive tasks comparable (Figure 1A and 1B), the volume of tones were individually determined at the beginning of the experiment. To achieve this, participants were asked to adjust the intensity of the volume of the tones while the scanner was acquiring images. Participants were instructed to repeatedly decrease the volume of the tones until the minimal not detectable level (they do not hear anything) and then increase it to one level higher (the first higher detectable level). They could use left, right index, and right middle finger to decrease, increase, and confirm the intensity of tones. This minimum detectable level was used for constructing the tone intensities in exteroceptive task in localizer and neuro-feedback sessions. The frequency of tones was 800 Hz, with a duration of 200 millisecond, a length that is comparable to the average duration of a heartbeat. To control for habituation effects, tones were presented in 3 different intensities, 1, 14, and 34db above the subject's threshold intensity. Additionally the inter tone interval was varied pseudo-randomly by 600, 800, 1000, 1200, 1400 millisecond. A Siemens Pulse oximeter (Physiological Monitoring Unit) was used for recording heartbeats by attaching the light sensor to the finger.

2.3. MRI data acquisition

Functional images were acquired using a 3.0 T MR scanner, with a standard 64-channel head coil (Siemens Prisma Magnetom, Erlangen, Germany). During feedback training, standard echo planar imaging (EPI) images consisting of twenty axially oriented slices (voxel size=3×3×3.3 mm³, slice gap=0.57 mm) were acquired (repetition time TR=1500 ms, matrix size=64×64, echo time TE=35 ms, flip angle $\alpha=79^\circ$, bandwidth=1.905 kHz/pixel). With the same parameters the localizer images acquired at TR=2000 ms. For superposition of functional maps upon brain anatomy a high resolution T1 weighted image of the whole brain was collected from each subject (ADNI, matrix size=256×232, 192 partitions, voxel size=1×1×1 mm³, TR=2000 ms, TE= 3.06 ms, TI=1100 ms, $\alpha=9^\circ$). In order to minimize head movements two foam cushions were positioned around participant's head.

2.4. Data Processing

2.4.1. Neurofeedback - online analyses

The MR images were exported in real time from the MRI console computer to the Turbo brain voyager computer. To avoid the T1 saturation effect, the first 10 images were discarded. The real time motion correction was applied by aligning all functional images to the first recorded volume in the first session, and images in all other sessions were aligned accordingly. Motion corrected functional images were then spatially smoothed by a kernel of 9 mm. Incoming images were considered for calculating feedback, the average BOLD activity within online selected ROIs in AIC, and SC. The participants were updated about their brain activity only during regulation by visually provided feedback in every TR. To have a smooth feedback, less prone to noise, the feedback value at each moment was calculated based on moving average of the current and the two previous combined BOLD activities of the ROIs. The more the average brain activity of AIC and SC was, the higher the number of gray lines inside the black thermometer.

2.4.2. Offline fMRI voxel-based data analysis

Functional imaging data were analyzed using SPM 8 (Wellcome Department of Cognitive Neurology, London, UK). All functional images were first motion corrected and realigned. The high-resolution T1 image was then co-registered to the mean image of the EPI series for each participant. Segmentation parameters were used to normalize the functional scans to a standard Montreal Neurological Institute (MNI) template. Normalized images were spatially smoothed with a 9mm full-width half-maximum Gaussian kernel. Low frequency drifts were removed using a high-pass filter with 128 seconds cut off. After functional data preprocessing, a general linear model was adopted to perform first level statistical analysis. For each participant, an analytic design matrix was constructed using the following type of events as regressors: baseline, regulation, interoception-preceded by regulation, interoception-preceded by baseline, exteroception-preceded by regulation, and exteroception-preceded by baseline. Conditions were modeled with a canonical hemodynamic response. In addition, a regressor considering key-pressed onsets was included to

cancel out residual hand movement-related variance. For each participant, contrast images of regulation versus baseline, and interoception vs exteroception were created. Contrast images were then entered into a second-level (random-effects) analysis to allow population-level inferences. One-sample t-tests on the contrast images imported from the first-level analysis were performed to assess group effects across all participants.

2.4.3. Offline fMRI ROI-based data analysis

2.4.3.1. Self-regulation effect-size

Information about the time courses of the voxels inside anatomically selected right secondary SC corresponding to supramarginal gyrus (BA40) and right AI were extracted, and linearly detrended. To factor out the stimulus-induced activity during regulation trial, and possible effect of BOLD activity from previous trial on the baseline trial, the 5 data points at the beginning of both trials were excluded. The neurofeedback training effect-size during regulation trial was then calculated separately for each ROI by calculating the following formula for all subjects and training sessions: $\text{Effect-size} = ((\text{BOLD_regulation} - \text{BOLD_baseline}) / \text{BOLD_baseline}) * 100$. Group analysis was performed by comparing the training effect-size over sessions using ANOVA and the paired t-test.

2.4.3.2. Functional connectivity analysis

Offline partial correlation analysis was performed to regress out any global fluctuation or unwanted movement artifact that possibly had not been corrected by preprocessing algorithms. For performing partial correlation analysis a control (third) region was selected from subcortical white matter far from AIC and SC in the temporal lobe (Sphere with a radius of 6 millimeters centered in $x=40, y=-40, z=7$ (MNI space)). Group analysis was performed by comparing the correlation between AIC and SC over sessions using the paired Wilcoxon signed rank test.

2.4.4. Behavioral data analysis

The interoceptive/exteroceptive sensitivities were calculated based on the real and the reported number for the heartbeats or auditory tones for each subject as follow:

$$\text{Sensitivity} = (\text{reported number} - \text{real number}) / \text{real number}$$

Regression analysis was performed between BOLD activity in both AI and SC, and interoceptive sensitivity across those participants who showed successful regulation of BOLD activity in both ROIs. The same analysis was performed between interoceptive sensitivity and the coupling among AI and SC. Average heart rate during regulation and its differences with respect to baseline were also calculated for each training session across all participants. To associate brain (regulation ability) and behaviour (sensitivity) to the individuals' imagery ability and awareness obtained from questionnaires and body mass index (BMI) multivariate regression analysis was performed.

3. Results

3.1. Self-regulation ability

3.1.1. BOLD activity

Nine participants were able to successfully regulate BOLD magnitude in the right anterior AI and SC. Neurofeedback training resulted in a significantly increased effect-size in both the right AI ($F(3,24)=3.65$, $p = 0.02$; $t = 2.39$, $p = 0.03$), and SC ($F(3,24)=2.11$, $p=0.1$; $t = 2.05$, $p = 0.03$) comparing session 4 to session1 (Figure 2).

3.1.2. Offline connectivity analysis

Offline connectivity analysis showed a significant increase of partial correlation between right AI and SC comparing session4 versus session1 only during regulation, and not baseline ($F(3,24)=1.89$, $p=0.15$; $p = 0.02$) (Figure 3).

3.1.3. Heart rate

Significant increase in heart rate was observed during regulation compared to baseline for each training session (session1: $p=0.01$; session2: $p=0.02$; session3: $p=0.02$; session4: $p=0.02$) (Figure 4). Between training sessions, there was no significant increase in heart rate during regulation (Figure 5).

3.2. Brain-behavior association

There was not meaningful relation between BOLD activities in any of AIC or SC ROIs with interoceptive sensitivity. The significant correlation between coupling among AIC and SC, and interoceptive sensitivity (IS) during baseline ($r=0.43$, $p=0.01$) (Figure 7) and regulation ($r= 0.45$, $p=0.009$) (Figure 6) was observed. Negative correlation between coupling among AIC and SC, and exteroceptive sensitivity was observed($r=-0.40$, $p=0.02$). Furthermore, connectivity between significantly activated clusters from statistical maps, such as thalamus, and basal ganglia with the right AIC

were tested for potential association with IS. Multivariate regression analysis showed a significant negative association between regulation-ability in AIC with awareness (Beta=-0.33, p=0.04).

3.3. Neural substrate of the learning effect

Group random effects analysis confirmed an increased BOLD-magnitude in the right AIC, right SC, right and left basal ganglia, right mid-cingulate and, right thalamus. All activation maps are generated from regulation> baseline comparing session 4 versus session 1, and projected on a single-subject T1 template. The activation map were thresholded at p=0.008.

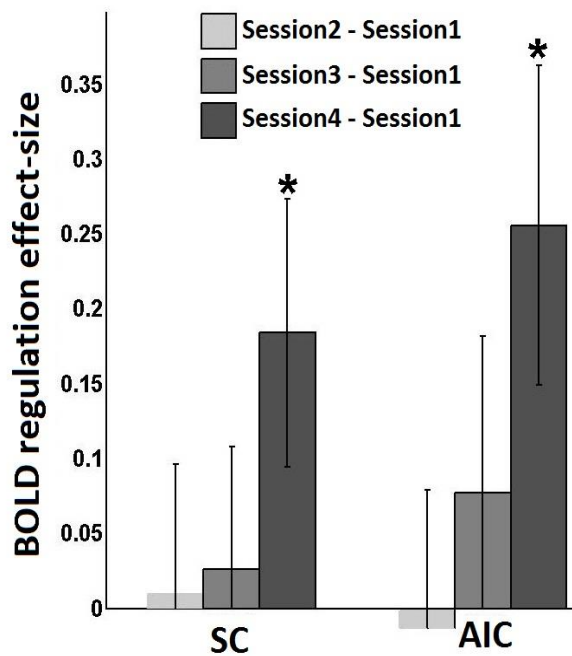


Figure 2: Feedback training BOLD regulation's effect-size – there is a significant increase of regulation effect-size between session4 and session1 in both SC and AIC.

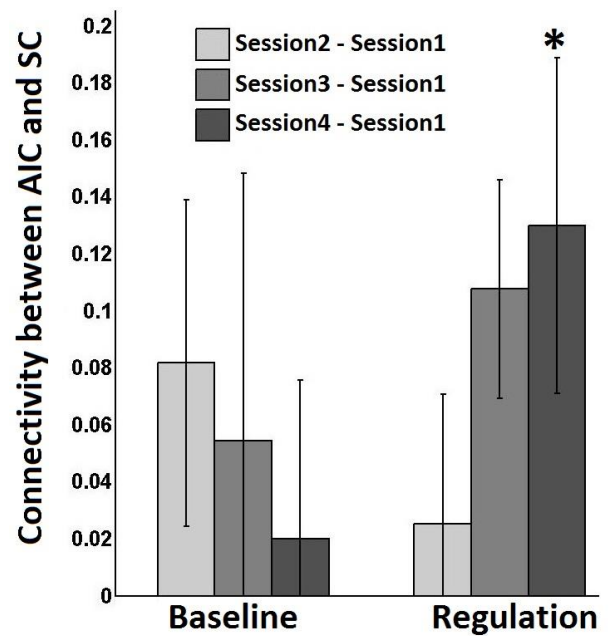


Figure 3: Offline functional connectivity - significant increase of connectivity (Partial correlation) between SC, and AIC over sessions and only during Regulation was observed.

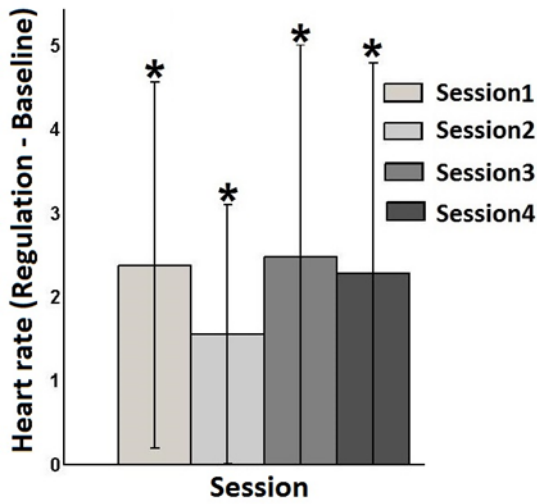


Figure 4: Heart rate differences- in each training session, a significant increase of heart rate in Regulation compared to Baseline was observed.

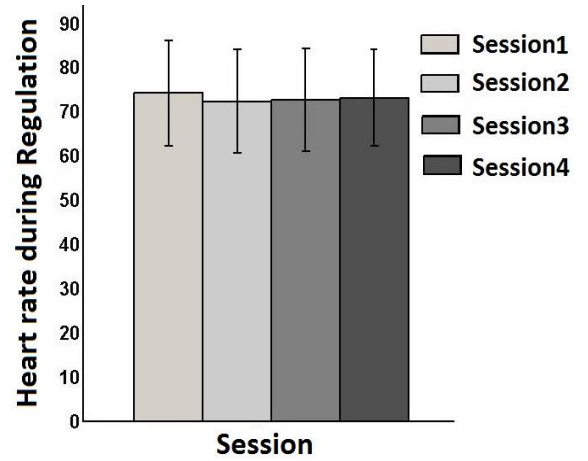


Figure 5: Heart rate – there is no significant difference in heart rate over sessions during regulation.

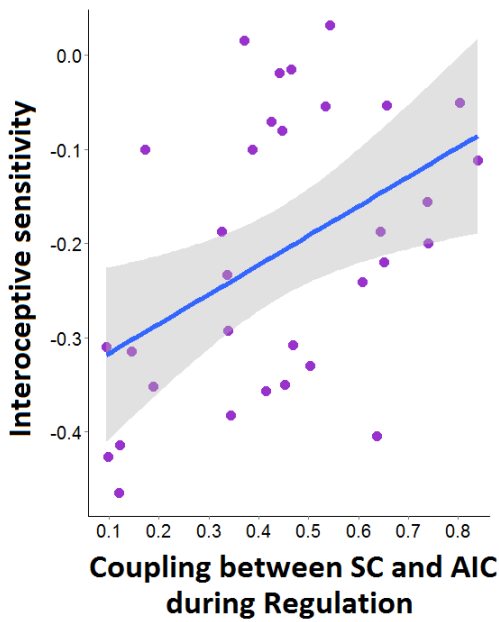


Figure 6. Coupling between SC and AIC during regulation versus interoceptive sensitivity ((reported – real)/real) including all training sessions across all subjects - Significant relationship was demonstrated by a significant correlation ($r=0.45$, $p=0.009$). Interoception trials subsequent to regulation were considered for this analysis.

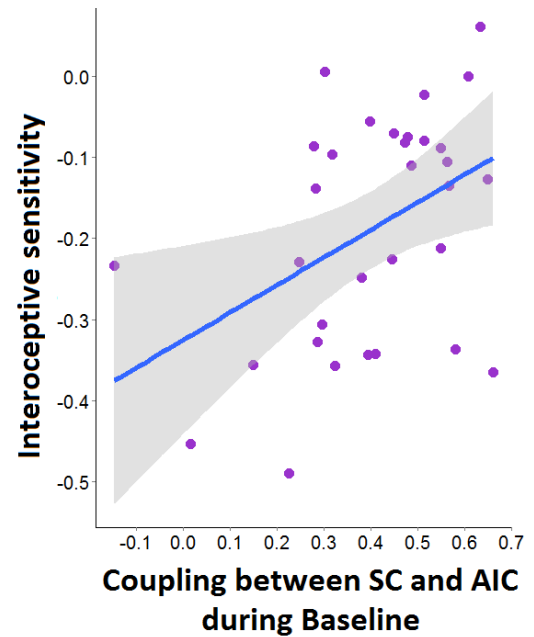


Figure 7. Coupling between SC and AIC during baseline versus interoceptive sensitivity ((reported – real)/real) including all training sessions across all subjects - Significant relationship was demonstrated by a significant correlation ($r=0.43$, $p=0.01$). Interoception trials subsequent to baseline were considered for this analysis.

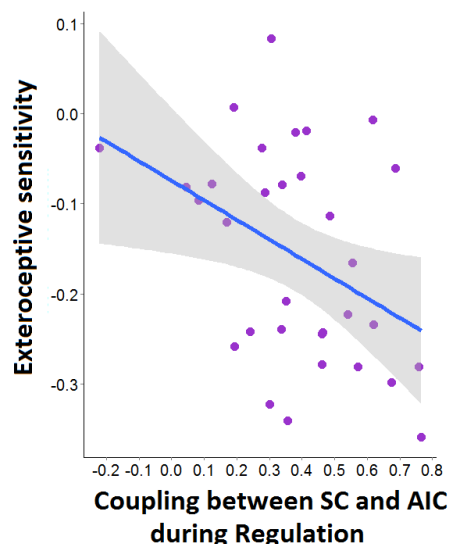


Figure 8. Coupling between SC and AIC during regulation versus exteroceptive sensitivity ((reported – real)/real) including all training sessions across all subjects. Exteroception trials subsequent to regulation were considered.

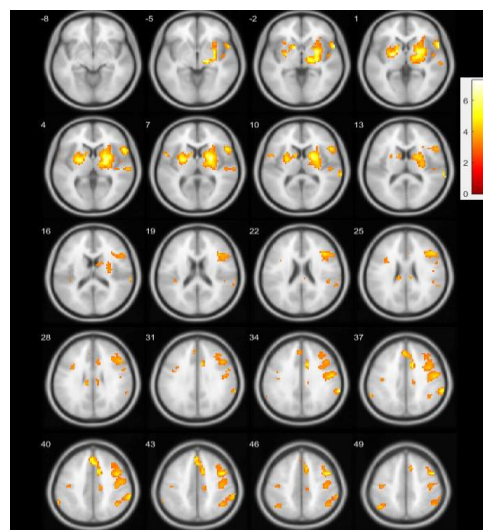


Figure 9. Brain regions underlying increased regulation ability - Random effects analysis on the experimental contrast confirmed an increased BOLD-magnitude in the right AIC, right SC, right and left basal ganglia, right mid-cingulate and, right thalamus. Activation map is generated from regulation > baseline comparing session4 versus session1, and projected on a single-subject T1 template.

Table 1: Brain regions underlying increased regulation ability (regulation>baseline)(session4) > (regulation>baseline)(session1)

Brain regions	K _E	Coordinates (MNI)			t-value
		X	y	Z	
Right Supramarginal gyrus	167	66	-40	34	7.25
Right Putamen	1321	24	-1	4	6.93
Right Thalamus	-	18	-19	5	6.88
Right Rolandic operculum	-	57	11	1	6.46
Left Putamen	217	-24	-7	-1	6.69
Left Pallidum	-	-12	8	-2	6.50
Left Caudate	-	-12	8	7	4.33
Mid-Cingulate	185	12	11	37	5.75
Right Anterior Insula	-	33	30	1	3.03
Left Frontal_Sup_Medial	-	0	29	40	5.52
Left Angular gyrus	43	-45	-61	49	4.67
Left Post central gyrus	75	-42	-28	58	3.99

4. Discussion

Brain is continuously updated about the physiological states of all body's tissues. Small-diameter sensory afferents from skin (via spinal laminar 1) and all viscera (carrying motivational information such as hunger, satiety, thirst, and the like via vagus and glossopharyngeal nerves terminating within NTS (nucleus of the solitary tract)) provide ongoing sensory inputs to the homeostatic cells in spinal and brain stem. In the Craig homeostatic model, primary interoceptive representation, the high-resolution representation of ongoing metabolic and vascular conditions, which are conveyed by the small-diameter sensory fibers, is embedded in the posterior insula. AIC (where conscious experience of emotion emerges) incorporates emotionally salient activity from limbic cortical regions (ACC, OFC), as well as social and cognitive activities from vmPFC, and dlPFC (Craig 2002, Craig 2009). Researchers have shown that differences in sensitivity to the internal bodily signals, interoceptive sensitivity, predicts the individual differences in the intensity of subjective emotional experiences (Critchley et al. 2004, Pollatos et al. 2007). However, the large-diameter skin sensory afferents projecting to the primary and secondary somatosensory cortices (SC: S1 and S2), which usually believed to support exteroception, independently from small-diameter sensory afferents to IC and ACC would enable awareness of the cardiovascular status of the body (Khalsa et al. 2009, Couto et al. 2014, Cameron et al. 2002, Rouse et al. 1998). Built on these previous findings, we hypothesized that the functional interconnection between AIC and SC organizes the processing of bodily signals from the viscera and somatic tissues which represents the core aspect of emotional regulation in the James-Lang concept of emotion, and its newer version of somatic marker (Damasio 1991).

In this study, we employed a novel neurofeedback approach to increase functional connectivity. Accordingly, by rewarding BOLD response in both AIC and SC simultaneously through rtfMRI-NF training we tightened their functional interconnection. Most of participants were able to regulate BOLD magnitude successfully in the right AIC and SC. Training resulted in a significantly increased BOLD activity, increased effect-size, in both the right AIC, and SC. Offline partial correlation connectivity analysis showed significant increase of correlation between right AI and SC over

sessions during regulation. This interesting finding shows that up-regulating simultaneous BOLD activity of two spatially separated brain regions could potentially be used for enhancing functional connectivity (FC) between those regions. Researchers have shown that there is a clear neuronal mechanism underlying learning regulation of BOLD activity (Birbaumer et al. 2013), therefore indirect modulation of FC by targeting BOLD activity rather than a measure of FC such as correlation would be easier to learn and might have stronger transfer effect.

At behavioral level, due to the significant increase of heart rate, probably higher anxiety level, during regulation compared to baseline, there was not a clear association between interoceptive sensitivity and BOLD activity in AIC or SC. However, we did observe an improvement in interoceptive sensitivity at the group level in those subjects who showed enhanced FC between the two regions. Furthermore, very interestingly, as we have postulated we observed that the modulation of FC between the AIC and SC predicted performance in the heartbeat perception task during both baseline and regulation. This finding elucidates that interoceptive awareness would be mediated by simultaneous action of both SC and AIC pathways, the higher FC the higher awareness. The possibility to manipulate interoceptive sensitivity through self-regulation of specific neuronal network activity might represent a novel approach for clinical application aiming at treating disorders of interoceptive awareness i.e. obesity and anorexia-bulimia.

5. Acknowledgements

The authors acknowledge the funding source EU Brain Train 602186. Niels Birbaumer is supported by the Deutsche Forschungsgemeinschaft (DFG BI 195/69-1 Koselleck), The Italian Ministry of Health progetto corrente RC 2614726, The Eva and Horst Köhler Stiftung, The Baden-Württemberg-Stiftung GRUENS, ROB-1, EMOIO-grant BMBF 16SV7196 German Ministry of Education and Research (Bundesministerium für Bildung und Forschung), Stiftung Volkswagen (VW-Stiftung 87819).

6. Literature

Bechara, A. and N. Naqvi (2004). "Listening to your heart: interoceptive awareness as a gateway to feeling." Nat Neurosci **7**: 102-103.

Birbaumer, N., et al. (2013). "Learned regulation of brain metabolism." Trends Cogn Sci **17**(6): 295-302.

Cameron, O. G. and M. Satoshi (2002). "Regional Brain Activation Due to Pharmacologically Induced Adrenergic Interoceptive Stimulation in Humans." Psychosomatic Medicine **64**: 851–861

Caria, A. and S. de Falco (2015). "Anterior insular cortex regulation in autism spectrum disorders." Front Behav Neurosci **9**: 38.

Caria, A., et al. (2012). "Real-time fMRI: a tool for local brain regulation." Neuroscientist **18**(5): 487-501.

Couto, B., et al. (2014). "The man who feels two hearts: the different pathways of interoception." Soc Cogn Affect Neurosci **9**(9): 1253-1260.

Craig, A. D. (2002). "How do you feel? Interoception: the sense of the physiological condition of the body." Nature Reviews Neuroscience **3**(8): 655-666.

Craig, A. D. (2002). "How do you feel? Interoception: the sense of the physiological condition of the body." NATURE REVIEWS **3**: 655-666.

Craig, A. D. (2003). "Interoception: the sense of the physiological condition of the body." Current Opinion in Neurobiology **13**(4): 500-505.

Craig, A. D. (2005). "Forebrain emotional asymmetry: a neuroanatomical basis?" Trends Cogn Sci **9**(12): 566-571.

Craig, A. D. (2009). "How do you feel—now? the anterior insula and human awareness." Nature Reviews Neuroscience **10**(1).

Craig, A. D. (2009). "How do you feel — now? The anterior insula and human awareness." Nature reviews, neuroscience **10**.

Craig, A. D. (2009). "How do you feel — now? The anterior insula and human awareness." ATURE REVIEWS **10**: 59-70.

Critchley, H. D. and N. A. Harrison (2013). "Visceral influences on brain and behavior." Neuron **77**(4): 624-638.

Critchley, H. D., et al. (2004). "Neural systems supporting interoceptive awareness." Nat Neurosci **7**(2): 189-195.

Damasio, A. R. (1991). "Behavior: Theory and Preliminary Testing." Frontal lobe function and dysfunction: 217.

Dickenson, J., et al. (2013). "Neural correlates of focused attention during a brief mindfulness induction." SCAN **8**: 40-47.

- Garfinkel, S. N., Critchley, H. D. (2013). "Interoception, emotion and brain: new insights link internal physiology to social behaviour. Commentary on: "Anterior insular cortex mediates bodily sensibility and social anxiety" by Terasawa et al. (2012)." Soc Cogn Affect Neurosci **8**(3): 231-234.
- Gu, X., et al. (2013). "Anterior insular cortex and emotional awareness." J Comp Neurol **521**(15): 3371-3388.
- Hebb, D. O. (1949). "The Organization of Behavior. New York: Wiley & Sons."
- Kashkouli Nejada, K., et al. (2015). "Supramarginal activity in interoceptive attention tasks." Neuroscience Letters **589** 42–46.
- Khalsa, S. S., et al. (2009). "The pathways of interoceptive awareness." Nat Neurosci **12**(12): 1494-1496.
- Kilpatrick, L. A., et al. (2011). "Impact of mindfulness-based stress reduction training on intrinsic brain connectivity." Neuroimage **56**: 290–298.
- Ondobaka, S., et al. (2015). "The role of interoceptive inference in theory of mind." Brain Cogn.
- Pollatos, O., et al. (2007). "Neural systems connecting interoceptive awareness and feelings." Hum Brain Mapp **28**(1): 9-18.
- Pollatos, O., et al. (2005). "Brain structures involved in interoceptive awareness and cardioafferent signal processing: a dipole source localization study." Hum Brain Mapp **26**(1): 54-64.
- Pollatos, O., et al. (2007). "Brain structures mediating cardiovascular arousal and interoceptive awareness." Brain Res **1141**: 178-187.
- Rouse, C. H., et al. (1998). "The effect of body composition and gender on cardiac awareness." Psychophysiology **25**(4): 400-407.
- Seth, A. K. (2013). "Interoceptive inference, emotion, and the embodied self." Trends Cogn Sci **17**(11): 565-573.
- Seth, A. K., et al. (2011). "An interoceptive predictive coding model of conscious presence." Front Psychol **2**: 395.
- Sulzer, J., et al. (2013). "Real-time fMRI neurofeedback: Progress and challenges." Neuroimage **76**: 386–399.
- Weiskopf, N. (2012). "Real-time fMRI and its application to neurofeedback." Neuroimage **62**(2): 682-692.
- Weiskopf, N., et al. (2007). "Real-time functional magnetic resonance imaging: methods and applications." Magn Reson Imaging **25**(6): 989-1003.
- Wiens, E. S. M., and Edward S. Katkin (2000). "Heartbeat detection and the experience of emotions." COGNITION AND EMOTION **14** (3): 417- 427.

Self-Regulation of Anterior Insula with real-Time fMRI and Its Behavioral Effects in Obsessive-Compulsive Disorder: A Feasibility Study

Korhan Buyukturkoglu^{1,2}, Hans Roettgers³, Jens Sommer³, Mohit Rana^{1,2,5}, Leonie Dietzsch³, Ezgi Belkis Arıkan³, Ralf Veit³, Rahim Malekshahi^{1,2}, Tilo Kircher³, Niels^{2,4} Birbaumer, Ranganatha Sitaram^{2,5}, Sergio Ruiz^{2,6}

¹Graduate School of Neural & Behavioural Sciences, International Max Planck Research School, University of Tübingen, Tuebingen, Germany,

²Institute for Medical Psychology and Behavioural Neurobiology, University of Tuebingen, Tuebingen, Germany,

³Department of Psychiatry and Psychotherapy, Philipps-University Marburg, Marburg, Germany,

⁴Ospedale San Camillo, Istituto di Ricovero e Cura a Carattere Scientifico, Venezia, Italy,

⁵Department of Biomedical Engineering, University of Florida, Gainesville, Florida, United States of America,

⁶Departamento de Psiquiatría, Escuela de Medicina, Centro Interdisciplinario de Neurociencia, Pontificia Universidad Católica de Chile, Santiago, Chile

RESEARCH ARTICLE

Self-Regulation of Anterior Insula with Real-Time fMRI and Its Behavioral Effects in Obsessive-Compulsive Disorder: A Feasibility Study

Korhan Buyukturkoglu^{1,2*}, Hans Roettgers^{3*}, Jens Sommer³, Mohit Rana^{1,2,5}, Leonie Dietzsch³, Ezgi Belkis Arikani³, Ralf Veit², Rahim Malekshahi^{1,2}, Tilo Kircher³, Niels Birbaumer^{2,4}, Ranganatha Sitaram^{2,5*}, Sergio Ruiz^{2,6*}

1 Graduate School of Neural & Behavioural Sciences, International Max Planck Research School, University of Tübingen, Tuebingen, Germany, **2** Institute for Medical Psychology and Behavioural Neurobiology, University of Tuebingen, Tuebingen, Germany, **3** Department of Psychiatry and Psychotherapy, Philipps-University Marburg, Marburg, Germany, **4** Ospedale San Camillo, Istituto di Ricovero e Cura a Carattere Scientifico, Venezia, Italy, **5** Department of Biomedical Engineering, University of Florida, Gainesville, Florida, United States of America, **6** Departamento de Psiquiatría, Escuela de Medicina, Centro Interdisciplinario de Neurociencia, Pontificia Universidad Católica de Chile, Santiago, Chile

* These authors contributed equally to this work.

* smruiz@med.puc.cl (SR); ranganatha.sitaram@bme.ufl.edu (RS)



CrossMark
click for updates

OPEN ACCESS

Citation: Buyukturkoglu K, Roettgers H, Sommer J, Rana M, Dietzsch L, Arikani EB, et al. (2015) Self-Regulation of Anterior Insula with Real-Time fMRI and Its Behavioral Effects in Obsessive-Compulsive Disorder: A Feasibility Study. PLoS ONE 10(8): e0135872. doi:10.1371/journal.pone.0135872

Editor: Aviv M. Weinstein, University of Ariel, ISRAEL

Received: March 3, 2015

Accepted: July 27, 2015

Published: August 24, 2015

Copyright: © 2015 Buyukturkoglu et al. This is an open access article distributed under the terms of the [Creative Commons Attribution License](https://creativecommons.org/licenses/by/4.0/), which permits unrestricted use, distribution, and reproduction in any medium, provided the original author and source are credited.

Data Availability Statement: Due to ethical restrictions imposed by the ethics committee of the Faculty of Medicine, University of Marburg, related to protecting patient confidentiality, all relevant data is available upon request to Dr. Korhan Buyukturkoglu (korhan.buyukturkoglu@mssm.edu).

Funding: This study was supported by the Center of Integrated Neurosciences-Tuebingen (CIN-Pool Project 2011-08) <http://www.cin.uni-tuebingen.de/>; RS SR NB; Comisión Nacional de Investigación Científica y Tecnológica de Chile (Conicyt) through Fondo Nacional de Desarrollo Científico y

Abstract

Introduction

Obsessive-compulsive disorder (OCD) is a common and chronic condition that can have disabling effects throughout the patient's lifespan. Frequent symptoms among OCD patients include fear of contamination and washing compulsions. Several studies have shown a link between contamination fears, disgust over-reactivity, and insula activation in OCD. In concordance with the role of insula in disgust processing, new neural models based on neuroimaging studies suggest that abnormally high activations of insula could be implicated in OCD psychopathology, at least in the subgroup of patients with contamination fears and washing compulsions.

Methods

In the current study, we used a Brain Computer Interface (BCI) based on real-time functional magnetic resonance imaging (rtfMRI) to aid OCD patients to achieve down-regulation of the Blood Oxygenation Level Dependent (BOLD) signal in anterior insula. Our first aim was to investigate whether patients with contamination obsessions and washing compulsions can learn to volitionally decrease (down-regulate) activity in the insula in the presence of disgust/anxiety provoking stimuli. Our second aim was to evaluate the effect of down-regulation on clinical, behavioural and physiological changes pertaining to OCD symptoms. Hence, several pre- and post-training measures were performed, i.e., confronting the patient with a disgust/anxiety inducing real-world object (Ecological Disgust

Tecnológico Fondecyt (project n°11121153) <http://www.conicyt.cl> SR; European Union and Indian collaboration grant (New INDIGO) <http://www.newindigo.eu/> RS; Badenwuerttemberg-Singapore Life Sciences grant RS; EU Collaborative Project BRAINTRAIN <http://www.braintrainproject.eu/> NB; Proyectos de Investigación Interdisciplinaria, Vicerrectoría de Investigación (VRI), Pontificia Universidad Católica de Chile, <http://www.uc.cl/> SR and Deutsche Forschungsgemeinschaft (DFG), Koselleck Award <http://www.dfg.de/> NB. The funders had no role in study design, data collection and analysis, decision to publish, or preparation of the manuscript.

Competing Interests: The authors have declared that no competing interests exist.

Test), and subjective rating and physiological responses (heart rate, skin conductance level) of disgust towards provoking pictures.

Results

Results of this pilot study, performed in 3 patients (2 females), show that OCD patients can gain self-control of the BOLD activity of insula, albeit to different degrees. In two patients positive changes in behaviour in the EDT were observed following the rtfMRI trainings. Behavioural changes were also confirmed by reductions in the negative valence and in the subjective perception of disgust towards symptom provoking images.

Conclusion

Although preliminary, results of this study confirmed that insula down-regulation is possible in patients suffering from OCD, and that volitional decreases of insula activation could be used for symptom alleviation in this disorder.

Introduction

Obsessive-compulsive disorder (OCD) is among the most disabling anxiety conditions and accounts for more than half of serious anxiety cases [1]. It can have disabling effects throughout the patient's lifespan. To be diagnosed with OCD, a person must have obsessions and/or compulsions [2]. Among the most common obsessions are contamination fears (usually followed by washing compulsions), which are intense and intrusive feelings of being polluted or infected by contact with the dirty, infectious or soiled objects [3,4].

Prior work on the neural basis of OCD with neuroimaging techniques suggested an abnormal activation of several brain areas including the prefrontal cortex, orbitofrontal cortex, parietal cortex, cingulate gyrus, putamen, globus pallidus, nucleus accumbens and thalamus [5–7]. Hence, current models of the disease hypothesize a dysfunction in the above cortico-subcortical circuitry [8–10].

Pharmacological therapy (performed by drugs that exert their action on the serotonergic neurotransmission), and cognitive behavioral therapy (CBT) are the most commonly used methods in the treatment of OCD [11–13]. Functional brain imaging (PET, SPECT, fMRI) studies exploring the brain activity of the OCD patients show decreased activity levels in several brain areas after successful treatment (with these and other therapeutic approaches), mainly in nucleus accumbens (NAc), anterior cingulate cortex (ACC), thalamus, orbitofrontal cortex (OFC) and insula in parallel with symptom improvement [14–20].

More recent efforts have tried to elucidate OCD's neural basis in concordance with the heterogenic presentation of the disorder. In this sense, several studies have shown a link between contamination fears, disgust over-reactivity, and insula activation. Activation in the insula is associated with interoceptive/subjective feelings (e.g., pain, temperature, or itch stimuli), and the anterior part of this paralimbic structure is involved in disgust processing as a part of the gustatory cortex, containing neurons that respond to pleasant and unpleasant taste [21, 22].

Several sources of evidence support the aforementioned link between contamination fears, disgust over-reactivity, and insula activation. First, disgust is strongly associated with the fear of contamination and subsequent washing compulsions [4, 23, 24]. Furthermore, heightened disgust feelings towards disgust-inducing stimuli, and greater behavioral avoidance from

disgusting objects, situations and places are commonly observed in OCD patients, especially those with contamination fears and washing compulsions [25–35]. On the other hand, findings from functional neuroimaging studies have indicated that when subjects are presented disgust inducing stimuli, the insula is highly activated in persons with OCD, especially in the group of patients with contamination fears [32, 36, 37].

In summary, there is strong evidence that disgust sensitivity and an over-activation in the anterior part of the insula might contribute to avoidance by increasing the aversiveness of exposure to certain stimuli, and strengthening beliefs about contamination [38]. These results suggest that a reduction of insula activity could enable a reduction in contamination anxiety in the subgroup of OCD patients who suffer predominantly from contamination fears and washing compulsions.

A Brain-Computer Interface (BCI) is a system that measures the neural activity in the central nervous system (CNS) and converts it into artificial outputs that can replace, restore, enhance, supplement, or improve a natural output [39]. BCIs can also transform brain signals into available sensory inputs that can in turn modify behavior. A variation of BCI that has recently attracted interest is the BCI-neurofeedback. With the introduction of real-time functional magnetic resonance imaging (rtfMRI) to the BCI approach (rtfMRI-neurofeedback), voluntary control over specific brain areas has been achieved both in healthy participants [40–42] and patients suffering from neuropsychiatric diseases, such as schizophrenia and depression [43–47] (for detailed reviews see [48–50]).

In a recent study, Scheinost and colleagues [51] explored the effect of rtfMRI-neurofeedback training on healthy individuals without a clinical diagnosis of anxiety disorder, but who suffered from contamination anxiety when disgust inducing stimuli were presented to them. Participants who successfully learned to control the activity of orbitofrontal cortex displayed changes in resting-state connectivity across different brain areas and an enhanced control over contamination anxiety many days after the completion of the training. These results encourage the application of rtfMRI-neurofeedback in OCD patients.

Based on the above data, we designed a pilot rtfMRI-neurofeedback study in OCD patients, with two major aims. Our first aim was to investigate whether patients suffering from OCD with predominantly contamination obsessions and washing compulsions can learn to volitionally decrease (down-regulate) the BOLD activity in the anterior insula. Our second aim was to evaluate the effect of down-regulation training on clinical, behavioral and physiological changes pertaining to OCD symptoms. The further goal of this study is to ascertain the feasibility and benefits of our method for a future larger study. Hence, in addition to evaluations related to clinical symptomatology, we include three assessments designed to evaluate how self-regulation affects individual responses towards disgust inducing stimuli outside the scanner environment: 1) Ecological disgust test (EDT), conducted in real-life conditions, in which OCD patients were confronted with real, disgusting objects (e.g., chewed gums, used toilet paper), to investigate how learned down-regulation of insula modulates the patient's ability to bear the proximity of a symptom-provoking object. 2) Disgust picture-rating test, in which patients rated disgust evoking pictures in different dimensions (valence, arousal and symptom provocation), outside the scanner, while performing down-regulation of insula without real-time feedback. In addition, physiological measures, namely, skin conductance level and heart rate variability were recorded in the same session. 3) During the rtfMRI-neurofeedback trainings, variability of heart rate and pupil size were measured in order to investigate the relationship between insula control and autonomic functions.

In view of the sample size for the pilot study, we have chosen to present individual patient data to assess the feasibility of our extensive experimental set-up, and from there to choose the most optimal clinical, behavioral, physiological, and fMRI parameters for a future larger study aimed at establishing a therapeutic intervention for OCD.

Material and Methods

Participants

Three adult OCD patients (2 females), diagnosed based on the Diagnostic and Statistical Manual of Mental Disorders [2] in control at the Department of Psychiatry and Psychotherapy, University of Marburg, Germany, participated in the study. Patients suffered from pronounced contamination obsessions and washing compulsions, as confirmed by a standardized clinical interview. All participants gave their written informed consent before participation. This study was approved by the ethics committee of the Faculty of Medicine, University of Marburg.

Experimental protocol

To measure the effects of rtfMRI-neurofeedback training on OCD patients, we applied several pre- and post-training tests. Between the pre- and post-test, patients underwent several sessions (days) of rtfMRI-neurofeedback trainings. Patients were trained to down-regulate the BOLD signal extracted from the left and right anterior insula. Pre- and post-tests were based on identical experimental protocols, but in the post-test patients used the cognitive strategies that they have learned inside the scanner used to down-regulate the anterior insula. The neurofeedback training and the pre- and post-tests were conducted over a duration of 10 days for each participant (see [Table 1](#)).

Screening

On the first day of the study, a trained clinical psychologist administered the scales and questionnaires, and obtained basic demographic information (such as gender, age, educational background), duration of the disease, previous psychotropic medications, and years using psychopharmacological medication. A vocabulary test, as a measure of verbal intelligence (Mehrfachwahl-Wortschatz-Intelligenztest, MWI) [52], and the Edinburgh Handedness Inventory [53] were also applied.

Pre-training clinical evaluation. The pre-training clinical evaluation included the following psychometric questionnaires and scales.

The German version of the Yale-Brown Obsessive Compulsive Scale (Y-BOCs) interview was performed to assess the severity of OCD symptoms [54]. In this test a score between 16 and 23 for compulsions and obsessions indicates moderate OCD pathology. Higher scores indicates higher levels of pathology.

The German version of the Beck Depression Inventory [55]. was used to clinically measure depression symptomatology. A score greater than 14 indicates clinically relevant depression.

Table 1. Experimental Protocol.

1 st Day	2 nd Day	3 rd Day	4 th -7 th Day	8 th Day	9 th Day	10 th Day
Edinburgh Handedness Scale, MWI, SCID-I, Y-BOCs, BDI-II, STAI Trait	Ecological Disgust (pre) Test	Picture ratings and physiological measurements (SCL, HR) Pre-test	rtfMRI-neurofeedback trainings and transfer runs, Inside the scanner heart rate measurements, STAI State	Ecological Disgust (post) Test	Picture ratings and physiological measurements (SCL, HR) Post-test	Y-BOCs

The neurofeedback training and the pre- and post-tests were conducted over a duration of 10 days.

doi:10.1371/journal.pone.0135872.t001

The German version of the state-trait-anxiety inventory (STAI) was used for measuring trait and state anxiety [56, 57]. Higher scores are positively correlated with higher levels of anxiety.

Real time fMRI-BCI neurofeedback training. On the first day, before beginning the rtfMRI-neurofeedback training, a functional localizer run and a structural scan were both acquired to select the regions of interest (ROI1: left anterior insula and ROI2: right anterior insula). We used both structural and functional information, as the latter is expected to improve the accuracy of ROI selection [58], while the former is considered to be clinically more useful [59].

During the functional localizer run, 30 symptom provocative pictures and 30 neutral pictures were presented to the patients in 5 blocks. These pictures were selected from a pool which contains 150 symptom provocative (e.g., pictures of body waste, rotten food, blood injury, rats, cockroaches, dead animal corpses, vomit, etc.) and 50 neutral pictures (landscapes, objects from daily life) obtained from the International Affective Picture System (IAPS) [60] and several internet sources. Twenty-five healthy subjects rated the pictures in the dimensions of disgust, anxiety and visual complexity prior to the experiments. Pictures with the highest disgust and anxiety ratings were selected to be used in the rtfMRI-neurofeedback trainings. Selected pictures were counterbalanced according to their visual complexity. Visual complexity was defined as the level of details and the intricacy in the presented pictures. Although some of the pictures from the pool matched with other pictures in the manner of disgust and anxiety inducement levels, if their visual complexity ratings were very different; i.e., more or less complex than others, they were not selected to be included in the picture set.

Each picture lasted for 3 seconds (2 TRs). Picture presentation blocks were followed by Rest blocks in which patients were instructed to look at the plus sign on the black screen and relax. Presentation (Neurobehavioral Systems, Berkeley, CA) was used as the software for the stimulus delivery. Brain data were analyzed in real-time with the commercially available software (Turbo-Brain Voyager 3.0, Brain Innovation, Maastricht, The Netherlands) [61]. A structural T2*-weighted localizer with identical slice orientation as the functional localizer was measured with a voxel size of 2.1x2.1x2mm³. The primary motor area was selected as a reference ROI, namely ROI3, to cancel out the effect of movement related activation and global, unspecific activations, and to nullify the effect of an imprecise activation on feedback.

Each rtfMRI-neurofeedback session (day) consisted of 4 training runs. Each training run consisted of 6 alternating blocks of baseline, down-regulation and neurofeedback and reward blocks. During baseline and down-regulation blocks, the same 30 disgust inducing images in the functional localizer run were projected on a screen at the back of the MRI scanner. The projected images could be viewed by the patients via a mirror mounted on the head coil of the MRI.

Baseline blocks were indicated by the discriminating stimulus, plus sign (+), on the right side of each disgust inducing image. Every block lasted for 30 seconds during which participants were instructed to look directly at the screen, view the images, and not suppress the feelings triggered by these images. For the down-regulation blocks (indicated by the discriminating stimulus, down arrow (↓), on the right side of the picture, 27 seconds each), participants were instructed to find an effective cognitive strategy to decrease the feedback signal while viewing the images. No specific cognitive strategy was suggested to the participants. Every image was used for both baseline and down-regulation blocks separately at least once through the runs. Fig 1 shows the flow chart of the rtfMRI-neurofeedback training runs.

The neurofeedback protocol was based on operant conditioning, wherein the visual display of monetary reward at the end of each neurofeedback trial served as the reinforcement. Reinforcement was calculated and presented immediately following each down-regulation block (at the interval of 3 seconds). The amount of monetary feedback was calculated by using the following

rtfMRI-BCI Neurofeedback Training

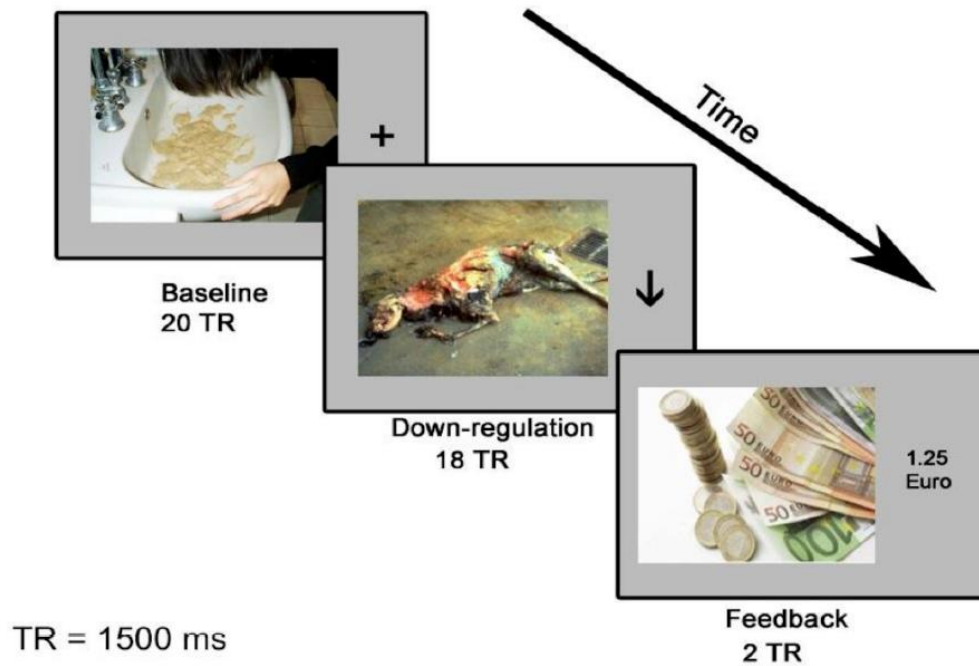


Fig 1. Flow of the rtfMRI-neurofeedback training run. Each run consisted of 6 baseline (duration: 30 seconds each) and 6 down-regulation blocks (duration: 27 seconds each). Immediately following each block of down-regulation, a monetary feedback was presented for 3 seconds. The same design was used for the transfer runs (5th run of the each session) but no feedback was presented.

doi:10.1371/journal.pone.0135872.g001

equation:

$$f = C \left\{ \text{mean} \left(\frac{ROI_1 + ROI_2}{2} - ROI_3 \right)_{\text{baseline}} - \text{mean} \left(\frac{ROI_1 + ROI_2}{2} - ROI_3 \right)_{\text{regulation}} \right\}$$

where, C was an arbitrary but fixed proportionality constant. A positive feedback value was presented when the mean BOLD value was reduced during the down-regulation condition relative to the baseline condition. If the mean BOLD level during down-regulation was the same or higher than the baseline value, the resulting feedback was presented as zero. Due to the potentially disturbing effect of the disgust pictures presented inside the scanner and the anxiety which might be triggered by the scanning process itself, we did not want to further induce a negative emotion led by either negative reinforcement or punishment. Hence, we presented only positive feedback values which signals to the participants that their response is correct [62].

Training runs with contingent feedback were interspersed with “transfer runs” in which the patients were asked to down-regulate the ROIs without the aid of the feedback, and by using the mental strategy learned during the neurofeedback training. Transfer runs were included in

order to train subjects to self-regulate in a real-world environment (outside the scanner). Twelve pictures from the neurofeedback runs were used as stimuli in the transfer run.

Brain data were analyzed in real-time with the Turbo-BrainVoyager [61], which includes on-line incremental 3D motion detection and correction, and drift removal. The software is capable of incrementally computing statistical maps based on the General Linear Model (GLM) and event-related averages. The visual feedback (“monetary reward”) was calculated from brain activity using Matlab 2012b (The MathWorks, Natick, MA) software running on a separate computer connected via a local area network (LAN) to the scanner and to the Turbo-Brain Voyager computer [63].

During the rtfMRI-neurofeedback training sessions heart rate (HR) measures were collected as an indicator of the OCD related sympathetic-parasympathetic activity. Heart rate variability (HRV) was monitored using a pulse oximeter. Inter-beat intervals were converted to heart rate in beats per minute (BPM). The distributions of the data were checked for normality with Shapiro-Wilk test. Differences between the baseline and the down-regulation conditions in the pre-test were statistically compared with the differences between the baseline and the down-regulation conditions in the post-test by applying paired samples t-tests with SPSS v19 (IBM, Armonk, NY).

Patients completed the German version of State-Trait Anxiety Inventory (STAI-State) before and after each session as a measure of their anxiety levels related to the fMRI measurement.

MR acquisition. MRI scans were acquired using a 3.0 Tesla body scanner, with standard 12-channel head coil (Siemens Magnetom Tim TRIO, Siemens, Erlangen, Germany) at the Department of Psychiatry, University of Marburg, Germany. A standard echo-planar imaging sequence was used for acquiring functional images (EPI; TR: 1.5 s, TE: 30 ms, matrix size: 64x64, flip angle α : 90°). Each volume consisted of 16 axial slices (voxel size: 3.3 x 3.3 x 5.0 mm³, slice gap of 1 mm) in AC-PC alignment. For the structural localizer we used T2*w images (56 axial slices, voxel size 2.1 x 2.1 x 2mm³, gap of 0.4 mm, TR: 4.5 s, TE: 35ms, matrix size: 100x100, flip angle α : 90°). In order to superimpose functional maps on brain anatomy, a high-resolution T1-weighted structural scan was collected in each session (MPRAGE, matrix size: 256 x 256, 176 sagittal slices, 1mm³ isotropic voxels, TR = 1900 ms, TE: 2.52 ms, TI: 900 ms, flip angle α : 9°).

Offline fMRI analysis. Hypothesis driven ROI analysis was performed using the ROIs previously selected for each patient during the rtfMRI sessions/neurofeedback runs. We performed fMRI pre-processing and statistical analysis using the FMRIB Software Library (FSL, <http://www.fmrib.ox.ac.uk/fsl>, Centre for Functional MRI of the Brain, Oxford University, UK). Data processing included rejection of the first 10 volumes, motion correction (MCFLIRT), slice timing correction, spatial smoothing (full width half maximum, 5mm) and high pass filtering (cutoff frequency 1/60Hz). Z (Gaussianised T/F) statistic images were thresholded using clusters determined by $Z > 2.3$ and $Z < -2.3$ and a (corrected) cluster significance threshold of $P = 0.05$.

fMRI data analysis packages like FSL, based on the GLM method, are more sensitive to mean differences in the BOLD signals between experimental conditions, and hence are more suitable for finding statistically significant differences in brain activity when neurofeedback training is sufficiently long and effective. However, the GLM is less sensitive to trial-by-trial variations in the form of systematic increases or decreases during the course of neurofeedback training. Furthermore, earlier studies by our group [41] showed that down-regulation of insula is relatively more difficult to achieve than up-regulation, especially when shorter durations of neurofeedback training was employed. In consideration of the above, we wanted to develop a more sensitive measure of down-regulation that can potentially detect a learning effect due to

neurofeedback training. Towards this end, we compared the BOLD signal level in the ROIs for every repetition time (TR) during the down-regulation blocks with the mean BOLD level during the previous baseline block. If the BOLD signal level in the down-regulation block was lower than the mean BOLD of the previous baseline block for that particular TR, it was counted as a "hit". Because each down-regulation block lasted 27 seconds (18 TRs), and there were 6 blocks through one run, the maximum number of hits for one run could be 108. We counted every hit of every down-regulation block during the run, and converted the total number of hits into the percentages. We named this analysis as the "hits analysis".

We reported results of both the GLM and the percentage of hits analyses for each patient, separately.

During the rtfMRI-neurofeedback training sessions, eye-tracker recordings (SR-Research, Eyelink 1000) were performed to evaluate whether patients were attending to the presented pictures during baseline and down-regulation conditions. Recordings indicated that patients attended to the pictures during the training sessions. None of the patients kept their eyes closed during any part of the experiment.

Pre and Post behavioral tests. These tests were conducted in each participant before and after the rtfMRI-neurofeedback training. Statistical analysis of behavioral and physiological data was performed by applying repeated measures two-way ANOVA (factors: time and condition) and post-hoc t-tests.

1. Ecological disgust test (EDT). The EDT was designed to evaluate each patient's response to a symptom-provoking stimulus in a naturalistic environment. Outside the scanner and in a separate room, patients were shown real-world disgusting objects, selected individually for each patient according to his/her own self-reports during the screening session. The object was placed in the first position on a wheeled table at a distance of 5 meters apart from the patient. On the left side of this object, a clearly visible '+' sign and/or a '↓' sign was shown. In each trial, the selected object was slowly brought towards the patient at a constant pace, either with the '+' sign or with the '↓' sign. There were 20 trials of this kind, each sign being presented 10 times. Patients were instructed to focus on the object, and say 'stop' when they feel that the object should not come any closer. As long as the patient does not say 'stop', the experimenter would move closer, and at the end bring the object in contact with the patient's hand. The distances between the starting point and the point at the "stop" moment were measured for '+' signed and '↓' signed blocks along the direction of movement of the experimenter for both pre-test and post-tests. The meanings of the signs ('+' = baseline, '↓' = insula down regulation) were not explained to the patients in the pre-test sessions. In the post-test, the same procedure and objects were used, but this time participants were instructed to use the cognitive strategies that they had learned during rtfMRI-neurofeedback trainings. Thus, in the above tests, participants were instructed to recreate mental strategies that they had used during the neurofeedback training of down-regulation (during presentation of the discriminating stimulus '↓') of anterior insula, but now in the absence of feedback and in real-life conditions.

We expected that down-regulation of anterior insula would allow the patient to stay closer to the disgust object than during baseline condition (once down-regulation was learned, i.e., in the post-test).

[Fig 2](#) shows the materials used in the Ecological Disgust Test.

2. Picture rating test. We tested patient responses to disgusting pictures in a naturalistic environment, outside the scanner, using a set of visual contamination, anxiety inducing stimuli. During the pre-test, another 50 pictures (30 contamination anxiety related, 20 neutral) taken from our previously constructed picture pool were presented to the patients (15 seconds each) two times, in two separate runs, in a counterbalanced order via a 21.5" LCD monitor. Patients were shown either a down arrow ('↓') or a plus sign ('+') on the right side of the screen attached

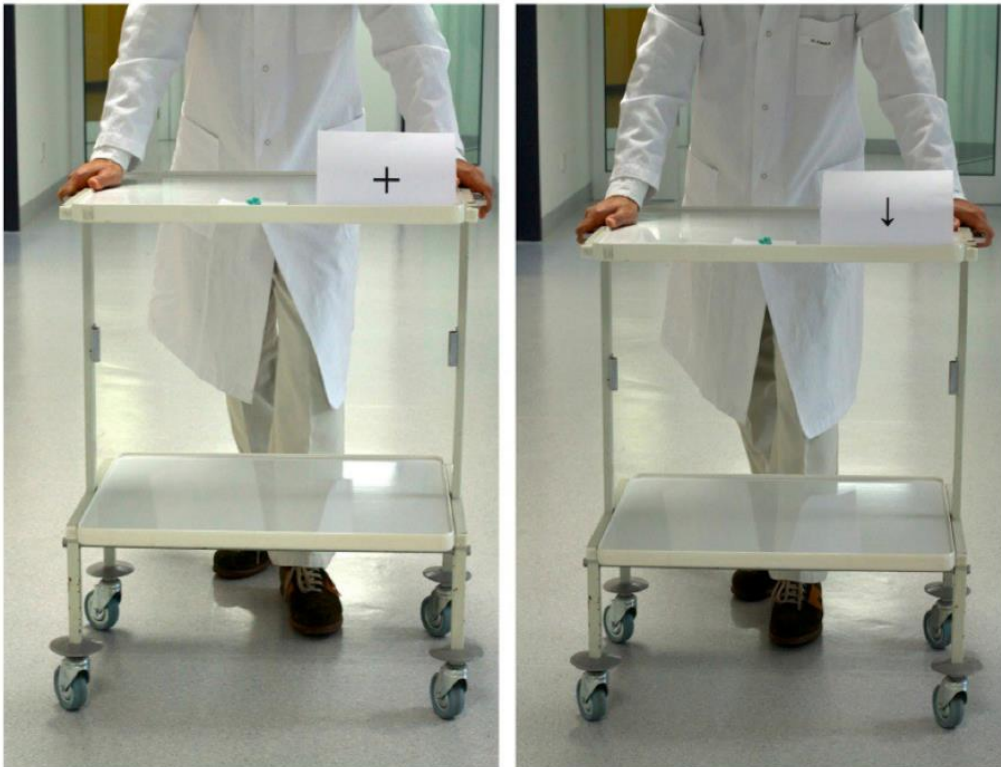


Fig 2. The Ecological Disgust Test and the flow of the experiment. The experimenter approached the patient with a real-life, disgust-inducing object from a distance of 5 meters either with a '↓' or '+' cue (10 times each). The patient focused on the object (two newly chewed gums in this picture) as the experimenter approached him/her, and said "stop" whenever he/she felt that the object should not come any closer. In the pre-test, the meanings of the cues are not explained to the patients. In the post-test, during down-arrowed runs, patients used the cognitive strategies that they had learned in the rtfMRI-neurofeedback training sessions.

doi:10.1371/journal.pone.0135872.g002

to each picture. Pictures that were presented with the ('+') sign (baseline condition) in the first run were presented with the ('↓') sign (down-regulation condition) in the second run. The meanings of these signs were not explained to the patients in the pre-test. Patients were asked to rate the pictures after each presentation in three dimensions, i.e. valence, arousal and OCD-symptom provocation by using a visual analogue scale (VAS) [64], with the help of the computer mouse. The positions of respondents' marks on the VAS were scaled as distinct points, resulting in codes from 1 to 1900. In the post-test, the same procedure was used, except for the fact that during the down-regulation conditions, patients were instructed to use the cognitive strategies that they had learned in rtfMRI-neurofeedback training.

We expected a modulation of the ratings toward the pictures during down-regulation compared to baseline (once down-regulation was learned, i.e., in the post-test).

Fig 3 shows the Picture Rating Test and the flow of the experiment.

3. Physiological measures during picture ratings (SCL & HR). Physiological responses, i.e. skin conductance level (SCL) and heart rate (HR) were measured by the NeXus-32 Wireless

Physiological Monitoring and Feedback System (Mind Media BV, The Netherlands) during the picture-rating test. Skin conductance was measured from 2 electrodes attached to the palms of the non-dominant hand. Mean skin conductance levels were calculated for two conditions (disgusting picture-baseline, disgusting picture-down-regulation, 15 seconds each). Heart rate variability was monitored using a pulse oximeter. Inter beat intervals were converted to heart rate in beats per minute.

On the 8th, 9th and 10th days of the study (6th, 7th and the 8th days for the first two patients) the post-tests (EDT, picture rating, SCL/HR measurements) were performed.

After the post-tests, the assessment of the general psychopathology was performed again (as in the pre-training clinical evaluation).

To differentiate the effects of variables other than neurofeedback training on the behavioral and physiological results e.g., habituation to the pictures/disgust stimuli, medication or other therapeutics, we compared the differences between baseline and down-regulation conditions (interspersed in the same runs) for both pre-test and post-test. Because the patients did not know the meanings of the ('↓') or ('+') signs in the pre-test, we did not expect any difference between baseline and down-regulation conditions in the pre-test.

Results

In this section, we shall elaborate on the results of each patient's pre-test, rtfMRI-neurofeedback training and post-test, separately. We have chosen to present individual patient data instead of group data due to the small sample size of this pilot study.

Patients No. 1 and No. 2 participated for 2 days in the rtfMRI-neurofeedback training (on the 4th and 5th days of their measurements) and continued with the post-tests on the 6th, 7th and 8th days, while patient 3 participated in four days of neurofeedback training and then continued with the post-tests on 8th, 9th and 10th days.

Patient 1

Patient 1 was a 19-year-old right-handed female. She was undergoing cognitive behavioral psychotherapy for 3 weeks during the measurements, and was not using psychotropic medication.

According to SCID-I interview, Patient 1 met the criteria for OCD with predominantly compulsive behavior. The Y-BOCs score also indicated mild OCD symptoms at the pre-test and the post-test. The BDI-II indicated severe depression. In comparison to healthy subjects, the patient suffered from higher anxiety levels according to the STAI trait.

Patient's pre-post questionnaire results are presented in [Table 2](#).

Real-time fMRI-BCI neurofeedback training analysis

Offline fMRI analysis. Due to technical difficulties, Patient 1 could complete only two runs of rtfMRI-neurofeedback training on the first day of rtfMRI-neurofeedback training.

Comparison of brain activity of Patient 1 for the down-regulation condition between the 1st and 2nd days showed increased activity in right superior frontal gyrus, right middle temporal gyrus, left postcentral gyrus, medial frontal cortex, brain stem and middle temporal gyrus/temporooccipital part on the second day of rtfMRI-neurofeedback training. Activity decreases on the second day as compared with the first day were observed in the supplementary motor area (SMA), precentral gyrus, anterior and posterior cingulate gyrus, middle frontal gyrus, left posterior supramarginal gyrus, orbitofrontal cortex (OFC), anterior insula, superior temporal gyrus, frontal pole, left and right caudate, left precuneus, lingual gyrus and occipital pole.

[Fig 4](#) shows comparison of brain activity for the down-regulation condition between the 1st and 2nd days of the rtfMRI-neurofeedback training.



Fig 3. Picture-rating test. Patients rate each picture at the dimensions of valence, arousal and OCD symptom provocation. During the ratings, skin conductance level and heart rate data were collected.

doi:10.1371/journal.pone.0135872.g003

Hits analysis. Fig 5 shows the percentage of hits for Patient 1 achieved during rtfMRI-neurofeedback training and the transfer runs from right and left anterior insula, respectively. On the second day, in the transfer run, the patient had 89 hits in the left insula, which corresponds to 82% of the possible total hits in a run. The patient used “thinking funny stories” as her cognitive strategy for down-regulation.

Table 2. Clinical evaluation of the Patient 1.

TEST	SCID I	Y-BOCs	BDI-II	STAI Trait	STAI State
Pre-test	F42.1 OCD, Predominantly compulsive acts	12	42	76	Pre-scan 69, Post-scan 68
Post-test	-	11	-	-	Pre-scan 48, Post-scan 40

doi:10.1371/journal.pone.0135872.t002

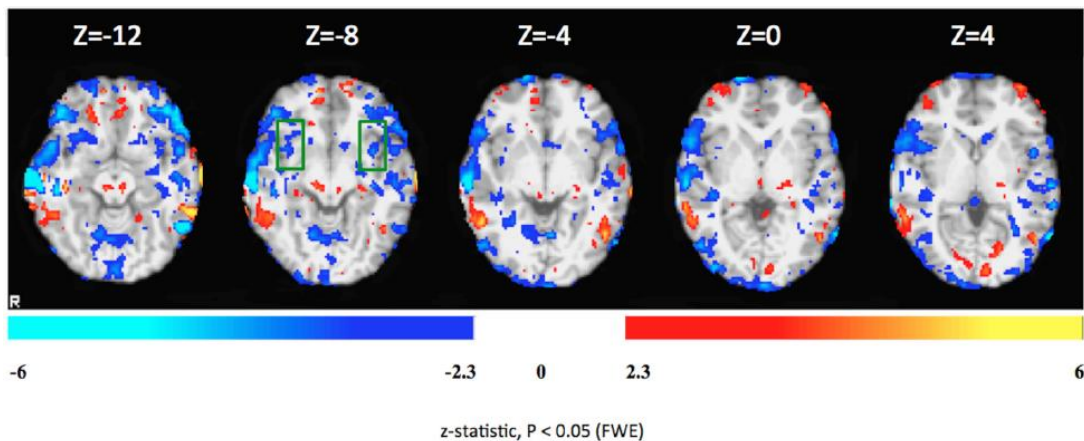


Fig 4. Differential brain activations during the down-regulation condition in Patient 1 on the first and second days of rtfMRI-neurofeedback training. Colors red-yellow: increased activity on the second day as compared to the first day. Blue-white: decreased activation the second day as compared to the first day. The colored functional maps were overlaid on T1-weighted structural images of four representative axial brain sections covering insula, which is delineated by the green rectangle. Statistical significance was based on z-statistic threshold of -2.3 and 2.3 followed by multiple comparisons correction at the cluster level using Family-Wise Error (FWE) at $p < 0.05$.

doi:10.1371/journal.pone.0135872.g004

Statistical comparisons (Wilcoxon signed-rank test) showed no significant difference between the 1st and 2nd day of trainings both for the right insula (day 1 mean number of hits = 60.5, sd = 2.12; day 2 mean number of hits = 50.2, sd = 5.11; $p = 0.18$), and the left insula (day 1 mean number of hits = 52.5, sd = 13.45; day 2 left mean number of hits = 62.4, sd = 19.2; $p = 0.655$).

No statistically significant difference was found between the left and right insula for both 1st ($p = 0.317$) and the 2nd day ($p = 0.223$) as well.

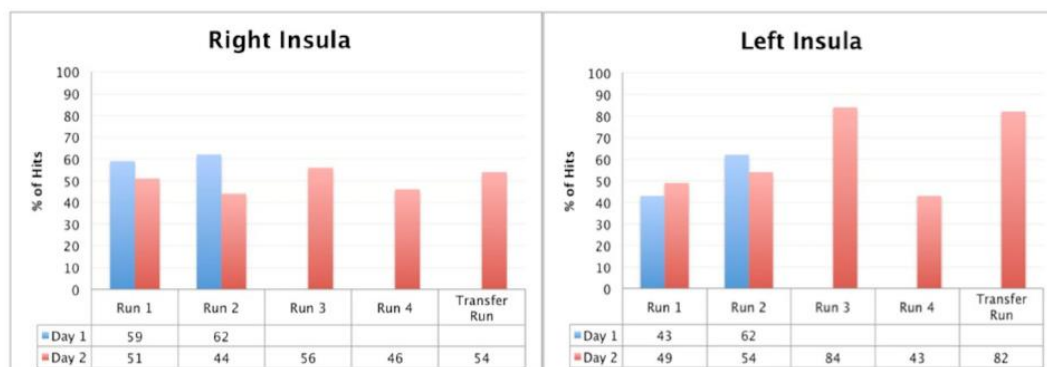


Fig 5. Patient 1, the percentage of the hits from the right and the left anterior insula through rtfMRI-neurofeedback trainings respectively. Blue columns show the percentage of the hits of the first, red columns show the second session of rtfMRI-neurofeedback training run by run. Due to technical difficulties, the first patient could complete only two runs of rtfMRI-neurofeedback training on the first session of rtfMRI-neurofeedback training.

doi:10.1371/journal.pone.0135872.g005

Heart rate measurements in the scanner. The first patient's HR scores as beats per minute (BPM) for baseline ($M = 90.03$, $sd = 1.67$), and down-regulation ($M = 87.25$, $sd = 1.68$) conditions on the first day of training were significantly different, $t(11) = 5.528$, $p < 0.01$. There was also a significant difference between baseline ($M = 91.24$, $sd = 3.79$) and down-regulation ($M = 90.36$, $sd = 3.87$) conditions in the second day of training, $t(23) = 2.275$, $p < 0.05$. In both days, HR was lower during the down-regulation blocks compared to the baseline blocks.

Ecological disgust test. In the EDT, two newly chewed gums were used as real-life, disgust objects. The distance between the starting point and the point at the "stop" moment were measured as meters for '+' signed baseline and '↓' signed down-regulation blocks for both pre-test and post-tests. We had 5 baseline and 5 down-regulation blocks in the pre-test for this patient.

Repeated measures two-way ANOVA analysis showed significant effect of time $F(1, 4) = 25.62$, $p < 0.01$ and condition $F(1, 4) = 14.18$, $p = 0.02$. The interaction between the time and the condition was significant as well $F(1, 4) = 7.323$, $p = 0.05$.

Post-hoc paired sample t-tests of the pre-test showed that there was no significant difference between baseline and down-regulation conditions in the patient's response to the disgust objects. A significant difference between baseline ($M = 4.45$ meters, $sd = 0.32$) and down-regulation ($M = 4.89$ meters, $sd = 0.27$) conditions was found in the post-test, $t(9) = -9.258$, $p < 0.01$. During the down-regulation conditions, the experimenter moved closer to the patient with the disgust object. On 3 post-test down-regulation trials, the patient allowed the experimenter to touch her hand with the chewed gum. The patient did not allow the experimenter to touch her with the chewed gum during the baseline trials.

Picture ratings. Repeated measures two-way ANOVA analysis results showed significant effect of time $F(1, 31) = 14.31$, $p < 0.01$ on the arousal ratings. No significant effect of condition $F(1, 31) = 0.224$, $p = 0.639$ and no interaction between time and condition was observed $F(1, 31) = 0.133$, $p = 0.718$.

We found significant effect of time $F(1, 31) = 89.85$, $p < 0.01$ and the condition $F(1, 31) = 23.04$, $p < 0.01$ on the valence ratings. Also, the interaction between time and the condition was found significant $F(1, 31) = 45.62$, $p < 0.01$.

Significant effect of time $F(1, 31) = 119.18$, $p < 0.01$ and condition $F(1, 31) = 40.75$, $p < 0.01$ on the symptom provocation ratings were also observed. There was a significant interaction between the time and the condition for the symptom provocation ratings $F(1, 31) = 81.24$, $p < 0.01$.

In the post-test, the patient rated the pictures as having less negative valence and as being less symptom provocative following the down-regulation blocks ($p < 0.01$ for both conditions).

Physiological measures during picture ratings (SCL & HR). No statistically significant difference was observed in SCL between baseline ($M = 12.22$, $sd = 0.59$) and down-regulation conditions ($M = 12.13$, $sd = 0.43$) in the pre-test in the picture rating test. The differences between baseline ($M = 17.26$, $sd = 7.61$) and down-regulation ($M = 15.03$, $sd = 3.71$) conditions did not reach significance in the post-test either. HR score differences as BPM between baseline ($M = 88.49$, $sd = 2.13$) and down-regulation ($M = 86.82$, $sd = 2.48$) conditions in the pre-test were not significant. Also, no significant difference was observed between baseline ($M = 80.10$, $sd = 3.16$) and down-regulation ($M = 79.79$, $sd = 1.61$) conditions in the post-test.

Patient 2

Patient 2 was a 25 years old right handed female. She was an in-patient, underwent cognitive behavioral psychotherapy for 3 weeks before the measurements and was using psychotropic medication (Setralin 150 mg).

Table 3. Clinical evaluation of the Patient 2.

TEST	SCID I	Y-BOCs	BDI-II	STAI Trait	STAI State
Pre-test	F42.1 OCD, Predominantly compulsive acts.	6	0	51	Pre-scan 40, Post-scan 40
Post-test	-	9	-	-	Pre-scan 31, Post-scan 42

doi:10.1371/journal.pone.0135872.t003

Patient 2 met SCID-I criteria for OCD predominantly with compulsive behavior, and had a low severity of symptomatology according to Y-BOCs. No clinically significant depression or anxiety was detected.

The patient’s pre-post clinical results are presented in [Table 3](#).

Real-time fMRI-BCI neurofeedback training analysis

Offline fMRI analysis. Between the first and the second day of rtfMRI-neurofeedback trainings, we observed an increase in activity in the left postcentral gyrus, posterior cingulate gyrus, right hippocampus and subcallosal cortex on the second day. Deactivations were observed on the second day as compared with the first day in SMA, anterior cingulate gyrus, middle frontal gyrus, frontal pole, thalamus, caudate, inferior frontal gyrus, OFC, insula, putamen, middle temporal gyrus, occipital fusiform gyrus, occipital pole and the lingual gyrus.

[Fig 6](#) shows comparison of brain activity for the down-regulation condition between the 1st and 2nd days of the rtfMRI-neurofeedback training.

Hits analysis. The patient showed similar down-regulation performances on the first and the second days of the rtfMRI-neurofeedback trainings. On the first day, during the transfer runs, she achieved 65 hits (60%) and 71 hits (65%) in the down-regulation of the right and the left insula, respectively. On the second day, the number of hits from the right insula decreased to 56 (51%) but an increase in the number of hits 75 (69%) was observed for left insula.

Statistical comparisons showed no significant difference between the 1st and 2nd day of trainings both for the right insula (day 1 mean number of hits = 71, sd = 14.3; day 2 mean

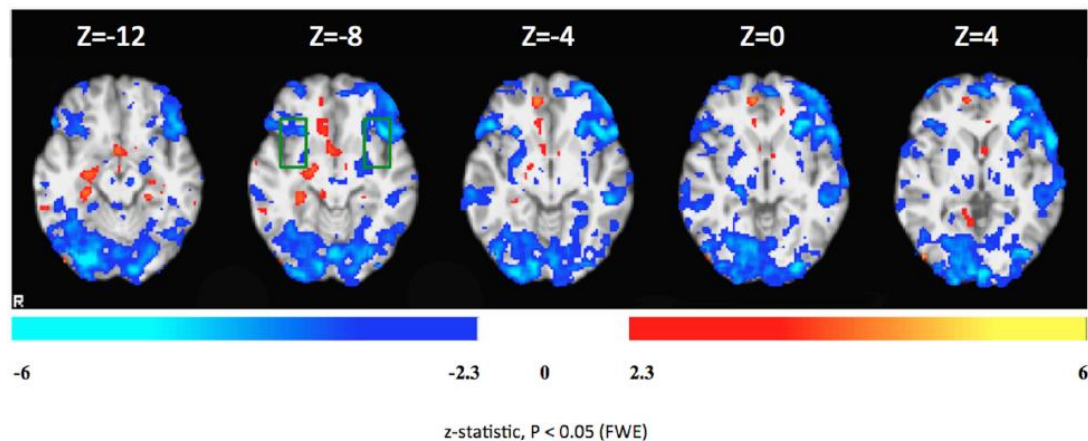


Fig 6. Differential brain activations during the down-regulation condition in Patient 2 on the first and second days of rtfMRI-neurofeedback training. Colors red-yellow: increased activity on the second day as compared to the first day. Blue-white: decreased activation the second day as compared to the first day. The colored functional maps were overlaid on T1-weighted structural images of four representative axial brain sections covering insula, which is delineated by the green rectangle. Statistical significance was based on z-statistic threshold of -2.3 and 2.3 followed by multiple comparisons correction at the cluster level using Family-Wise Error (FWE) at $p < 0.05$.

doi:10.1371/journal.pone.0135872.g006

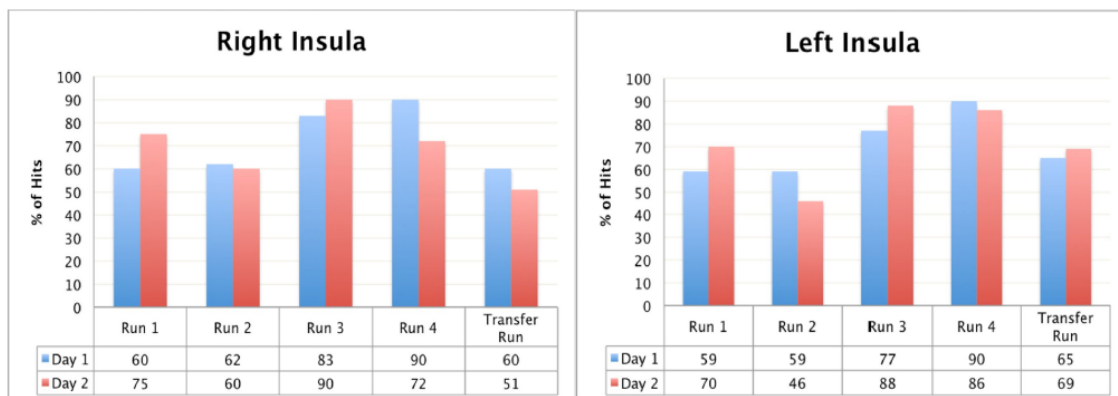


Fig 7. Patient 2, the percentage of the hits from the right and the left anterior insula through rtfMRI-neurofeedback trainings respectively. Blue columns show the percentage of the hits of the first, red columns show the second session of rtfMRI-neurofeedback training run by run.

doi:10.1371/journal.pone.0135872.g007

number of hits = 69.6, $sd = 14.9$; $p = 0.686$), and the left insula (day 1 mean number of hits = 70, $sd = 13.3$; day 2 mean number of hits = 71.8, $sd = 16.8$, $p = 0.785$).

No statistically significant difference was found between the left and right insula for both the 1st ($p = 0.465$) and the 2nd days ($p = 0.786$).

The patient reported “thinking herself lying on the grass” as her cognitive strategy for down-regulation conditions.

Fig 7 shows the percentage of the hits that the patient had through rtfMRI-neurofeedback training and the transfer runs from right anterior insula and left anterior insula, respectively.

Heart rate measurements in the scanner. Patient’s HR scores as BPM for baseline ($M = 82.20$, $sd = 1.46$) and down-regulation ($M = 80.97$, $sd = 2.25$) conditions on the first day of training were significantly different, $t(23) = 2.692$, $p < 0.05$. In the down-regulation condition, the patient showed significantly lower HR compared to the baseline condition. On the second day of training, although the patient continued to show a lower HR in the down-regulation condition, the difference between the baseline ($M = 93.76$, $sd = 2.79$) and the down-regulation ($M = 92.92$, $sd = 2.66$) conditions did not reach significance.

Ecological Disgust Test. In the EDT trials, used toilet papers, taken from a toilet bin and placed inside an open-mouthed nylon bag, were used as disgust objects.

Repeated measures two-way ANOVA analysis showed significant effect of time $F(1, 9) = 45.92$, $p < 0.01$. However no significant effect of condition $F(1, 9) = 2.273$, $p = 0.166$ and time x condition interaction $F(1, 9) = 0.115$, $p = 0.743$ was observed.

Picture rating test. Repeated measures two-way ANOVA analysis showed significant effect of time $F(1, 29) = 16.91$, $p < 0.01$ on the arousal ratings. No effect of condition $F(1, 29) = 0.01$, $p = 0.92$ and interaction between time and condition was observed $F(1, 29) = 1.41$, $p = 0.244$.

Significant effect of time $F(1, 29) = 20.89$, $p < 0.01$ was found on the valence ratings as well. However, no effect of condition $F(1, 29) = 0.218$, $p = 0.644$ and no significant interaction between the time and the condition $F(1, 29) = 0.006$, $p = 0.940$ was observed.

Effects of time on the symptom provocation ratings was significant $F(1, 29) = 14.338$, $p < 0.01$. No significant effect of condition $F(1, 29) = 0.076$, $p = 0.785$ and no interaction effect between the time and the condition was found ($1, 29) = 0.288$, $p = 0.596$.

Table 4. Clinical evaluation of the Patient 3.

SCID I	Y-BOCS	BDI-II	STAI Trait	STAI State
F42.2 OCD, Mixed obsessional thoughts and compulsive acts. Major Depression	Pre-test 36, Post-test 33	35	79	Pre-scan 57, Post-scan 57, Pre-scan 54, Post-scan 55, Pre-scan 65, Post-scan 55, Pre-scan 60, Post-scan 53

doi:10.1371/journal.pone.0135872.t004

Physiological measures during picture ratings (SCL & HR). The difference in SCR between the baseline ($M = 4.83$, $sd = 0.9$) and the down-regulation ($M = 5.21$, $sd = 0.98$) conditions was significant in the pre-test ($p = 0.013$). SCL was higher during down-regulation conditions than the baseline condition. In the post-test SCL differences between the baseline ($M = 2.66$, $sd = 0.51$) and the down-regulation ($M = 2.56$, $sd = 0.63$) conditions were not significantly different.

HR difference as BPM between baseline ($M = 81.89$, $sd = 4.24$) and the down-regulation ($M = 81.84$, $sd = 3.60$) in the pre-test was not significant, but we found a significant difference between the conditions in the post-test ($p = 0.013$). HR was higher in the down-regulation ($M = 90.73$, $sd = 3.25$) condition as compared to the baseline ($M = 89.36$, $sd = 2.43$).

Patient 3

The third patient was a 26-year old left handed male. He was under psychotropic medication (Setralin 125 mg, Risperdal 0.5 mg.), but not undergoing psychotherapy during the measurements. This patient received 4 days of rtfMRI-neurofeedback training.

Patient 3 met criteria for OCD and major depression in accordance with BDI-II. A decrease in the Y-BOCS score was observed after training. Patient 3 showed high levels of anxiety before and during the experiments. Patient’s pre-post questionnaire results are presented in [Table 4](#).

Real-time fMRI-BCI neurofeedback training analysis

Offline fMRI analysis. As compared with the 1st day, Patient 3 showed significantly increased BOLD responses during the down-regulation condition in the left lateral occipital cortex/superior division left, hippocampus, right amygdala and brain stem on the 4th day.

Statistical comparisons of the 1st and the 4th days yielded decreased activity in superior frontal gyrus, SMA, middle frontal gyrus, precentral gyrus, posterior supramarginal gyrus, anterior and posterior cingulate gyrus, precuneus, insula, putamen, caudate, thalamus, OFC, frontal pole, occipital pole, posterior middle temporal gyrus, right anterior supramarginal gyrus and precentral gyrus.

[Fig 8](#) shows comparison between the 1st and 4th days of FSL analyses of the rtfMRI-neurofeedback training.

Hits analysis. Statistical comparisons showed no significant difference between the 1st and 4th day of trainings both for the right insula (day 1 mean number of hits = 65.8, $sd = 10.9$; day 4 mean number of hits = 69.8, $sd = 15.1$; $p = 0.354$), and the left insula (day 1 mean number of hits = 51.8, $sd = 18.8$; day 4 mean number of hits = 54.8, $sd = 17.3$; $p = 0.686$).

No statistically significant difference was found between the left and the right insula for both 1st ($p = 0.225$) and 4th day ($p = 0.43$).

As the mental strategy for down-regulation, the patient mentally replaced the “ugly” parts in the pictures with “nicer” objects. On the third day of training the patient changed his strategy through the runs (e.g., thinking on nice memories and concentrating on colors of the objects). In this session, his overall number of hits was the lowest as compared with the other days.

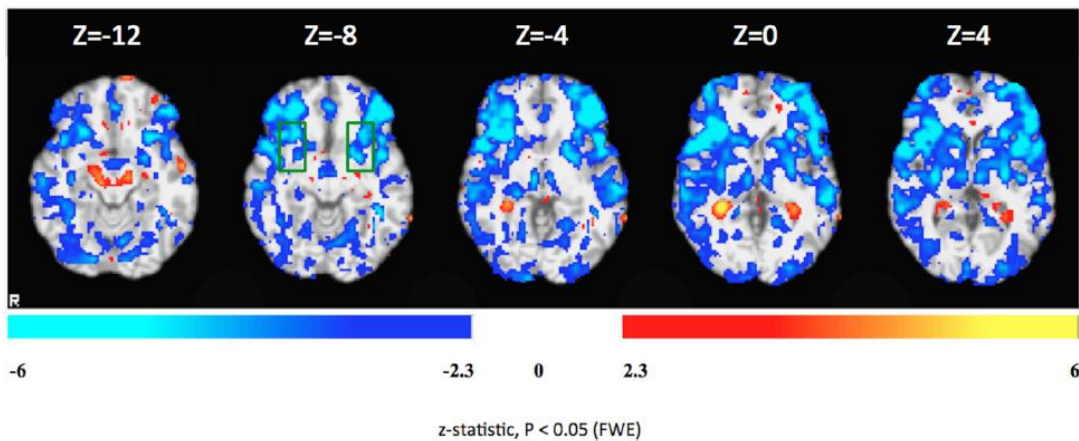


Fig 8. Differential brain activations during the down-regulation condition in Patient 3 on the first and second days of rtfMRI-neurofeedback training. Colors red-yellow: increased activity on the second day as compared to the first day. Blue-white: decreased activation the second day as compared to the first day. The colored functional maps were overlaid on T1-weighted structural images of four representative axial brain sections covering insula, which is delineated by the green rectangle. Statistical significance was based on z-statistic threshold of -2.3 and 2.3 followed by multiple comparisons correction at the cluster level using Family-Wise Error (FWE) at $p < 0.05$.

doi:10.1371/journal.pone.0135872.g008

Fig 9 shows the percentage of the hits that patient had through rtfMRI-neurofeedback training and the transfer runs for four days.

Heart rate measurements in the scanner. In contrast to the previous two patients, the third patient showed increased HR during the down-regulation conditions as compared to the baseline through the rtfMRI-neurofeedback training sessions. On the first day of the training, the scores as BPM for baseline ($M = 72.89$, $sd = 1.26$) and down-regulation ($M = 73.89$, $sd = 1.64$) conditions were significantly different, $t(17) = -2.359$, $p < 0.05$. There was also a significant difference between baseline ($M = 78.51$, $sd = 1.87$) and down-regulation ($M = 79.21$, $sd = 2.19$) conditions on the second day of trainings, $t(23) = -2.536$, $p < 0.05$. For the third day,

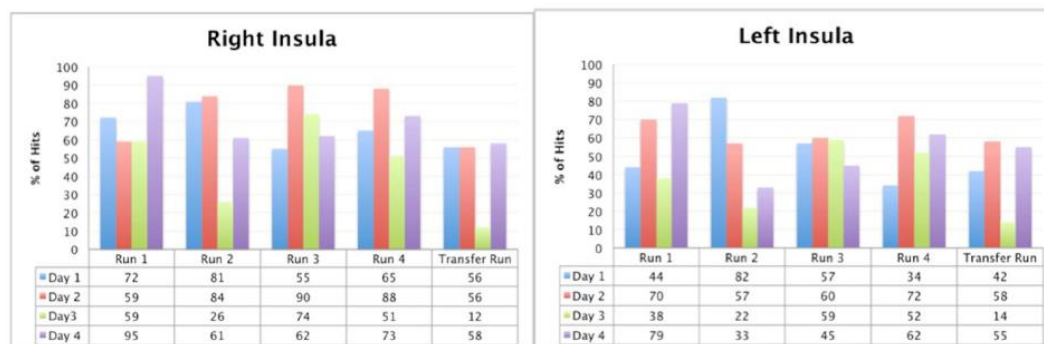


Fig 9. Patient 3, the percentage of the hits from the right and the left anterior insula through rtfMRI-neurofeedback trainings respectively. Blue columns show the percentage of the hits of the first, red columns show the second, green columns show the third and purple columns show the fourth session of rtfMRI-neurofeedback training by run.

doi:10.1371/journal.pone.0135872.g009

no significant difference was found between baseline ($M = 79.43$, $sd = 1.98$) and regulation ($M = 80.21$, $sd = 2.24$) conditions. Likewise, there was no significant difference between baseline ($M = 83.45$, $sd = 3.25$) and down-regulation ($M = 83.91$, $sd = 3.69$) conditions on the fourth day.

Ecological Disgust Test. For this patient, used toilet papers were the real-life disgust objects (similar to that of the second patient). These disgust objects were put into a nylon bag and the nylon bag's mouth was left open.

Repeated measures two-way ANOVA analysis results showed significant time $F(1, 9) = 10.028$, $p = 0.01$ condition $F(1, 9) = 37.166$, $p < 0.01$ and time x condition interaction $F(1, 9) = 11.423$, $p < 0.01$ effects on EDT.

Post-hoc paired samples t-tests revealed that, the difference in the patient's response between baseline ($M = 4.25$ meters, $sd = 0.10$) and down-regulation ($M = 4.27$ meters, $sd = 0.06$) conditions in pre-test did not reach significance. There was a significant difference in the patient's response between baseline ($M = 4.26$ meters, $sd = 0.13$) and down-regulation ($M = 4.49$ meters, $sd = 0.15$) conditions in the post-test, $t(9) = -5.314$, $p < 0.01$. The experimenter could get closer to the patient with the disgust object while the patient used his cognitive strategies during the down-regulation conditions.

Picture rating test. Repeated measures two-way ANOVA analysis results showed no significant effect of time $F(1, 29) = 0.530$, $p = 0.472$, and condition $F(1, 29) = 1.74$, $p = 0.198$ on the arousal ratings. No interaction between time and condition was observed either $F(1, 29) = 0.247$, $p = 0.623$.

No significant effect of time $F(1, 29) = 0.02$, $p = 0.89$ and the condition $F(1, 29) = 2.385$, $p = 0.133$ was observed on the valence ratings too. Also, the interaction between time and the condition was not significant $F(1, 29) = 1.256$, $p = 0.272$.

Effect of time $F(1, 29) = 2.201$, $p = 0.149$ and condition $F(1, 29) = 2.325$, $p = 0.138$ on the symptom provocation ratings were found non-significant. There was no significant interaction between the time and the condition for the symptom provocation ratings $F(1, 29) = 1.293$, $p = 0.265$.

Although no time, condition and time x condition interaction effect were observed on arousal, valence and the symptom provocation ratings, paired samples t-tests revealed significant differences on valence and the symptom provocation ratings between the baseline and down-regulation conditions in the post-test. The patient rated the pictures as less symptom provocative and having less negative valence in the post-test down-regulation conditions (Valence baseline $M = 1884.5$, $std = 95.76$, down-regulation $M = 1825.33$, $std = 166.06$, $p = 0.05$; symptom provocation baseline $M = 1708.07$, $std = 232.47$, down-regulation $M = 1633.53$, $std = 240.25$, $p < 0.05$).

Physiological measures during picture ratings (SCL & HR). We did not observe a statistically significant difference in the SCL between baseline ($M = 1.43$, $sd = 0.18$) and the down-regulation ($M = 1.43$, $sd = 0.22$) conditions in the pre-test. The difference between the conditions for the SCL in the post-test was not significant either (Baseline $M = 1.39$, $sd = 0.31$; Down-regulation $M = 1.42$, $sd = 0.28$).

Also, HR difference between baseline ($M = 81.96$, $sd = 4.94$) and the down-regulation ($M = 81.77$, $sd = 2.42$) in the pre-test and post-test did not show any significance (Baseline $M = 84.92$, $sd = 1.89$; Down-regulation $M = 85.05$, $sd = 2.86$).

Discussion

Recent evidence suggest that OCD involving contamination obsessions and washing compulsions might be characterized by a disorder in disgust processing. Hyperactivity in the insula

may play a particularly important role in mediating such putative disruptions [24, 25, 35]. In light of these findings, we designed a pilot study to explore the effects of rtfMRI-neurofeedback based anterior insula down-regulation on several behavioral, physiological and clinical measures of OCD patients with contamination fears and washing compulsions. Also, we aimed to examine the feasibility of our study procedures, validity of the tools, and overall approach for a larger study developing an rtfMRI-neurofeedback treatment approach for OCD. Yet, a further purpose was to introduce/present our methods, some of which were used for the first time (e.g., Ecological Disgust Test) in rtfMRI-neurofeedback studies.

GLM analysis show that down-regulation of the anterior insula is possible in OCD patients. In fact, all patients could decrease the BOLD signal with rtfMRI-neurofeedback in insula, albeit to different degrees, in the presence of disgust inducing stimuli. Although all patients showed increased activity in the anterior insula during the down-regulation condition on the first rtfMRI-neurofeedback training day, they showed a decrease in activity in the same ROI through the following sessions. In addition to the decreased activity in the anterior insula, an increased activity during the down-regulation conditions in the middle temporal gyrus and left postcentral gyrus was observed in all the patients.

Patients were less successful at down-regulation during the transfer runs in comparison to the regular training runs. Hence, including more transfer runs in the experimental protocol would be crucial in future experiments, in order to improve the behavioral results measured outside the scanner environment. Some further steps which can be taken to improve the self-regulation performance are discussed below.

In operant conditioning, the success in learning a new behavior is determined by the contingency of the behavior-consequence associations [65]. In rtfMRI-neurofeedback experiments, the association between a mental strategy that successfully regulates a neural signal (behavior) and feedback (consequence) can be affected by the temporal delay of the feedback signal [63]. In the great majority of rtfMRI-neurofeedback studies, feedback is continuously presented with minimal delay, approximately 2s [50]. However, because of insula's role in feeling, motivation and self-monitoring [21, 66], we anticipated that there could be potential activity increases in the insula due to reward processing when the feedback is presented in real-time. To prevent such an increase in insula activity in opposition to the desired decrease of this study, we followed a different approach of providing delayed feedback [67, 68]. According to this method, BOLD amplitudes in the anterior insula during the down-regulation block was averaged, and a proportional level of monetary reward was computed and presented to the patient at the end of each down-regulation block instead of presenting the reward values in real-time. However, some studies have suggested that uncoupling the cognitive task from the feedback by providing the feedback at shorter intervals might be a better way to achieve a particular behavior-consequence association when mental imagery is used during self-regulation [69, 70]. In line with the above suggestion, with an objective to improve the contingency of the feedback, in our followup study it might be useful to provide patients information about their ongoing brain activity at 10 s intervals (three times throughout each down-regulation block). To avoid cognitive or visual distractions, which can be caused by the presence of the graphical thermometer next to the disgust inducing pictures in the screen, it would be beneficial to locate each picture inside a frame which can provide neurofeedback, for example by color changes. In this manner, it would be possible to separate the neurofeedback information, which is presented more often from the reward, which will be presented only at the end of each block.

As an alternate approach to feedback computation, it might also be interesting to consider the "hits" approach (currently used only as an offline analytical approach) for the feedback calculation in the follow-up studies in combination with an intermittent feedback to gain sensitivity to trial-by-trial variations.

In addition, the target regions selected for self-regulation and the direction of regulation (either up or down) are crucial aspects in brain self-regulation experiments. The majority of previous rtfMRI-neurofeedback studies used single ROI up-regulation paradigms in which participants were been trained to increase activity of one target region [48–50]. However, relatively fewer rtfMRI studies showed that subjects could learn to down-regulate the brain activity e.g., in amygdala [71], subgenual anterior cingulate [72], auditory cortex [73] and anterior cingulate cortex [74]. Decreasing the BOLD signal might be harder as compared to increasing it [41]. Our preliminary results are important in showing the possibility of down-regulation of an abnormally activated brain region in psychiatric populations.

Considering that OCD affects a distributed fronto-striatal circuit, a connectivity-based or a pattern classifier-based neurofeedback study design, instead of a single ROI design, might be an interesting possibility in future experiments. In a recent study, Weygandt and colleagues [75] investigated whether fear, disgust and neutral emotional states can be decoded from brain patterns of fMRI information in OCD patients and healthy controls. Their results indicated that fMRI data contains information about OCD-relevant fear stimuli, and using this information it is possible to distinguish between OCD patients and healthy controls. These results suggest that future studies could also investigate the use of classifier-based neurofeedback for the treatment of OCD.

Regarding the behavioral effects due to rtfMRI-neurofeedback training, it is not possible to make clear conclusions from this pilot study with only 3 patients. However, in two patients (Patient 1 and Patient 3) positive changes in the behavioural tests were observed. The aforementioned patients improved their capability to bear the physical proximity of a real-world, disgusting, symptom-provoking object, by employing their successful cognitive strategies for down-regulation after the training. These results are forward-looking and trend-setting for the further development rtfMRI-neurofeedback, in light of previous studies that were limited to testing the immediate effects of self-regulation on behavior and symptoms by conducting tests inside the scanner environment [40, 44, 46, 76]. Novel symptom-specific tests, like EDT, would represent significant progress in the field for exploring the transfer and application of self-regulation skills to real-world situations.

It is important to stress that as both down-regulation and baseline conditions were interspersed in the same runs (both in the pre- and post-training test), the differences in behavioral/physiological measurements between baseline and down-regulation can not be attributed to habituation, effect of time, or general therapy that patients underwent, as those would have influenced both conditions. However, although all the stimuli presented in the pre- and the post behavioral tests were the same, there was an asymmetry in the pre- and the post-test instructions. We had assumed that there would not be differences between the baseline and the down-regulation conditions in the pre-tests but that there would be differences between these conditions in the post-test depending on the success in learning self-regulation. In accordance with the above assumption, we did not instruct the patients to use any cognitive strategy in the pre-test. Further, we supposed that this would allow us to observe the baseline behavioral and physiological values before the training. However, it would have been better if we had instructed the patients exactly the same way in both the pre- and post-tests as it would have allowed us to observe the instructions on brain activity during the pre-test. This potential limitation of the present study should be taken into account in future study designs.

In parallel with the EDT results, the same two patients also showed improvements in the picture rating test in two dimensions, i.e., valence and OCD symptom provocation. During the post-tests, patients rated the disgust evoking pictures with less negative valence, and as less symptom provocative following down-regulation blocks.

Patient 2, did not display any improvement in these dimensions. In fact, the patient's Y-BOCs scores were higher at the end of the experiments. Because the questionnaires used as

clinical measures, are self-administered, and because we do not ask patients to use their mental strategies during the administration of the questionnaires, it is not possible to be certain whether the positive or negative changes in the scores could be attributed to the rtfMRI-neurofeedback training, or to other factors active during this period.

Because the main purpose of this study was to see the feasibility of the method and optimization of the measurements for a controlled, future study, we wanted to keep the heterogeneity of the patients to figure out the possible effects of the rtfMRI-neurofeedback training on different patient subgroups. In light of Patient-2's lack of behavioral improvement and relatively low Y-BOCs scores at the beginning of the measurements, in future studies it might be useful to define a threshold for the clinical symptomatology (measured by Y-BOCs) for selecting only the patients whose scores are above that threshold.

Non-consistent results were observed for HR measures collected inside the scanner. Two patients (patient 1 and patient 2), displayed decreased heart rates during the down-regulation conditions. However, patient 3 had higher heart rates while down-regulating through the runs. HR measures, recorded while the patients were looking at the disgust inducing pictures outside the scanner, did not reveal a significant difference between the baseline and the down-regulation conditions, in the post-tests, in all three patients.

Previous psycho-physiological investigations exploring responses towards disgust inducing stimuli are limited in number and provide conflicting results, including heart rate. Although some studies show elevated HR in the conditions when healthy subjects are presented with symptom provoking pictures [77–81], others point to a deceleration in the HR as an indicator of parasympathetic activity [82–84]. Studies that have measured OCD patients' physiological responses towards disgust inducing stimuli reported contradictory results as well. While some experimenters found elevated autonomic nervous system activity and HR [85–88], other studies reported HR decelerations which is interpreted as a sign of orientation and not avoidance or stimulus rejection [89–92]. One of the reasons for these conflicting findings might be the type of the stimuli used in the experiments. While the disgust emotion elicited in relation to contamination and pollution (e.g., pictures of dirty toilets, cockroaches, maggots on food, foul smells, facial expressions of expelling food), is characterized by HR acceleration, disgust elicited in relation to mutilation, injury and blood (e.g., injections, mutilation scenes, bloody injuries), seems to be characterized by a pattern of HR deceleration [93]. In our set of stimuli we included both contamination and mutilation types of images. Therefore, and depending on the heterogeneity of the OCD patients, using both kind of pictures together in the same measurement might cause a neutralizing effect in HR measures. The differences on anxiety levels in our small group of patients might have also contributed to this inconsistency in HR results. Patient 3, who showed elevated HR during the down-regulation conditions in the scanner, showed also the highest anxiety level (both in trait and state-anxiety measures). Patients' elevated HR during down-regulation conditions might also be attributed to performance anxiety and reward expectancies.

Disgust is consistently reported to be associated with increased electrodermal activity [93]. However, we did not observe a significant difference between disgust provoking and neutral pictures and skin conductance level levels. There were no significant differences in levels between baseline and down-regulation blocks while patients were viewing disgust inducing pictures either. Because we measured the mean skin conductance levels throughout baseline and the down-regulation blocks, these results might be due to the presentation of mixed type of disgust inducing pictures.

Subjective reports of patients at the end of the rtfMRI-neurofeedback training periods indicate that patients used reappraisal or suppression strategies to gain control over the feedback signal. With continued training, subjects modified their strategy to maximize their feedback

and reward. Because different emotional regulation mechanisms may have different effects on physiological responses such categorization could partly explain the heterogeneity in the heart rate and the skin conductance level measurements as well.

Finally, an important question as to whether the BOLD up- or down-regulation directly leads to the physiological and clinical changes observed in the patients, or the invoking of the appropriate mental imagery and cognitive strategies leads to those physiological changes, or both mechanisms are interwoven remains unanswered in this or any of the rtfMRI-neurofeedback studies so far. This is a topic of ongoing and future research.

In summary, in this pilot study we investigated the application of rtfMRI-neurofeedback for the down-regulation of BOLD activity in the anterior insula in OCD patients. We also explored the feasibility of several behavioral and physiological pre- and post-training tests and clinical assessments that could be used in a future long-term study. Our results indicate that with sufficient training OCD patients can down-regulate the BOLD activity in their anterior insula in the presence of disgust inducing stimuli. The two tests that were designed to examine the effect of this self-control in real-world conditions outside the scanner (picture rating tests and the EDT) have important implications for future studies.

To improve the consistency of self-regulation, it might be crucial to combine rtfMRI-neurofeedback sessions with extended neurofeedback training outside the scanner using portable EEG and/or functional near infrared spectroscopy (fNIRS). For this purpose, it would be useful to identify the EEG and/or fNIRS correlates of down-regulation of the BOLD signal in the anterior insula in a patient-specific manner.

Author Contributions

Conceived and designed the experiments: KB RS SR JS MR HR NB. Performed the experiments: KB JS LD EA. Analyzed the data: KB JS LD EA RV RM. Contributed reagents/materials/analysis tools: KB JS RS SR TK MR. Wrote the paper: KB RS SR JS TK NB.

References

1. Ruscio AM, Stein DJ, Chiu WT, Kessler RC. The epidemiology of obsessive-compulsive disorder in the National Comorbidity Survey Replication. *Mol Psychiatry*. 2010; 15(1):53–63. Epub 2008 Aug 26. doi: [10.1038/mp.2008.94](https://doi.org/10.1038/mp.2008.94) PMID: [18725912](https://pubmed.ncbi.nlm.nih.gov/18725912/)
2. APA—American Psychiatric Association. *Diagnostic and Statistical Manual of Mental Disorders—DSM-IV-TR* (4th edition, Text Revision). Washington, D.C.: American Psychiatric Association; 2000.
3. Rachman S. Fear of contamination. *Behaviour Research and Therapy*. 2004; 42(11), 1227–1255. PMID: [15381436](https://pubmed.ncbi.nlm.nih.gov/15381436/)
4. Broderick J, Grisham JR, Weidemann G. Disgust and fear responding in contamination-based obsessive-compulsive disorder during pictorial exposure. *Behav Ther*. 2013; Mar; 44(1):27–38. doi: [10.1016/j.beth.2012.05.005](https://doi.org/10.1016/j.beth.2012.05.005) PMID: [23312424](https://pubmed.ncbi.nlm.nih.gov/23312424/)
5. Millet B, Dondaine T, Reymann JM, Bourguignon A, Naudet F, Jaafari N, et al. Obsessive compulsive disorder networks: positron emission tomography and neuropsychology provide new insights. *PLoS One*. 2013; 8(1):e53241. doi: [10.1371/journal.pone.0053241](https://doi.org/10.1371/journal.pone.0053241) PMID: [23326403](https://pubmed.ncbi.nlm.nih.gov/23326403/)
6. Rotge JY, Guehl D, Dilharreguy B, Cuny E, Tignol J, Bioulac B, et al. Provocation of obsessive-compulsive symptoms: a quantitative voxel-based meta-analysis of functional neuroimaging studies. *J Psychiatry Neurosci*. 2008; 33: 405–412. PMID: [18787662](https://pubmed.ncbi.nlm.nih.gov/18787662/)
7. Kwon JS, Jang JH, Choi JS, Kang DH. Neuroimaging in obsessive-compulsive disorder. *Expert Rev Neurother*. 2009; 9: 255–269. doi: [10.1586/14737175.9.2.255](https://doi.org/10.1586/14737175.9.2.255) PMID: [19210199](https://pubmed.ncbi.nlm.nih.gov/19210199/)
8. Graybiel AM, Rauch SL. Toward a Neurobiology of Obsessive-Compulsive Disorder. *Neuron*. 2000; Vol. 28, 343–347, November.
9. Auouizerate B, Guehl D, Cuny E, Rougier A, Bioulac B, Tignol J, et al. Pathophysiology of obsessive-compulsive disorder: a necessary link between phenomenology, neuropsychology, imagery and physiology. *Prog Neurobiol*. 2004; 72:195–221. PMID: [15130710](https://pubmed.ncbi.nlm.nih.gov/15130710/)

10. Menzies L, Chamberlain SR, Laird AR, Thelen SM, Sahakian BJ, Bullmore ET. Integrating evidence from neuroimaging and neuropsychological studies of obsessive-compulsive disorder: the orbitofronto-striatal model revisited. *Neurosci Biobehav Rev*. 2008; 32(3):525–549. PMID: [18061263](#)
11. Ougrin D. Efficacy of exposure versus cognitive therapy in anxiety disorders: systematic review and meta-analysis. *BMC Psychiatry*. 2011; Dec 20; 11:200. doi: [10.1186/1471-244X-11-200](#) PMID: [22185596](#)
12. Doron G, Moulding R. Cognitive behavioral treatment of obsessive-compulsive disorder: a broader framework. *Isr J Psychiatry Relat Sci*. 2009; 46(4): 257–63 PMID: [20635772](#)
13. Seibell PJ, Hollander E. Management of obsessive-compulsive disorder. *F1000Prime Rep*. 2014; Aug 1; 6:68. doi: [10.12703/P6-68](#) PMID: [25165567](#)
14. Schiepek G, Tominschek I, Heinzel S, Aigner M, Dold M, Unger A, et al. Discontinuous patterns of brain activation in the psychotherapy process of obsessive-compulsive disorder: converging results from repeated fMRI and daily self-reports. *PLoS One*. 2013; Aug 15; 8(8):e71863 doi: [10.1371/journal.pone.0071863](#) PMID: [23977168](#)
15. Mindus P, Ericson K, Greitz T, Meyerson BA, Nyman H, Sjögren I. Regional cerebral glucose metabolism in anxiety disorders studied with positron emission tomography before and after psychosurgical intervention. A preliminary report. *Acta Radiol Suppl*. 1986; 369:444–8. PMID: [2980522](#)
16. Schwartz JM, Stoessel PW, Baxter LR Jr, Martin KM, Phelps ME. Systematic changes in cerebral glucose metabolic rate after successful behavior modification treatment of obsessive-compulsive disorder. *Arch Gen Psychiatry*. 1996; Feb; 53(2):109–13. PMID: [8629886](#)
17. Swedo SE, Pietrini P, Leonard HL, Schapiro MB, Rettew DC, Goldberger EL, et al. Cerebral glucose metabolism in childhood-onset obsessive-compulsive disorder. Revisualization during pharmacotherapy. *Arch Gen Psychiatry*. 1992; Sep; 49(9):690–4. PMID: [1514873](#)
18. Figeo M, Luigjes J, Smolders R, Valencia-Alfonso CE, van Wingen G, de Kwaasteniet B, et al. Deep brain stimulation restores frontostriatal network activity in obsessive-compulsive disorder. *Nat Neurosci*. 2013; Apr; 16(4):386–7. doi: [10.1038/nn.3344](#) PMID: [23434914](#)
19. Baxter LR Jr, Schwartz JM, Bergman KS, Szuba MP, Guze BH, Mazziotta JC, et al. Caudate glucose metabolic rate changes with both drug and behavior therapy for obsessive-compulsive disorder. *Arch Gen Psychiatry*. 1992; Sep; 49(9):681–9. PMID: [1514872](#)
20. Nakao T, Nakagawa A, Yoshiura T, Nakatani E, Nabeyama M, Yoshizato C, et al. Brain activation of patients with obsessive-compulsive disorder during neuropsychological and symptom provocation tasks before and after symptom improvement: A functional magnetic resonance imaging study. *Biological Psychiatry*. 2005; 57, 901–910. PMID: [15820711](#)
21. Craig B. How do you feel now? The anterior insula and human awareness. *Nat. Rev. Neurosci*. 2011; 10, 59–70.
22. Wright P, He G, Shapira NA, Goodman WK, Liu Y. Disgust and the insula: fMRI responses to pictures of mutilation and contamination. *Neuroreport*. 2004; Oct 25; 15(15):2347–51. PMID: [15640753](#)
23. Olatunji BO, Sawchuk CN, Lohr JM, de Jong PJ. Disgust domains in the prediction of contamination fear. *Behaviour Research and Therapy*. 2004; 42(1), 93–104. PMID: [14744526](#)
24. Stein DJ, Arya M, Pietrini P, Rapoport JL, Swedo SE. Neurocircuitry of disgust and anxiety in obsessive-compulsive disorder: a positron emission tomography study. *Metabolic Brain Disease*. 2006; 21(2–3), 267–277. PMID: [16850255](#)
25. Starcevic V, Berle D, Brakoulias V, Sammut P, Moses K, Milicevic D, et al. Functions of compulsions in obsessive-compulsive disorder. *Aust N Z J Psychiatry*. 2011; Jun; 45(6):449–57. doi: [10.3109/00048674.2011.567243](#) PMID: [21510720](#)
26. Olatunji BO, Cisler JM, Deacon BJ, Connolly K, Lohr JM. The disgust propensity and sensitivity scale-revised: Psychometric properties and specificity in relation to anxiety disorder symptoms. *Journal of Anxiety Disorders*. 2007; 21, 918–930. PMID: [17236747](#)
27. Tsao SD, McKay D. Behavioral avoidance tests and disgust in contamination fears: distinctions from trait anxiety. *Behav Res Ther*. 2004; Feb. 42(2):207–16 PMID: [14975781](#)
28. Cisler JM, Olatunji BO, Lohr JM. Disgust, fear, and the anxiety disorders: A critical review. *Journal of Anxiety Disorders*. 2009; 29(1), 34–46.
29. Muris P, van der Heiden S, Rassin E. Disgust sensitivity and psychopathological symptoms in non-clinical children. *J Behav Ther Exp Psychiatry*. 2008; Jun. 39(2):133–46. Epub 2007 Mar 12. PMID: [17433251](#)
30. Schienle A, Dietmaier G, Ille R, Leutgeb V. Eine Skala zur Erfassung der Ekelempfindlichkeit. *Zeitschrift für Klinische Psychologie und Psychotherapie*. 2002; 39, 80–86.
31. Schienle A, Schäfer A, Stark R, Walter B, Kirsch P, Vaitl D. Disgust processing in phobia of blood-injection-injury: an fMRI study. *Journal of Psychophysiology*. 2003; 17, 87–93.

32. Phillips ML, Marks IM, Senior C, Lythgoe D, O'Dwyer AM, Meehan O, et al. A differential neural response in obsessive-compulsive disorder patients with washing compared with checking symptoms to disgust. *Psychol Med*. 2000; 30(5):1037–50. PMID: [12027041](#)
33. Mataix-Cols D, Wooderson S, Lawrence N, Brammer MJ, Speckens A, Phillips ML. Distinct neural correlates of washing, checking, and hoarding symptom dimensions in obsessive-compulsive disorder. *Arch Gen Psychiatry*. 2004; 61(6):564–76. PMID: [15184236](#)
34. Moretz MW, McKay D. Disgust sensitivity as a predictor of obsessive-compulsive contamination symptoms and associated cognitions. *J Anxiety Disord*. 2008; 22(4):707–15. PMID: [17719199](#)
35. Goetz AR, Lee HJ, Cogle JR. The association between health anxiety and disgust reactions in a contamination-based behavioral approach task. *Anxiety Stress Coping*. 2013; 26(4): 431–46. doi: [10.1080/10615806.2012.684241](#) PMID: [22607189](#)
36. Shapira NA, Liu Y, He AG, Bradley MM, Lessig MC, James GA, et al. Brain activation by disgust-inducing pictures in obsessive-compulsive disorder. *Biological Psychiatry*. 2003; 54(7), 751–756. PMID: [14512216](#)
37. Stein DJ, Arya M, Pietrini P, Rapoport JL, Swedo SE. (2006). Neurocircuitry of disgust and anxiety in obsessive-compulsive disorder: a positron emission tomography study. *Metabolic Brain Disease*. 2006; 21 (2–3), 255–265.
38. Berle D, Phillips ES. Disgust and obsessive-compulsive disorder: an update. *Psychiatry*. 2006; Fall; 69 (3): 228–38. PMID: [17040174](#)
39. Birbaumer N, Cohen LG. Brain-computer interfaces: communication and restoration of movement in paralysis. *J Physiol*. 2007; Mar 15; 579(Pt 3):621–36 PMID: [17234696](#)
40. Caria A, Sitaram R, Veit R, Begliomini C, Birbaumer N. Volitional control of anterior insula activity modulates the response to aversive stimuli. A real-time functional magnetic resonance imaging study. *Biol Psychiatry*. 2010; 68 (5), 425–432. doi: [10.1016/j.biopsych.2010.04.020](#) PMID: [20570245](#)
41. Veit R, Singh V, Sitaram R, Caria A, Rauss K, Birbaumer N. Using real-time fMRI to learn voluntary regulation of the anterior insula in the presence of threat-related stimuli. *Soc Cogn Affect Neurosci*. 2012; Aug; 7(6):623–34. doi: [10.1093/scan/nsr061](#) PMID: [21983794](#)
42. Sitaram R, Lee S, Ruiz S, Rana M, Veit R, Birbaumer N. Real-time support vector classification and feedback of multiple emotional brain states. *Neuroimage*. 2010; May 15; 56(2):753–65. doi: [10.1016/j.neuroimage.2010.08.007](#) PMID: [20692351](#)
43. Sitaram R, Caria A, Veit R, Gaber T. Volitional control of insula using an fMRI Brain-Computer Interface in criminal psychopaths enhances functional connectivity of the emotional network. 38th annual meeting of the Society for Neuroscience, Washington. 2008a.
44. Sitaram R, Veit R, Stevens B, Caria A, Gerloff C, Birbaumer N, et al. Acquired control of ventral premotor cortex activity by feedback training: an exploratory real-time fMRI and TMS study. *Neurorehabil Neural Repair*. 2012; Mar-Apr. 26(3):256–65. doi: [10.1177/1545968311418345](#) PMID: [21903976](#)
45. Sitaram R, Caria A, Veit R, Gaber T, Ruiz S, Birbaumer N. Volitional control of the anterior insula in criminal psychopaths using real-time fMRI neurofeedback: a pilot study. *Front Behav Neurosci*. 2014; Oct 14; 8:344. doi: [10.3389/fnbeh.2014.00344](#) PMID: [25352793](#)
46. Ruiz S, Lee S, Soekadar SR, Caria A, Veit R, Kircher T, et al. Acquired self-control of insula cortex modulates emotion recognition and brain network connectivity in schizophrenia. *Hum Brain Mapp*. 2013; 34 (1), 200–212. doi: [10.1002/hbm.21427](#) PMID: [22021045](#)
47. Linden DE, Habes I, Johnston SJ, Linden S, Tatineni R, Subramanian L, et al. Real-time self-regulation of emotion networks in patients with depression. *PLoS ONE*. 2012; 7, e38115. doi: [10.1371/journal.pone.0038115](#) PMID: [22675513](#)
48. Ruiz S, Buyukturkoglu K, Rana M, Birbaumer N, Sitaram R. Real-time fMRI brain computer interfaces: Self-regulation of single brain regions to networks *Biol Psychol*. 2014; Jan; 95:4–20. doi: [10.1016/j.biopsycho.2013.04.010](#) PMID: [23643926](#)
49. Birbaumer N, Ruiz S, Sitaram R. Learned regulation of brain metabolism. *Trends Cogn Sci*. 2013; Jun; 17(6):295–302. doi: [10.1016/j.tics.2013.04.009](#) PMID: [23664452](#)
50. Sulzer J, Haller S, Scharnowski F, Weiskopf N, Birbaumer N, Blefari M, et al. Real-time fMRI neurofeedback: progress and challenges. *Neuroimage*. 2013; 76, 386–399. doi: [10.1016/j.neuroimage.2013.03.033](#) PMID: [23541800](#)
51. Scheinost D, Stoica T, Saks J, Papademetris X, Constable RT, Pittenger C, et al. Orbitofrontal cortex neurofeedback produces lasting changes in contamination anxiety and resting-state connectivity. *Transl Psychiatry*. 2013; Apr 30; 3:e250. doi: [10.1038/tp.2013.24](#) PMID: [23632454](#)
52. Lehl S. Mehrfachwahl-Wortschatz-Intelligenztest: MWT-B (3.überarbeitete Auflage). Balingen: PERI-MED-spitta, 1995.

53. Oldfield RC. The assessment and analysis of handedness: the Edinburgh inventory. *Neuropsychologia*. 1971; Mar; 9(1):97–113. PMID: [5146491](#)
54. Hand I, Büttner-Westphal H. Die Yale-Brown Obsessive Compulsive Scale (Y-BOCS): Ein halbstrukturiertes Interview zur Beurteilung des Schweregrades von Denk- und Handlungszwängen. *Verhaltenstherapie*. 1991; 1(3): 223–5.
55. Hautzinger M, Keller F, Kühner Ch. BDI-II. Beck-Depressions-Inventar. Revision. 2. edition. Pearson Assessment: Frankfurt; 2009.
56. Spielberger CD, Gorsuch RL, Lushene RE. Manual for the State-Trait Anxiety Inventory. Palo Alto, CA: Consulting Psychologists Press; 1970.
57. Laux L, Glanzmann P, Schaffner P, Spielberger C.D. Das State-Trait-Angstinventar. Theoretische Grundlagen und Handanweisung. Weinheim: Beltz Test GmbH; 1981.
58. Lawrence EJ, Su L, Barker GJ, Medford N, Dalton J, Williams SC, et al. Self-regulation of the anterior insula: Reinforcement learning using real-time fMRI neurofeedback. *Neuroimage*. 2014; Nov 11; 88C:113–124.
59. Saxe R, Brett M, Kanwisher N. Divide and conquer: a defense of functional localizers. *Neuroimage*. 2006; 30:1088–96, discussion 1097–89. PMID: [16635578](#)
60. Lang PJ, Bradley MM, Cuthbert BN. International affective picture system (IAPS): affective ratings of pictures and instruction manual. Technical report A-6. Gainesville, FL: Center for Research in Psychophysiology, University of Florida, 2005.
61. Goebel R. Cortex-based real-time fMRI. *Neuroimage*. 2001; 13, S129.
62. Ashby FG, O'Brien JB. The effects of positive versus negative feedback on information-integration category learning. *Percept Psychophys*. 2007 Aug; 69(6):865–78. PMID: [18018967](#)
63. Caria A, Sitaram R, Birbaumer N. Real-time fMRI: a tool for local brain regulation. *Neuroscientist*. 2012; 18 (5), 487–501. PMID: [21652587](#)
64. Gerich J. Visual analogue scales for mode-independent measurement in self-administered questionnaires. *Behav Res Methods*. 2007; Nov; 39(4):985–92. PMID: [18183916](#)
65. Schacter DL, Gilbert DT, Wegner DM. *Psychology* (2nd Edition). New York: Worth, 2011.
66. Bray S, Shimojo S, O'Doherty JP. Direct instrumental conditioning of neural activity using functional magnetic resonance imaging-derived reward feedback. *J. Neurosci*. 2007; 27 (28), 7498–7507. PMID: [17626211](#)
67. Ninaus M, Kober SE, Witte M, Koschutnig K, Stangl M, Neuper C, et al. Neural substrates of cognitive control under the belief of getting neurofeedback training. *Front Hum Neurosci*. 2013 Dec 26; 7:914. doi: [10.3389/fnhum.2013.00914](#) eCollection 2013. PMID: [24421765](#)
68. Posse S, Fitzgerald D, Gao K, Habel U, Rosenberg D, Moore GJ, et al. Real-time fMRI of temporolimbic regions detects amygdala activation during single-trial self-induced sadness. *NeuroImage*. 2003; 18 (3), 760–768. PMID: [12667853](#)
69. Yoo SS, Jolesz FA. Functional MRI for neurofeedback: feasibility study on a hand motor task. *Neuroreport*. 2002; 13 (11), 1377. PMID: [12167756](#)
70. Johnson KA, Hartwell K, LeMatty T, Borckardt J, Morgan PS, Govindarajan K, et al. Intermittent “real-time” fMRI feedback is superior to continuous presentation for a motor imagery task: a pilot study. *J. Neuroimaging*. 2012; 22 (1), 58–66. doi: [10.1111/j.1552-6569.2010.00529.x](#) PMID: [20977537](#)
71. Dewiputri WI, Schweizer R, Auer T, Frahm J. Uncoupling task and feedback processing during cognitive fMRI neurofeedback training. Poster session presented at the Organization of Human Brain Mapping OHBM, 2013.
72. Brühl AB, Scherpiet S, Sulzer J, Stämpfli P, Seifritz E, Herwig U. Real-time neurofeedback using functional MRI could improve down-regulation of amygdala activity during emotional stimulation: a proof-of-concept study. *Brain Topogr*. 2014; Jan; 27(1):138–48. doi: [10.1007/s10548-013-0331-9](#) PMID: [24241476](#)
73. Hamilton JP, Glover GH, Hsu JJ, Johnson RF, Gotlib IH. Modulation of subgenual anterior cingulate cortex activity with real-time neurofeedback. *Human Brain Mapping*. 2011; 32 (1), 22–31 doi: [10.1002/hbm.20997](#) PMID: [21157877](#)
74. Haller S, Birbaumer N, Veit R. Real-time fMRI feedback training may improve chronic tinnitus. *Eur. Radiol*. 2010; 20 (3), 696–703. doi: [10.1007/s00330-009-1595-z](#) PMID: [19760238](#)
75. Li X, Hartwell KJ, Borckardt J, Prisciandaro JJ, Saladin ME, Morgan PS, et al. Volitional reduction of anterior cingulate cortex activity produces decreased cue craving in smoking cessation: a preliminary real-time fMRI study. *Addict Biol*. 2013; Jul; 18(4):739–48. doi: [10.1111/j.1369-1600.2012.00449.x](#) PMID: [22458676](#)

76. Weygandt M, Blecker CR, Schäfer A, Hackmack K, Haynes JD, Vaitl D, et al. fMRI pattern recognition in obsessive-compulsive disorder. *Neuroimage*. 2012; Apr 2; 60(2):1186–93. doi: [10.1016/j.neuroimage.2012.01.064](https://doi.org/10.1016/j.neuroimage.2012.01.064) PMID: [22281674](https://pubmed.ncbi.nlm.nih.gov/22281674/)
77. Buyukturkoglu K, Rana M, Ruiz S, Hackley SA, Soekadar SR, Birbaumer N, et al. Volitional Regulation of the Supplementary Motor Area with fMRI-BCI neurofeedback in Parkinson's disease: A Pilot Study. Conference Proceeding. Neural Engineering (NER), 6th International IEEE/EMBS Conference on 6–8 Nov 2013. San Diego, CA. Page(s): 677–681.
78. Lang PJ, Bradley MM, Cuthbert BN. "Motivated attention: affect, activation and action," in *Attention and Orienting: Sensory and Motivational Processes*, eds Lang P. J., Simons R. F., and Balaban M. T. (Hillsdale, NJ: Erlbaum), 97–135. 1997.
79. Alaoui-Ismaïli O, Robin O, Rada H, Dittmar A, Vernet-Maury E. Basic emotions evoked by odorants: comparison between autonomic responses and self-evaluation. *Physiology & Behaviour*. 1997; 62, 713–720.
80. Schienle A, Stark R, Vaitl D. Evaluative conditioning: A possible explanation for the acquisition of disgust responses? *Learning and Motivation*. 2001; 32(1), 65–83.
81. Vrana SR. Startle reflex response during sensory modality specific disgust, anger, and neutral imagery. *Journal of Psychophysiology*. 1994; 8(3), 211–218.
82. Gross JJ. Antecedent- and response-focused emotion mregulation: Divergent consequences for experience, expression, and physiology. *Journal of Personality and Social Psychology*. 1998; 74(1), 224–237. PMID: [9457784](https://pubmed.ncbi.nlm.nih.gov/9457784/)
83. Gross JJ, Levenson RW. Emotional suppression: Physiology, self-report, and expressive behavior. *Journal of Personality and Social Psychology*. 1993; 64(6), 970–986. PMID: [8326473](https://pubmed.ncbi.nlm.nih.gov/8326473/)
84. Johnsen BH, Thayer JF, Hugdahl K. Affective judgment of the Ekman faces: A dimensional approach. *mJournal of Psychophysiology*. 1995; 9(3), 193–202.
85. Levenson RW. Autonomic nervous system differences among emotions. *Psychological Science*. 1992; 3(1), 23–27.
86. Benkelfat C, Mefford IN, Masters CF, Nordahl TE, King AC, Cohen RM, et al. Plasma catecholamines and their metabolites in obsessive-compulsive disorder. *Psychiatry Research*. 1991; 37(3), 321–331. PMID: [1891512](https://pubmed.ncbi.nlm.nih.gov/1891512/)
87. Insel TR, Zahn T, Murphy DL. Obsessive-compulsive disorder: an anxiety disorder. In: Tuma AT, & Maser J (Eds.), *Anxiety and the anxiety disorders* (pp. 577–589). Hillsdale, NJ: Lawrence Erlbaum & Associates. 1985.
88. Rabavilas AD, Boulougouris JC, Stefanis C. Synchrony and concordance on subjective and psychophysiological measures after beta-blockade and flooding in obsessive-compulsive patients. In: Boulougouris J. C., & Rabavilas A. D. (Eds.), *The treatment of phobic and obsessive-compulsive patients* (pp. 115–125). Oxford: Pergamon. 1977.
89. Hoehn-Saric R, McLeod DR, Hipsley P. Is hyperarousal essential to obsessive compulsive disorder? Diminished physiologic flexibility, but not hyperarousal, characterizes patients with obsessive-compulsive disorder. *Archives of General Psychiatry*. 1995; 52(8), 688–693. PMID: [7632122](https://pubmed.ncbi.nlm.nih.gov/7632122/)
90. Hollander E, DeCaria C, Nitsescu A, Cooper T, Stover B, Gully R, et al. Noradrenergic function in obsessive-compulsive disorder: behavioral and neuroendocrine responses to clonidine and comparison to healthy controls. *Psychiatry Research*. 1991; 37(2), 161–177. PMID: [1876628](https://pubmed.ncbi.nlm.nih.gov/1876628/)
91. McCarthy PR, Ray WJ, Foa EB. Cognitive influences on electrocortical and heart rate activity in obsessive-compulsive disorder. *International Journal of Psychophysiology*. 1995; 19(3), 215–222. PMID: [7558988](https://pubmed.ncbi.nlm.nih.gov/7558988/)
92. Zahn TP, Leonard HL, Swedo SE, Rapoport JL. Autonomic activity in children and adolescents with obsessive-compulsive disorder. *Psychiatry Research*. 1996; 60(1), 67–76. PMID: [8852868](https://pubmed.ncbi.nlm.nih.gov/8852868/)
93. Olatunji BO, Davis ML, Powers MB, Smits JA. Cognitive-behavioral therapy for obsessive-compulsive disorder: a meta-analysis of treatment outcome and moderators. *J Psychiatr Res*. 2013; Jan; 47(1):33–41. doi: [10.1016/j.jpsychires.2012.08.020](https://doi.org/10.1016/j.jpsychires.2012.08.020) PMID: [22999486](https://pubmed.ncbi.nlm.nih.gov/22999486/)